Zeitschrift: IABSE congress report = Rapport du congrès AIPC = IVBH Kongressbericht

Band: 12 (1984)

Rubrik: VI. Wind effects on structures

SEMINAR

VI

Wind Effects on Structures

Effets du vent sur les structures

Windeinwirkungen auf Tragwerke

Chairman: A.G. Davenport, Canada

Coordinator: E. Gehri, Switzerland

General Reporter: W. Melbourne, Australia

The theme has been introduced by the General Reporter in the Introductory Report of the 12th Congress, available at the IABSE Secretariat.

Leere Seite
Blank page
Page vide

Wind Tunnel Tests of Long Span Bridges

Essais en soufflerie sur des ponts de longue portée

Windkanalversuche an Brücken mit grosser Spannweite

Peter IRWIN
Dir. Techn. Serv.
Morrison Hershfield Ltd.
Guelph, ON, Canada

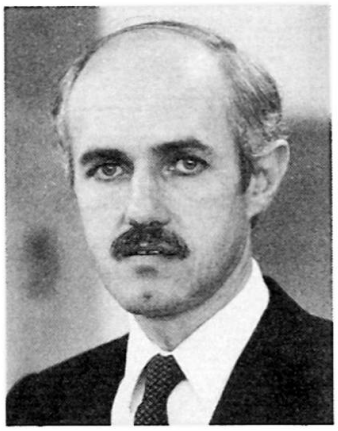

Peter Irwin was born in 1945, obtained his aeronautical engineering degree at the University of Southampton, U.K. and his Ph.D. from McGill University, Montreal, Quebec. Since 1974 he has been involved in research and consulting in wind engineering, first at the National Research Council, Ottawa, and, since 1980, at the wind tunnel laboratories of Morrison Hershfield Limited.

SUMMARY

Recent experiences in wind tunnel testing a number of long span bridge projects are described. These experiences include the aerodynamic stability of plate girder decks, the use of baffle plates and other methods to eliminate vortex excitation, the effects of wind turbulence, the effect on flutter of offset centre of rotation for torsional oscillations, the use of part-span fairings, and the effectiveness of tuned-mass dampers.

RESUME

Des expériences récentes lors d'essais en soufflerie sur des ponts de longue portée sont décrites. Ces expériences concernent la stabilité aérodynamique des tabliers, l'emploi de revêtements insonorisants et d'autres façons de lutter contre les effets des tourbillons, l'effet sur la stabilité aérodynamique d'un centre de rotation compensé pour les oscillations de torsion, l'emploi de profilés de travée partielle, et l'effet des amortisseurs de vibration.

ZUSAMMENFASSUNG

Die neuesten Erfahrungen aus den Windkanalversuchen mit einer Anzahl Brücken grosser Spannweite werden beschrieben. Die Erkenntnisse umfassen die aerodynamische Stabilität der Fahrbahnplatten von Balkenbrücken, die Verwendung von Prallplatten und anderer Vorkehrungen für das Vermeiden von Resonanzschwingungen, den Einfluss von Turbulenzen, die Auswirkung einer Verschiebung des Drehpunktes auf die Torsions- und Biegeschwingungen, die Wirkung einer strömungsgünstigen Verkleidung und die Wirksamkeit einer abgestimmten Dämpfungsvorrichtung.

1. INTRODUCTION

The object of this paper is to record some of the more interesting findings that have emerged from various wind tunnel tests that the author has been involved with including the new Annacis Island cable-stayed bridge near Vancouver[1]. The wind tunnel tests have ranged from simple sectional model tests in smooth uniform flow to full aeroelastic model investigations with wind turbulence simulated. One general observation is that the behaviour of a particular bridge in strong winds is influenced by many factors: overall deck shape; edge details; natural frequencies; deflection shapes of the modes of vibration; structural damping; the mass distribution of the deck and other major components; wind turbulence; height above the water; local topography; adjacent bridges; snow and ice accumulations; and alignment of the bridge relative to the most probable strong wind directions. The following selected experiences illustrate how some of the above mentioned factors have come into play in particular cases.

2. NOTATION

b	= width of deck	r	= offset of centre of rotation
I	= moment of inertia per unit length	r_G	= radius of gyration
U	= mean wind speed	R	= r for sectional model
u'	= rms value of wind speed	m	= mass per unit length
ζ	= damping ratio	N_V	= vertical frequency
ρ	= air density	N_T	= torsional frequency

3. USE OF PLATE GIRDERS ON ANNACIS ISLAND BRIDGE, VANCOUVER

Some bridge decks with plate girders have experienced serious aerodynamic instabilities. However, in the right circumstances they can have more than an adequate stability. Data on plate girder sections indicate that shallow girders and a girder location inboard of the deck edge are preferable aerodynamically and these concepts were applied to the new cable-stayed, 465 main span, Annacis Island Bridge [1,2]. Figure 1 shows the torsional response for three of the various cross-sections tested in Morrison Hershfield Limited's Guelph wind tunnel using 1:60 scale sectional models [1]. Cross-section 1 possessed the best aerodynamic stability but was less efficient structurally than cross-section 2 on which the cables could be directly attached to the girders. As can be seen in Figure 1 the torsional stability of cross-section 2 was not as good as for 1. However, by increasing the depth of the vertical plate at the extreme edge of the deck, as in cross-section 3, the torsional stability was significantly improved. This was attributed to the edge plate acting as a wind deflector that assisted the smooth passage of the flow around the bottom of the girder. The onset of torsional instability for cross-section 3 began at a nondimensional wind speed of 3.0 but was limited to an amplitude of less than 1 degree. This initial instability was attributed to vortex excitation. The strong flutter type of instability did not begin until a non-dimensional speed of 4.5. Both cross-sections 1 and 3 had sufficient aerodynamic stability for the site. Tests in turbulent wind indicated the torsional instability was not greatly altered by turbulence. The optimum shape, cross section 3, thus resulted from simultaneous considerations of structural economy and the aerodynamics of both the overall deck shape and edge details. In another paper in this conference, Taylor [2] describes the evolution of the Annacis design in more depth.

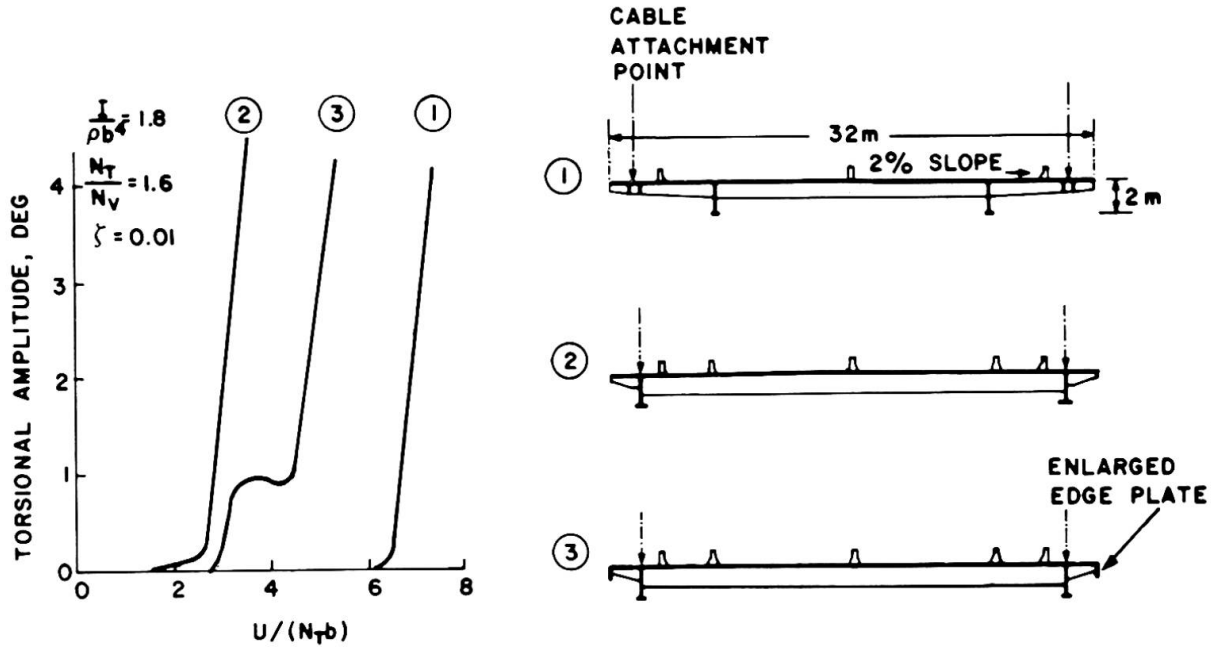

FIGURE 1 - TORSIONAL RESPONSE OF ANNACIS ISLAND BRIDGE

4. USE OF BAFFLE PLATES ON THE PROPOSED DAMES POINT STEEL BRIDGE

The evolution of the final steel version of Dames Point Bridge, Jacksonville, Florida, in Figure 2 took place in the course of sectional model tests in smooth flow at the National Research Council, Ottawa [3]. Although a number of details of the cross-section contributed towards providing good aerodynamic stability, the most important were the vertical baffle plates at approximately the 1/4-chord position under the road deck. These broke up vortices that otherwise tended to form under the deck on the original cross-section, as illustrated in Figure 2, and greatly reduced vortex excitation. Furthermore they provided a 40% increase in the critical wind speed for the onset of flutter. The baffle plate principle has subsequently been tested in other investigations for the Annacis Island bridge [1] and the Thousand Islands Bridge [4], and again found to be very beneficial for aerodynamic stability.

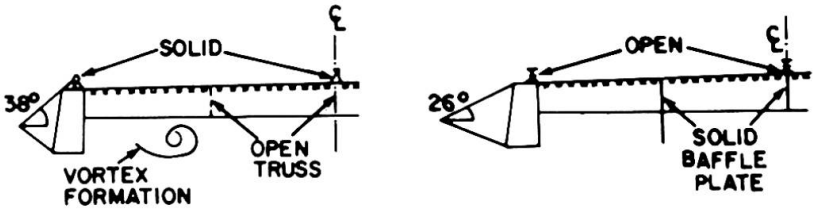

FIGURE 2 - DAMES POINT BRIDGE CROSS-SECTIONS

5. EXAMPLES OF THE EFFECTS OF WIND TURBULENCE

The importance of wind turbulence for aerodynamic stability was first brought to the fore by Davenport, Isyumov and Miyata [5] and then was strikingly illustrated on a 1:110 scale full aeroelastic model of Lions Gate Bridge, Vancouver [6]. Figure 3 shows the torsional response of the model which represented a modified version of this existing truss-stiffened bridge. Two experimental curves are shown, one for smooth wind and one for an accurately simulated natural wind with turbulence intensity $u'/U = 0.11$. It can be seen

that the torsional response in smooth wind exhibited a sudden flutter instability at a nondimensional wind speed of $U/(N_t b) = 6.5$, similar to that observed in smooth flow sectional tests [7], whereas in the turbulent wind the instability was not evident. Clearly, in this case the neglect of turbulence would have led to overly pessimistic results for the torsional stability.

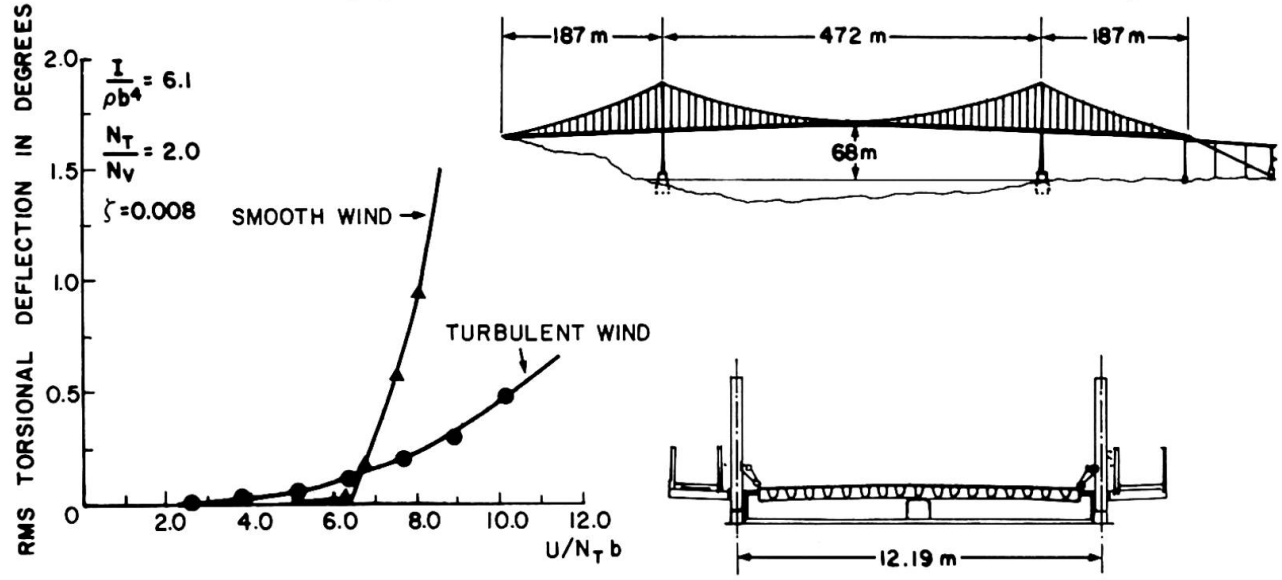

FIGURE 3 - EFFECT OF WIND TURBULENCE ON LIONS GATE BRIDGE

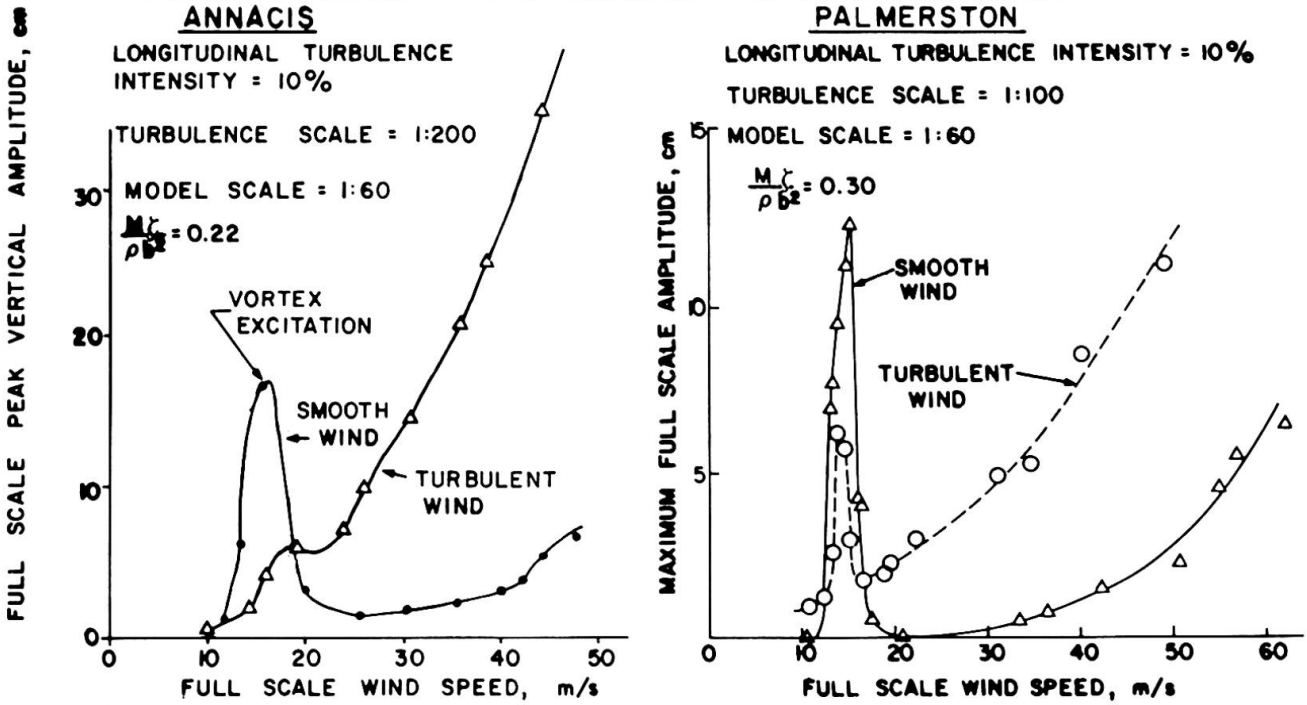

FIGURE 4 - EFFECT OF TURBULENCE ON VORTEX EXCITATION

Examples of the effect of turbulence on vortex induced vertical oscillations of models of the Palmerston girder bridge, Pugwash, Nova Scotia [8] and the Annacis Island bridge [1] are shown in Figure 4. The cross-section of the former bridge is shown in Figure 5. It is evident that turbulence has a significant mitigating effect on the vertical excitation of these decks. However, the Longs Creek bridge [9], which has a plate girder deck with similar overall dimensions to the Palmerston Bridge, is an example of serious vortex excitation actually occurring at full scale, indicating turbulence cannot be relied

upon to quell vortex excitation in all cases. One contributing factor for Longs Creek may well have been the light weight and low damping of the steel deck. Figure 5 includes additional results from the Palmerston Bridge tests where the effect of varying the mass damping parameter, $m\zeta/\rho b^2$, was investigated. It is clear that the effect of turbulence is far less pronounced for low mass damping parameters and the Longs Greek value of m / b^2 would not have provided a very significant alleviation of vortex-induced oscillations. It is worth noting that both these decks were significantly affected by the proximity of the water surface.

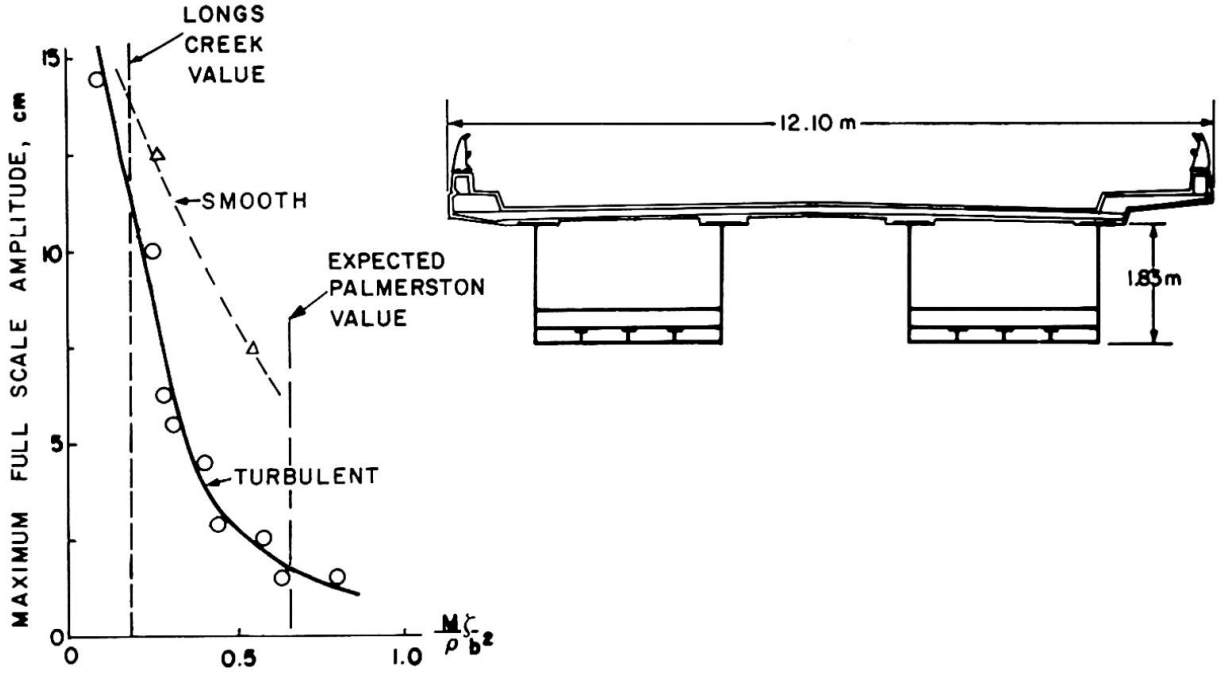

FIGURE 5 - PALMERSTON BRIDGE CROSS-SECTION AND EFFECT OF MASS-DAMPING PARAMETER

This section has discussed the effect of wind turbulence on stability. However, in high winds even a stable bridge is excited to large motions by the buffeting action of wind turbulence. Theoretical methods for computing the dynamic loads induced by buffeting are described in References 6 and 10. They involve a number of empirical assumptions and are therefore best used in conjunction with a wind tunnel investigation.

6. SIMILKAMEEN ORE CONVEYOR BRIDGE

Figure 6 illustrates this 396m span conveyor bridge. Sectional model tests [11] in smooth wind indicated that the bridge would experience vertical oscillations due to vortex excitation. These were eliminated on the model by cutting slots in the conveyor cover walls and removing short sections of the cover roof at line-stands as illustrated in Figure 6. The effect of various width wall slots on the response is shown in Figure 7. The ratio of open area to total cover area, as seen in elevation normal to the span, was 42% in the final configuration. The object of the cover was to prevent the conveyor belt being blown off its runners. It was verified in the tests that even with the openings in the cover it would still perform this function satisfactorily. An important factor for this structure was the large contribution to the overall oscillating mass that came from the cables and towers. This helped to reduce vertical oscillations and for torsional motion eliminated all forms of instability.

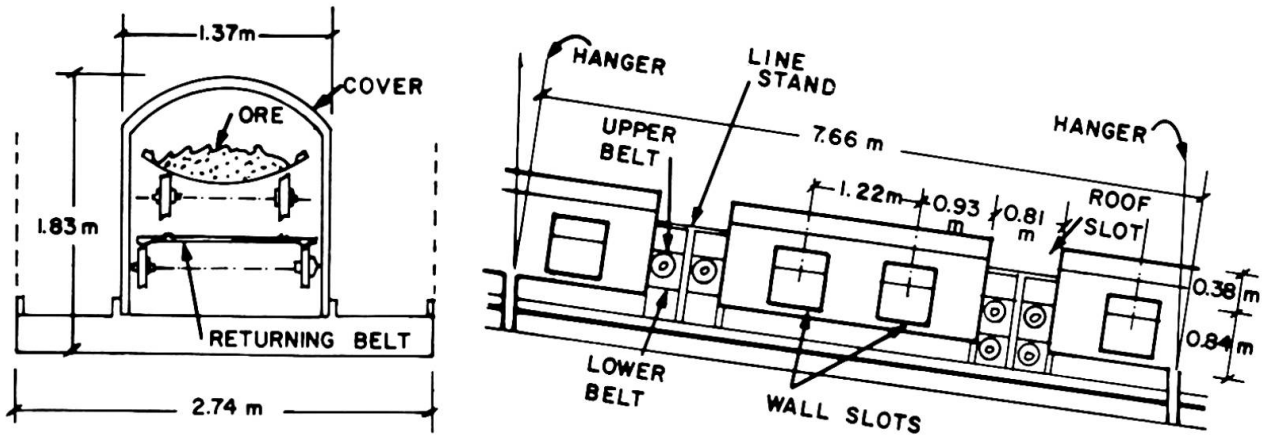

FIGURE 6 - 396m SIMILKAMEEN SUSPENDED ORE CONVEYOR BRIDGE

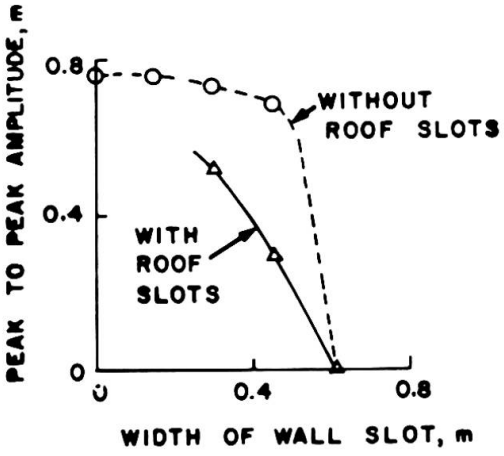

FIGURE 7 - EFFECT OF SLOTS ON SIMILKAMEEN BRIDGE

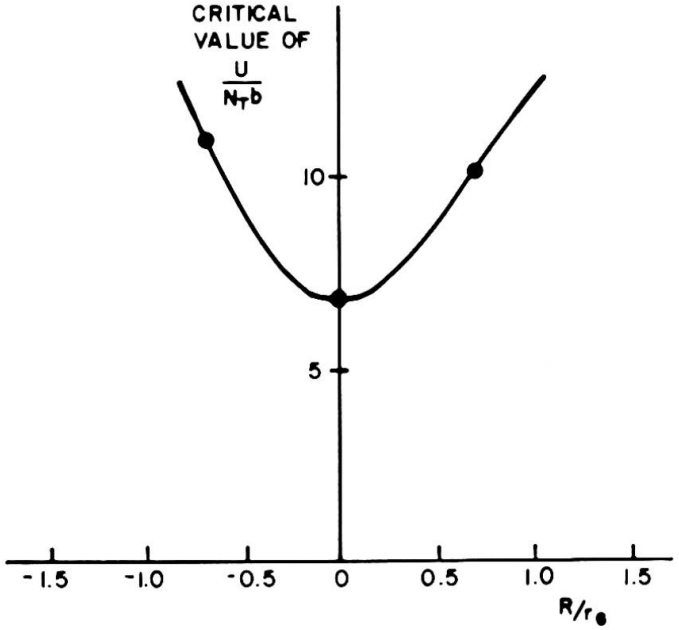

FIGURE 8 - CENTRE OF ROTATION EFFECT ON ON ORIGINAL LIONS GATE BRIDGE

7. EFFECT OF CENTRE OF ROTATION FOR TORSION

For bridges where the shear centre of the deck cross-section is substantially above or below the centre of mass the modes of vibration involving twist and horizontal motion normal to the span can no longer be classified as pure torsional or horizontal modes. Each mode involves simultaneous torsional and horizontal motions and this affects the aerodynamic stability. This type of motion can, however, be thought of as pure torsional motion, if the centre of rotation is taken to be an appropriate distance, r, above (or below) the deck centre of mass. Since r usually varies along the span, to simulate the centre of rotation effect on a sectional model it is necessary to select a representative single value for r which is denoted by R. Reference [11] gives an expression for calculating R. Figure 9 shows the effect of centre of rotation on the torsional instability of the original Lions' Gate Bridge [7, 12] in smooth wind. Since R/r_G was 1.05 for the first symmetric mode the critical wind speed can be seen in Figure 9 to be increased by 40% compared with $R/r_G = 0$. This illustrates how important the centre of rotation can be for some decks.

8. USE OF PART-SPAN FAIRINGS

Wind tunnel tests to develop fairings, an extensive topic in itself, have usually been done on sectional models (e.g. References 1, 3, 5, 7, 8, 9) which cannot be used to accurately assess the use of fairings on only part of the bridge length. However, in the full aeroelastic tests on Lions Gate Bridge [6] the use of part-span fairings was investigated. Figure 9 illustrates how fairings on only about one-eighth of total bridge length were very effective in eliminating torsional instability on one version of this bridge. The fairings were located on the centre section of the main span. Theoretical estimates [1] indicate that when fairings are used they need only be put along portions of the span where the amplitude is highest.

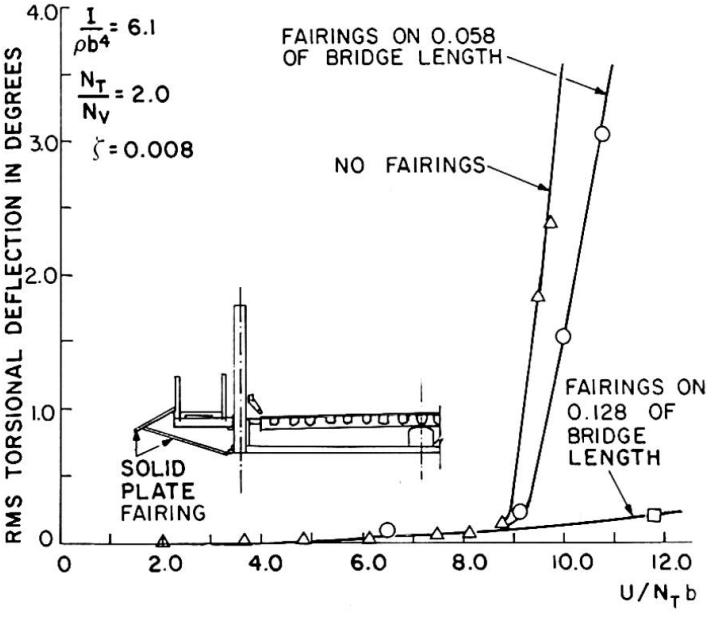

FIGURE 9 - EFFECT OF PART-SPAN FAIRINGS, LIONS GATE BRIDGE

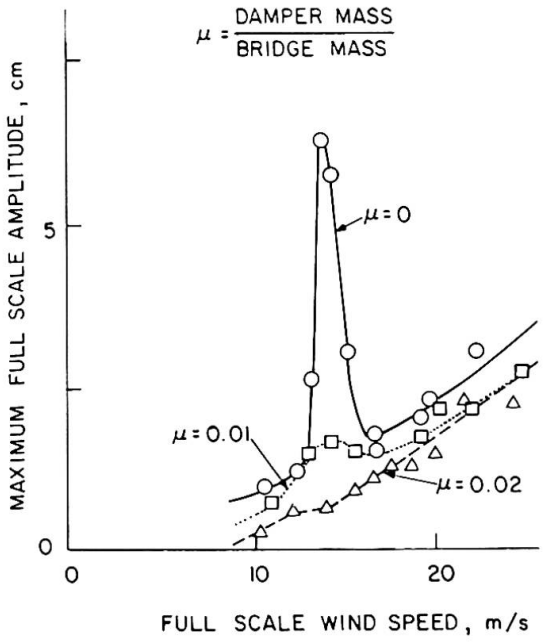

FIGURE 10 -EFFECT OF TUNED MASS DAMPER, PALMERSTON BRIDGE

9. EFFECTIVENESS OF TUNED MASS DAMPERS

A tuned mass damper consists of a damped mass spring system with a natural frequency nearly equal to that of mode of vibration it is desired to damp. The ratio of damper mass to bridge mass is denoted here by μ . Figure 10 shows the great effectiveness of a tuned mass damper in quelling vortex excitation on the Palmerston Bridge model [8] in turbulent wind.

10. CONCLUSION

The foregoing observations illustrate some of the many factors that affect a bridge's aerodynamic stability. It is important to consider the likely effects of as many of these factors as possible since any one of them may emerge as dominant for a particular bridge.

Acknowledgements

There would not be space to acknowledge individually all the numerous contributions from others in the various wind tunnel investigations. These came from the bridge authorities, the structural engineers, co-authors and

other colleagues. However, the author particularly benefited from discussions with R. L. Wardlaw while at the National Research Council. Also, many valuable inputs came from P.G. Buckland and P. R. Taylor of Buckland and Taylor Ltd. during the investigations for the Lions Gate, Similkameen and Annacis Island bridges.

References

1) IRWIN, P.A. and SCHUYLER, G.D. "Wind Tunnel Tests on the proposed Annacis Island Bridge", Morrison Hershfield Limited Reports 4821961, 48215021, 48318091, 4841501; 1983-1984.

2) TAYLOR, P.R. "Evolution of a Hybrid Design for the World's Longest Cable-Stayed Bridge", IABSE Congress, Vancouver, 1984.

3) IRWIN, P.A., SAVAGE, M.G. and WARDLAW, R.L. "A Wind Tunnel Investigation of a Steel Design for the St. Johns River Bridge, Jacksonville, Florida", National Research Council, NAE Report LTR-LA-220, 1978.

4) IRWIN, P.A. and SCHUYLER, G.D. "Wind Tunnel Tests of the 1000 Island Bridge American Crossing", Morrison Hershfield Limited Report 48315011, 1983.

5) DAVENPORT, A.G. ISYUMOV, N. and MIYATA, T. "The Experimental Determination of the Response of Suspension Bridges to Turbulent Wind", Proc. 3rd Int. Conf. on Wind Effects on Buildings and Structures, p.1207, 1971.

6) IRWIN, P.A. and SCHUYLER, G.D. "Wind Effects on a Full Aeroelastic Bridge Model" ASCE Spring Convention, 1978, Pittsburgh, preprint 3628. (National Research Council, NAE Reports LTR-LA-206 and LTR-LA-210).

7) IRWIN, P.A. and WARDLAW, R.L. "Sectional Model Experiments on Lions' Gate Bridge, Vancouver", National Research Council, NAE Report LTR-LA-205, 1975.

8) IRWIN, P.A., DUFFY, K. and SAVAGE, M.G. "Wind Tunnel Investigation of the Palmerston Bridge, Pugwash, Nova Scotia", National Research Council, NAE Report LTR-LA-244, 1980.

9) WARDLAW, R.L. and GOETTLER, L.L. "A Wind Tunnel Study of Modifications to Improve the Aerodynamic Stability of the Longs Creek Bridge", National Research Council, NAE Report LTR-LA-8, 1968.

10) DAVENPORT, A.G. "Buffeting of a Suspension Bridge by Storm Winds", Proceedings of the ASCE, Journal of Structural Division, p.223, 1962.

11) IRWIN, P.A. and SAVAGE, M.G. "Investigation of Wind Effects on a Suspended Ore Conveyor, Similkameen River, British Columbia", National Research Council, NAE Report LTR-LA-232, 1979.

12) IRWIN, P.A. "Centre of Rotation for Torsional Vibration of Bridges", Journal of Industrial Aerodynamics, 4, pp. 123-132, 1979.

Torsional Flutter of a Suspension Bridge

Effets de la turbulence du vent sur les vibrations de torsion dans les ponts suspendus

Torsionflattern von Hängebrücken

Manabu ITO
Professor, Dr. Eng.
University of Tokyo
Tokyo, Japan

Manabu Ito graduated in 1953, and received his Dr. Eng. degree in 1959, from the University of Tokyo. He has been engaged in teaching and research on bridge engineering and structural dynamics at the same university, and is now Professor of Civil Engineering.

Hiroki YAMAGUCHI
Lecturer, Dr. Eng.
Saitama University
Urawa, Japan

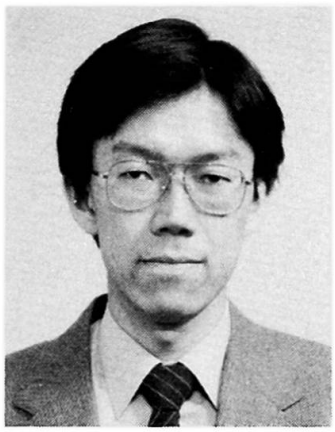

Hiroki Yamaguchi got his bachelor degree from Saitama University in 1975, and Dr. Eng. degree from the University of Tokyo in 1980. Starting his teaching career at the University of Tokyo, he is now engaged in teaching and research on structural mechanics at Saitama University.

SUMMARY

The effects of two types of phenomena existing under strong wind on the torsional flutter of a suspension bridge are discussed; one is the effects of wind-induced deformation of the structure, and another is those of the limited-amplitude cross-wind oscillation due to, for instance, vertical component of turbulent air flow. With the aid of sectional model experiment in a wind tunnel, it was found that the both effects mentioned above might raise the critical flutter speed to some extent.

RESUME

Cet article décrit les deux causes des vibrations torsionnelles des ponts suspendus sous l'effet de vents violents. L'une est due à la déformation de la structure créée par le vent et l'autre aux turbulences. Ce fait a été mis en évidence en soufflerie par des essais sur modèle.

ZUSAMMENFASSUNG

Zwei Arten von Erscheinungen, die bei starkem Wind auf das Torsionsflattern von Hängebrücken einwirken, werden diskutiert: der Einfluss von windinduzierten Verformungen des Tragwerkes und die beschränkte Amplitude von Querwindschwingungen, bedingt z.B. durch die lotrechte Komponente der turbulenten Windströmung. Mit Hilfe von Modellversuchen im Windkanal wurde festgestellt, dass beide genannten Einflüsse die kritische Flattergeschwindigkeit zu erhöhen vermögen.

1. INTRODUCTION

Self-excited vibrations of very flexible structures subject to wind, if occurred, are most catastrophic. Although various investigations concerned have been conducted since the well-known collapse of the old Tacoma Narrows Bridge, more realistic considerations seem to be needed to achieve the rational design of these structures.

This contribution deals with the effects of two types of phenomena existing under the action of strong wind on the torsional flutter of a suspension bridge; one is the effects of wind-induced deformation of the structure, and another is those of the limited-amplitude cross-wind oscillation due to, for instance, vertical component of turbulent air flow. The torsional flutter dominates often the design of a long-span suspension bridge, the stiffening frame of which is a truss with closed deck or a relatively shallow plate girder type.

2. EFFECTS OF WIND-INDUCED DEFORMATION

2.1 Coupled Free Oscillations

The dynamic characteristics of a long-span suspension bridge under strong wind will be more or less different from those at unloaded state, because the structure is so flexible as to cause considerable deformations due to wind pressure (Fig. 1). Fig. 2 shows an example of the first torsion-dominant vibration mode of a suspension bridge subject to very strong wind. It is found that the torsional component and the corresponding natural frequency under wind loading are not so much different from those at unloaded state, whereas the coupling between torsional, lateral and vertical components tends to be introduced by the static deformations due to wind force.

These coupled oscillations are associated with the rotational motion about a certain axis shown in Fig. 3. This centre of rotation locates at the point shifting from the shear centre of the bridge deck cross section as seen in the same figure. Fig. 4 shows the range of possible position of the centre of rotation, S_V and S_H, versus the maximum lateral displacement in the centre span of the bridge. Here we can find that the horizontal shift of rotation centre increases almost linearly with increasing lateral deflection while vertical shift changes slightly. It was also observed that the equivalent polar moment of inertia, that is the generalized mass for torsional mode, increased notably with increasing lateral deflection of the bridge.

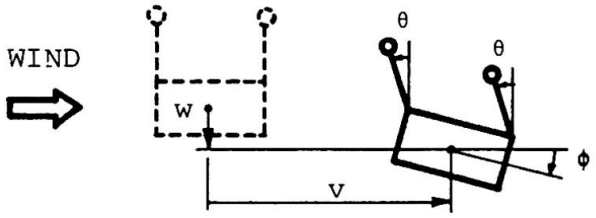

Fig. 1 Static deformation due to strong wind

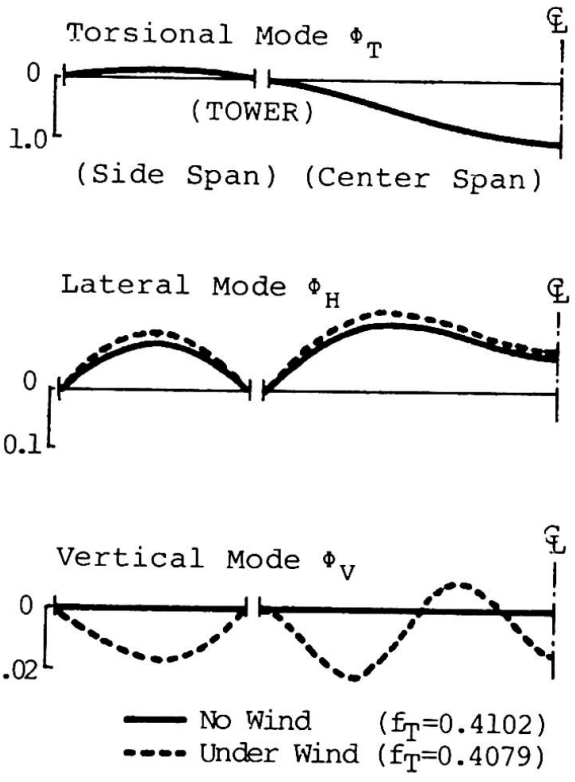

Fig. 2 Coupling in the first torsional mode of vibration

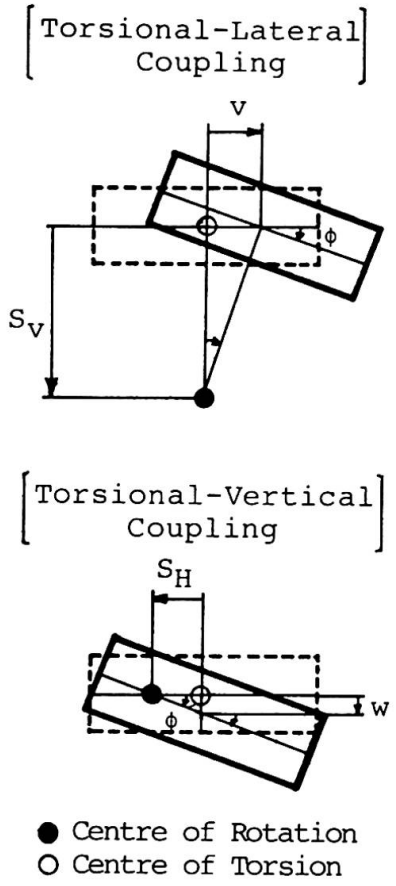

Fig. 3 Centre of rotation in coupled motion

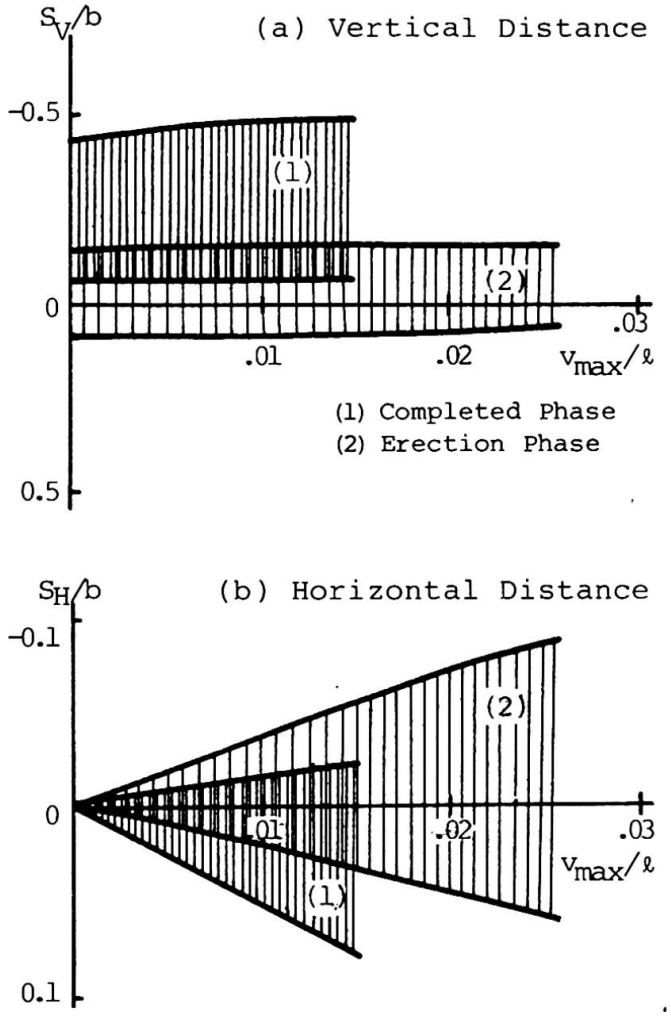

Fig. 4 Position of centre of rotation under static deformation

2.2 Critical Wind Speed for Torsional Flutter

As found in the preceding section, when a flexible suspension bridge deforms due to wind force, its dynamic characteristics change from those at unloaded state. In consequence the aerodynamic stability of the structure may also change to some extent. In order to verify these situation, utilizing the analytical results for static deformation and coupled vibration modes, the aeroelastic wind tunnel test with the sectional model of a truss-stiffened suspension bridge was conducted in a smooth air flow. The prototype bridge has a main span length of about 800m and the structural damping was set at $\delta_s = 0.01$ in logarithmic decrement.

Fig. 5 (a) and (b) show the relation between the reduced wind speed $U_r = U/f_T B$ and the double amplitude in torsion for different values of vertical and horizontal shift, respectively, of centre of rotation, where U is wind speed, f_T is the natural frequency of torsion, and B is the width of bridge deck. These experimental results indicate that the vertical shift of centre of rotation gives no significant effect on the aerodynamic stability of the structure. This agrees with the past experiences conducted elsewhere [1], [2]. On the other hand, the critical wind speed for flutter is clearly increased with the horizontal shift of centre of rotation which may be accompanied by lateral deformation of the structure. As also seen in Fig. 5(b), the slope of response curve becomes more gentle as the centre of roration moves away from the centre of section to upstream side ($S_H/B > 0$), and vice versa.

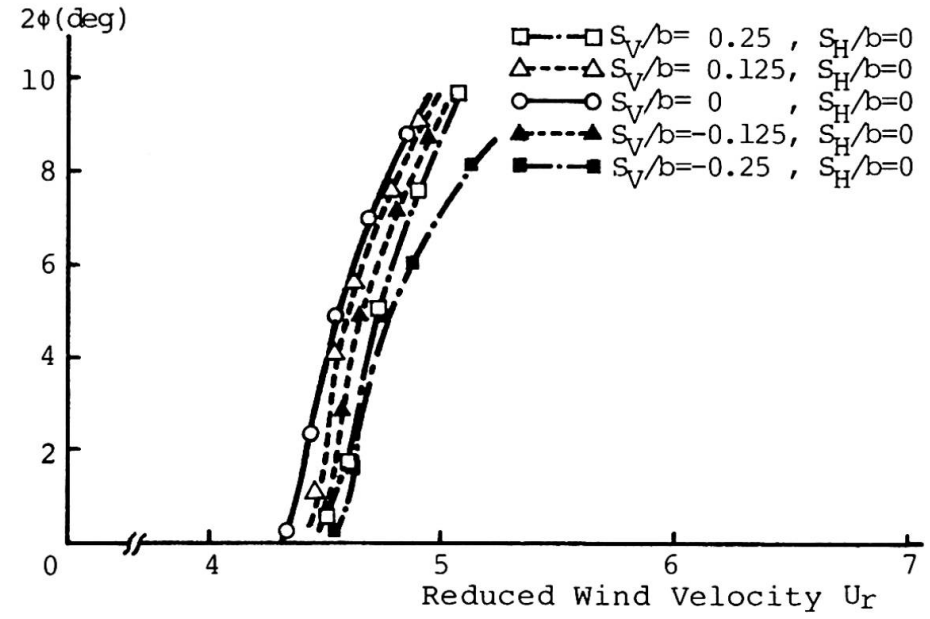

(a) Effect of vertical shift

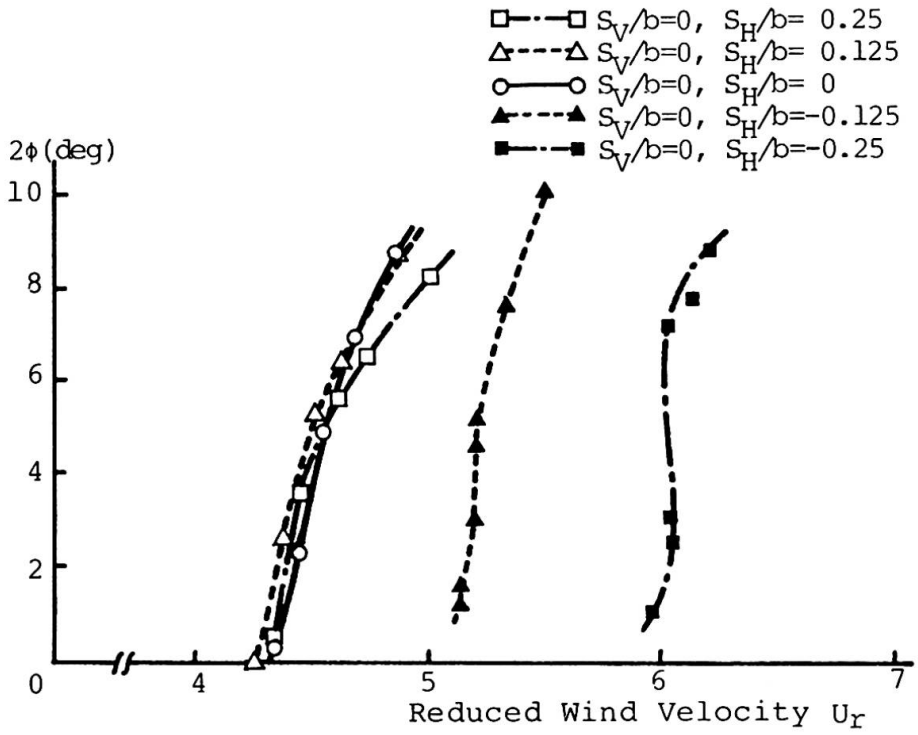

(b) Effect of horizontal shift

Fig. 5 Effects of position of centre of rotation on flutter response

Fig. 6 illustrates the critical reduced velocities for flutter for different structural damping. In the case of small damping, the critical velocity changes slightly when the centre of rotation moves forward, while it is substantially increased when the centre of rotation moves backward. With large structural damping, however, the increase of critical velocity is achieved by the horizontal shift of rotation centre irrespectively of its direction.

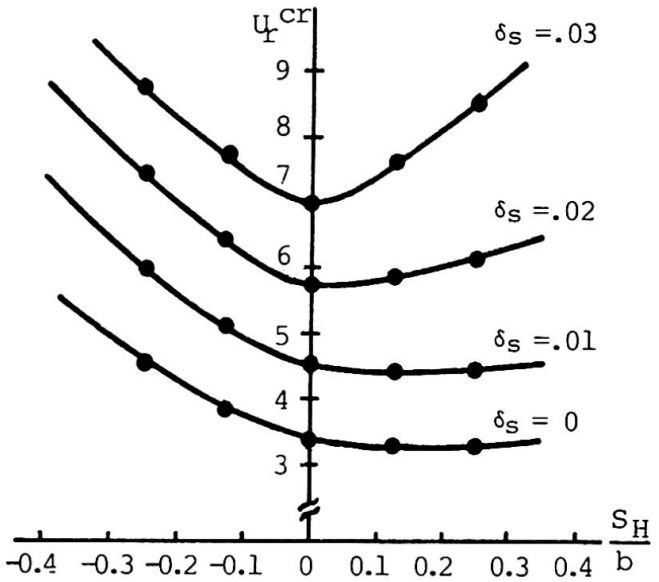

Fig. 6 Critical flutter speed vs. horizontal shift of centre of rotation

3. EFFECTS OF CROSS-WIND MOTION

The second aspect of the present contribution is the effect of the limited-amplitude oscillations, such as turbulence or vortex excitation, on the torsional flutter of a suspension bridge. For the sake of simplicity, given one-mode vertical oscillation of constant amplitude and specified natural frequency, the sectional model tests in the wind tunnel were carried out. The configuration of the bridge deck model was intentionally selected to cause torsional flutter. The experiment was conducted in a smooth air flow. Thus the vertical forced oscillation and the torsional flutter were dealt with independently.

Expressing the unsteady aerodynamic moment M as

$$M = \frac{1}{2} \rho U^2 B^2 (C_{MR} + i\, C_{MI}) \frac{\phi}{\phi_0}$$

Fig. 7 and 8 show the aerodynamic coefficient C_{MI}, which exerts the aerodynamic damping effect on the structure and was obtained from the sectional model test. In the above equation, ρ is the air density, B is the width of bridge deck, $\phi = \phi_0 \exp(i \cdot 2\pi f t)$ is the torsional displacement and $i = \sqrt{-1}$.

Fig. 7 demonstrates that the existence of the vertical oscillation gives little influence on the negative aerodynamic damping in the region $U_r > 5$, while it clearly affects on the aerodynamic characteristics at U_r = 3-4, where the aerodynamic damping turns from positive to negative. This latter effect decreases as the amplitudes of torsional flutter become large. It might be observed that the existence of vertical oscillation tends to weaken the nonlinearity of unsteady aerodynamic force with respect to amplitude.

In order to know the effects of cross-wind motion more thoroughly, the results for the torsional amplitude $2\phi_0 = 3^0$ were rearranged in Fig. 8 (a) and (b) which illustrate the influence of the amplitude and frequency of vertical oscillation, respectively. From these figures, it is found that the critical wind speed for torsional flutter is generally raised with the increase of both the amplitude and the frequency of vertical oscillation.

Finally the effect of vertical oscillation modes on the torsional flutter response will be discussed. The response was numerically estimated by applying the unsteady aerodynamic force obtained above to the three-dimensional structure which oscillates vertically. The applicability of strip theory is presupposed here and the structural damping was assumed as $\delta s = 0.03$ in logarithmic decrement. The results are shown in Fig. 9. Again it is observed that the existence of cross-wind oscillation tends to augment the critical wind speed for torsional flutter and this trend is more marked, with some exception, in the

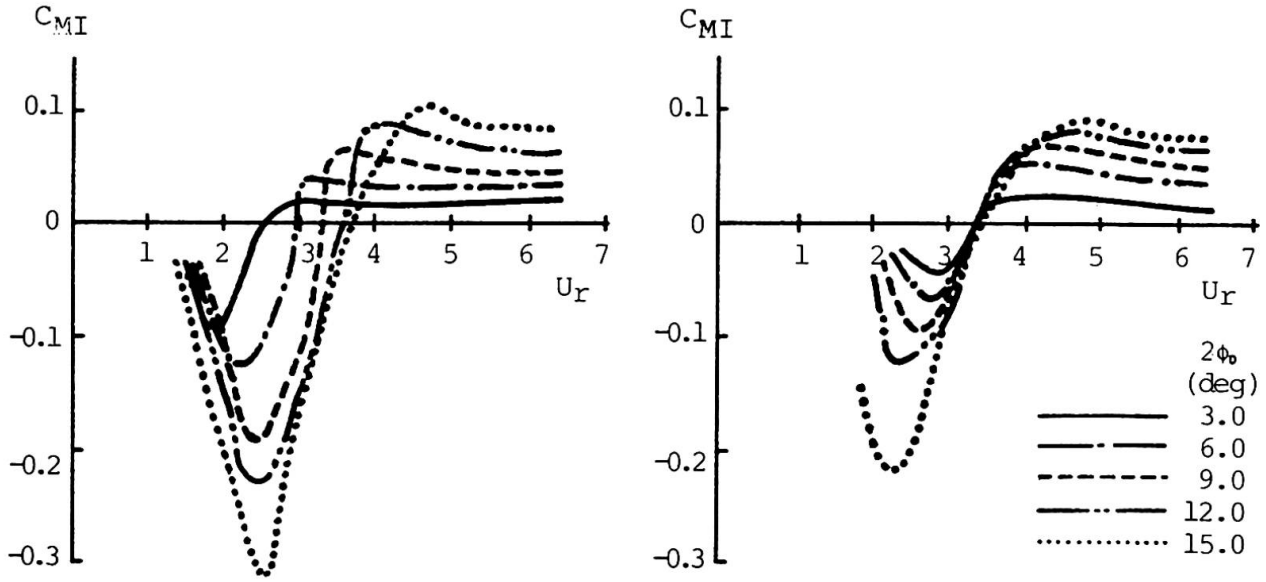

(a) Without vertical motion

(b) Under vertical motion (f_V/f_T = 1.12, $2h_0/B$ = 0.105)

Fig. 7 Unsteady aerodynamic coefficient C_{MI}

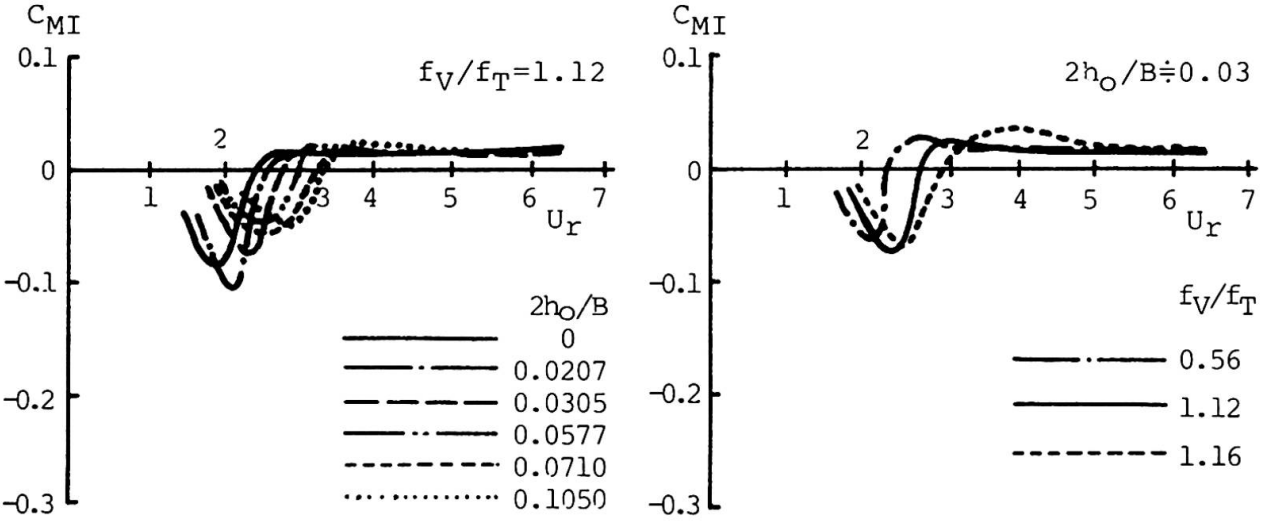

(a) Effect of amplitude (f_V/f_T = 1.12)

(b) Effect of frequency ratio ($2h_0/B$ = 0.03)

Fig. 8 Effects of vertical motion on C_{MI} at $2\phi_0$ = 3°

case of higher modes of vertical oscillations. Once the flutter occurs, however, the development of flutter response is more rapid in general when the vertical oscillation exists.

4. CONCLUSIONS

When a flexible suspension bridge is deformed by wind force, the coupling between vertical, lateral and torsional displacement component in its oscillatory behaviour is more pronounced. This coupling leads to the horizontal shift of rotation centre, and in its consequence, the critical wind speed for torsional flutter increases to some extent.

The existence of limited-amplitude oscillation of vertical bending may also

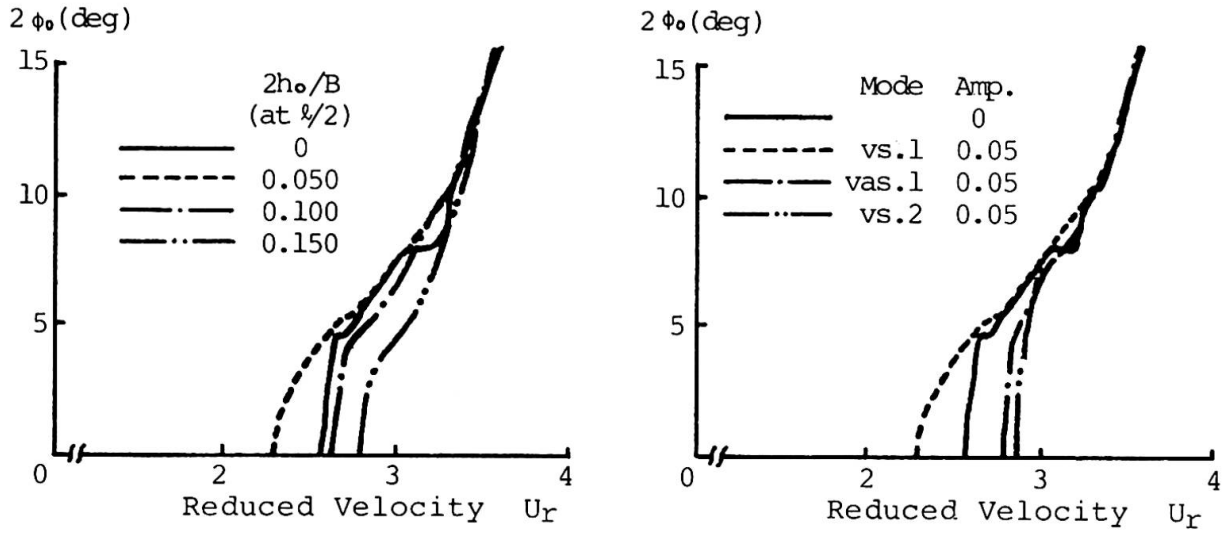

(a) Effect of amplitude: 1st symmetric mode of vertical oscillation

(b) Effect of mode of vertical oscillation

Fig. 9 Effects of vertical motion on flutter response

augment the critical wind speed for torsional flutter of a suspension bridge. However, this effect seems not so remarkable in practical sense, whereas the development of flutter response in the range beyond the critical wind speed becomes more abrupt. Therefore, it will be unable to be concluded that the coexistent cross-wind motion, such as due to air turbulence, may improve the torsional instability. If the effect of buffeting on aerodynamic instabilities of a structure is to be studied more realistically, the effect of air turbulence on aerodynamic force and the unsteadiness of buffeting response should be taken into account.

NOTATIONS

b : half width of bridge deck
B : width of bridge deck (=2b)
C_{MR}: real part of aerodynamic moment coefficient
C_{MI}: imaginary part of aerodynamic moment coefficient
f_T : natural frequency of torsional vibration
f_V : frequency of vertical bending vibration
h_0 : amplitude of vertical bending vibration
i : unit of imaginary number
l : span length
M : unsteady aerodynamic moment
t : time
U : wind velocity
U_r : reduced wind velocity
δ_s : structural damping in logarithmic decrement
ρ : air density
ϕ : torsional displacement
ϕ_0 : amplitude of torsional vibration

ACKNOWLEDGMENTS

The analytical and experimental works reported in this paper were supported by the Grant in Aid for Scientific Research, Ministry of Education, Japan. The authors also wish to acknowledge the collaboration of Messrs. H. Yokoyama and T.

Shimizu, formerly graduate students at the University of Tokyo, during the course of the present investigation.

REFERENCES

1. Irwin, H.P.A.H.: Centre of rotation for torsional vibration of bridges, Jour. Industrial Aerodynamics, Vol. 4, No. 2, March 1979.
2. Honshu-Shikoku Bridge Authority: Report of wind tunnel tests on construction of In-noshima Bridge (in Japanese), Oct. 1981.

Dynamic Wind Forces on Long Span Bridges

Effets dynamiques du vent sur les ponts de grande portée

Dynamische Windlasten auf weitgespannte Brücken

A.G. DAVENPORT
University of Western Ontario
London, ON, Canada

Alan Davenport, obtained his B.A. and M.A. from Cambridge University England in 1954 and 1958. In 1957 he received his M.A. Sc. from the University of Toronto and a Ph. D. from the University of Bristol in 1961. He is a Professor in Civil Engineering and the Director of the Boundary Layer Wind Tunnel Laboratory. He has advised on the construction and design of a number of long span bridges and structures.

J.P.C. KING
University of Western Ontario
London, ON, Canada

Peter King got his Civil Engineering degree in 1973 from the University of Western Ontario and his Masters from the same institution in 1978 following three years of practice in the field of bridge engineering. He is completing his Ph.D. and is currently on staff at the Boundary Layer Wind Tunnel Laboratory.

SUMMARY

This paper describes a method for defining static wind loads acting on a long span bridge equivalent to the important dynamic motions due to gust buffeting and wake excitation, as well as the influence of the aeroelastic stability characteristics of the deck. The new approach makes use of the results of wind tunnel experiments in a turbulent airstream on dynamically mounted section models and uses theory to adjust these results to the conditions of full scale.

RESUME

Une méthode est proposée pour déterminer les charges statiques du vent sur un pont de grande portée, équivalentes aux effets dynamiques et aux mouvements dus à des coups de vent, et tenant compte des caractéristiques aéroélastiques du tablier. Cette nouvelle méthode tient compte des résultats d'essais en soufflerie, avec des turbulences, sur des modèles soumis à des charges dynamiques et fait appel à la théorie pour ajuster les résultats aux conditions réelles.

ZUSAMMENFASSUNG

Dieser Beitrag beschreibt eine Methode zur Bestimmung von statischen Ersatzlasten auf weitgespannte Brücken, aequivalent den dynamischen Beanspruchungen durch Windstösse und durch Anregung durch Luftturbulenzen. Ferner beschreibt er den Einfluss der Charakteristik der aero-elastischen Stabilität des Brückendecks. Die neue Näherung resultiert aus Experimenten im Windtunnel mit turbulenten Luftströmen an dynamisch gelagerten Querschnittsmodellen, unter Anwendung einer Theorie zur Angleichung dieser Resultate an die Verhältnisse der Gesamtstruktur.

1. INTRODUCTION

The conventional treatment of wind loading on long span bridges has tended to consider the static design wind loading used in normal strength design, and the aerodynamic stability as two separate and distinct aspects. The procedure described in this paper takes a more unified approach. It depends on the measurement of the dynamic response of section models to grid turbulence rather than smooth flow. The response is corrected for discrepancies in the intensity and spectrum of turbulence, the damping, and the joint acceptance function for the mode shape. A small correction is also added for the deficiency in low frequency excitation from grid turbulence. The design loads are found from the estimates of dynamic motion in the lowest symmetric and asymmetric modes a well as the mean load. This approach is an outgrowth of earlier studies in turbulent flow on the Murray MacKay Bridge (1), the Bronx-Whitestone Bridge (2), and Sunshine Skyway Bridge (3).

2. THE DESCRIPTION OF DESIGN LOADS

The persistent movements of any long span bridge (4,5) in strong wind are organized through its various mode shapes - horizontal, vertical and torsional. They cover a range of frequencies but take place mostly at or near the natural frequencies of the individual modes and have a random character due to the continual shifts in phase and amplitude.

To summarize the variety of load actions which the dynamic movements will produce in a severe wind storm, a wind load description for design has been proposed as in Fig. 1.

$$W_x(\eta) = \overline{W}_x \bar{\alpha}(\eta) \pm \gamma \tilde{W}_{1_x} \alpha_1(\eta) \pm \gamma \tilde{W}_{2_x} \alpha_2(\eta) \qquad (1a)$$

$$W_z(\eta) = \overline{W}_z \bar{\alpha}(\eta) \pm \gamma \tilde{W}_{1_z} \alpha_1(\eta) \pm \gamma \tilde{W}_{2_z} \alpha_2(\eta) \qquad (1b)$$

$$W_\theta(\theta) = \overline{W}_\theta \bar{\alpha}(\eta) \pm \gamma \tilde{W}_{1_\theta} \alpha_1(\eta) \pm \gamma \tilde{W}_{2_\theta} \alpha_2(\eta) \qquad (1c)$$

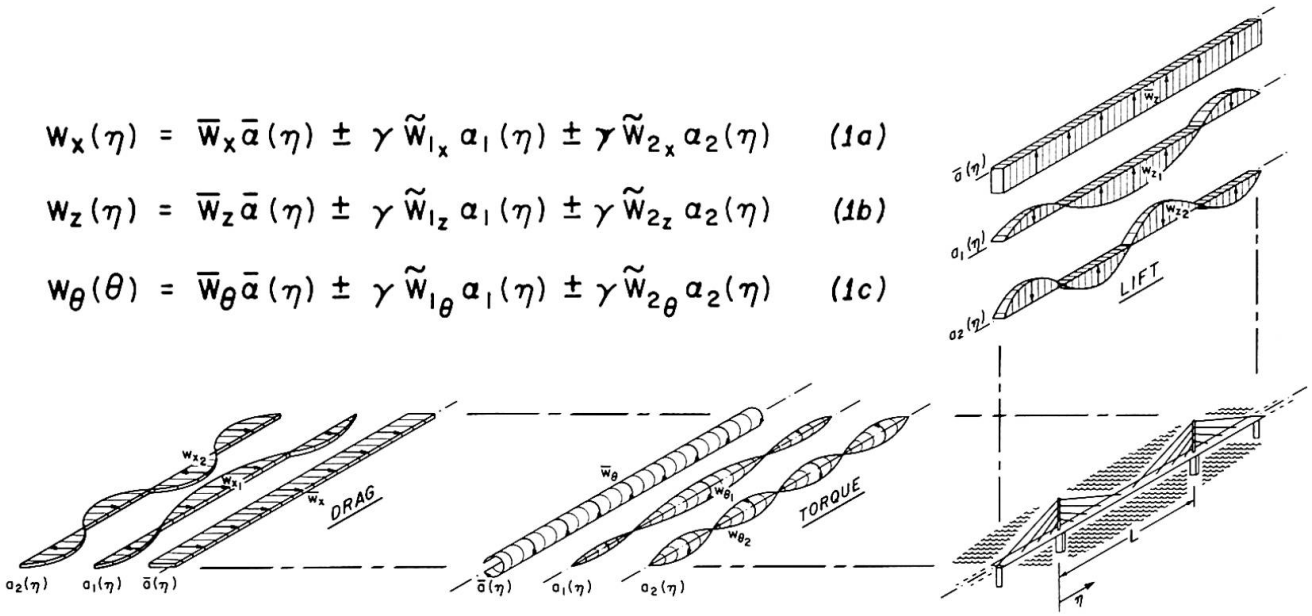

Fig. 1 Distributed Wind Load Components

In this x, z and θ denote the horizontal (downwind), vertical (upward) and torsional (nose-up) components; (see Fig. 2); $\overline{W}$, $\tilde{W}_1$ and $\tilde{W}_2$ are the mean, symmetric and antisymmetric load components per unit length of deck; $\bar{\alpha}(\eta)$, $\alpha_1(\eta)$ and $\alpha_2(\eta)$ are the mean and modal load distribution functions; γ_1 and γ_2 are statistical load combination factors and take on values $\pm$ 1.0 if only one modal term is included; $\pm$ 0.8 for two terms; $\pm$ 0.7 for three terms and $\pm$ 0.6 for four or more terms.

The description of the mean time average wind load components produced by the mean wind is straightforward. They are defined through the force coefficients $C_x(a)$, $C_z(a)$ and $C_\theta(a)$ which may be measured for a range of angles of attack a, the deck width B, and the mean reference velocity pressure at deck height H, $q_H = \frac{1}{2}\rho U_H^2$. The three mean forces per unit length are then:

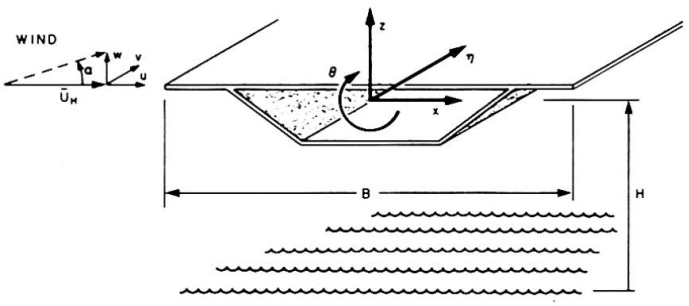

Fig. 2 Notation

$$\overline{W}_x = q_H B C_x(0); \quad \overline{W}_z = q_H B C_z(0); \quad \overline{W}_\theta = q_H B^2 C_\theta(0) \qquad (2)$$

Two points should be made. First the coefficients in turbulent flow may differ from those in smooth flow. Second, normally only horizontal mean winds need to be considered. Only in steep mountainous valleys is there likely to be any appreciable inclination to the mean flow.

3. EVALUATION OF THE MODAL LOAD COMPONENTS W_1 AND W_2

Although the response of a suspension bridge deck has been represented by coupled vertical and torsional equations of motion (6,7), in fact the aerodynamic coupling terms are usually negligible, and the aerodynamic stiffness terms are usually small in comparison to the stiffness of the bridge itself. This leaves the aerodynamic damping as the most significant aerodynamic force induced by motion. If this is negative and numerically greater than the structural damping, large motion will result. The response of each uncoupled mode of vibration to the turbulent wind can be studied separately and superimposed at the end; usually, only the lowest modes are significant.

We can represent the peak modal load amplitude by the following: -

$$W = g\sqrt{\sigma^2 W_b + \sigma^2 W_r} \qquad (3)$$

where g is a statistical peak factor, $\sigma^2 W_b$ is the mean square background excitation acting quasi-statically, and $\sigma^2 W_r$ is the mean square excitation at or near the resonant frequency.

The two components of the excitation can be identified in the typical power spectrum shown in Fig. 3. The background excitation covers a broad frequency band below the natural frequency; the resonant excitation is concentrated in a peak at the natural frequency, the height of which is controlled by the damping. The two components can be estimated from the following expressions:

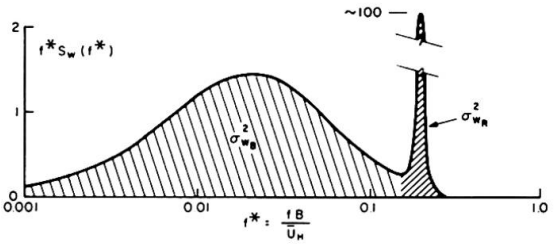

Fig. 3 Spectrum of Modal Load Amplitude

$$\sigma^2 W_{b_{x,z,\theta}} = \int_0^\infty f^* S_{F_{x,z,\theta}}(f^*) \cdot |J_{x,z,\theta}(f^*)|^2 \cdot d(\ln f^*) \qquad (4a)$$

$$\sigma^2 W_{r_{x,z,\theta}} = \frac{(\pi/4)}{(\zeta_s + \zeta_a(f^*_o))} \cdot f^*_o S_{F_{x,z,\theta}}(f^*_o) \cdot |J_{x,z,\theta}(f^*_o)|^2 \qquad (4b)$$

In the above the subscripts x, z, θ imply the equations are written for each variable in turn; f^* and $f_o{}^*$ are the reduced frequencies fB/U_H and $f_o B/U_H$; ζ_s and $\zeta_a(f^*)$ are the structural damping and aerodynamic damping at frequency f^*; $f^* S_{F_{x,z,\theta}}(f^*)$ is the power spectral density of the externally induced x,z,θ components on a cross-section of the bridge deck at the reduced frequency f^*; $|J_{x,z,\theta}(f^*)|^2$ is the "joint acceptance function", relating the generalized modal force component with the mode shape and the force components at frequency f^* at cross-sections of the bridge and involves the spanwise correlation of the forces.

The external forces on a bridge cross-section arise from either the direct action of turbulence in the wind or through the action of flow fluctuations in the wake. The latter are commonly described as vortex shedding. We can write:

$$f^* S_F(f^*) = (f^* S_F(f^*))_{turb} + (f^* S_F(f^*))_{wake} \tag{5}$$

The turbulent term can be written

$$(f^* S_F(f^*))_{turb} = (q_H B)^2 \cdot (C^2_{x,z,\theta} \; |A(f^*)|^2) \cdot (f^* S_{u,v,w,}(f^*)) \tag{6}$$

where $f^* S_{u,v,w}(f^*)$ = the power spectra of the turbulent velocity fluctuations u, v and w;

$A(f^*)$ = "aerodynamic admittance" which translates the turbulent fluctuations into forces on a cross-section; and

$C_{x,z,\theta}$ = a reference aerodynamic coefficient.

The contributions of the turbulence to the expressions for $\sigma^2 W_b$ and $\sigma^2 W_r$ can be written as follows. To simplify the notation we will consider the lift (z) force and only include the vertical (w) component of turbulence, which normally will dominate.

$$(\sigma^2 W_{b_z}) = (q_H B C'_z)^2 \left(\frac{\sigma_w}{U_H}\right)^2 \int_o^\infty \frac{f^* S_w(f^*)}{\sigma^2_w} |A_z(f^*)|^2 |J_z(f^*)|^2 d \ln f^* \tag{7}$$

$$(\sigma^2 W_{r_z}) = (q_H B C'_z)^2 \left(\frac{\sigma_w}{U_H}\right)^2 \frac{f^*_o S_w(f^*_o)}{\sigma^2_w} |A_z(f^*)|^2 |J_z(f^*_o)|^2 \cdot \frac{(\pi/4)}{(\zeta_s + \zeta_a(f^*_o))} \tag{8}$$

The coefficient C'_z denotes $(\partial C_z/\partial_\alpha)$. Similar expressions for the torsion can be written with θ replacing z and introducing an additional factor B^2. For the drag direction $2 C_x$ replaces C'_z and u replaces w.

If the left hand terms are normalized by the $(q_H B C'_z)^2$ term the response is a function primarily of the reduced frequency f^* and the intensity of turbulence (σ_w/U_H), two homologous quantities which link the full-scale bridge behaviour with any dynamically scaled model. Otherwise the turbulence controlled response is bound up in the functional form of the turbulence spectrum, S_w, the aerodynamic admittance, A_z, the joint acceptance function, J_z, and the aerodynamic damping ζ_a.

The aerodynamic admittance reflects the efficiency of the bridge deck as a lift generator, as well as the correlation of the flow in the vicinity of the deck. The theoretical and observed form of this function is shown in Fig. 8. The joint acceptance function can be written

$$|J(f^*)|^2 = \int_0^L \int_0^L R_{F_1 F_2}(\eta_1, \eta_2; f^*)\ \mu(\eta_1)\,\mu(\eta_2)\, d\eta_1\, d\eta_2 \qquad (9)$$

where $\mu(\eta)$ = mode shape with unit mean square amplitude; and

$$R_{F_1 F_2}(\eta_1, \eta_2; f^*) = \exp\left(-c f^* \frac{L}{B} \frac{|\eta_1 - \eta_2|}{L}\right) \qquad (10)$$

in which c is a constant which defines the effective width of the correlation. A similar expression can be written for the spanwise cross-correlation of the velocity component in which case $c \simeq 8$ is representative. It is reasonable to assume the same value holds for the forces F_1 and F_2 on the basis of the "strip assumption".

Equations (7) and (8) apply to both the full scale bridge and a model in a turbulent wind tunnel flow. Ideally the latter should be an exact scaling of the former. This ideal, however, is difficult to satisfy in the wind tunnel and some compromises may have to be made. There are significant advantages to using an elongated section model in a turbulent flow generated behind a coarse grid. Although the turbulence scale and intensity cannot be made to exactly correspond to full scale, the values can be made sufficiently close.

To adapt the results of the dynamic section model testing to full scale, corrections need to be applied as follows: (a) Corrections of the low frequency quasi-static, "background", response, $\sigma^2_{W_b}$, largely omitted from the section model due to the deficit in the vertical velocity spectrum generated by the grid. This can be estimated with reasonable accuracy from equation (7) using either theoretical or experimental data as outlined below. (b) Correction of the terms in the resonant response $\sigma^2_{W_r}$ for the discrepancies in the turbulent intensity, vertical velocity spectrum, joint acceptance function and damping. No correction is needed in the aerodynamic admittance. The following formula encompasses these corrections:

$$(\sigma^2_{W_r})_{full\ scale} = (\sigma^2_{W_r})_{model}\ \phi_{\sigma_w}\, \phi_{S_w}\, \phi_J\, \phi_\zeta \qquad (11)$$

where the terms ϕ_{σ_w}, ϕ_{S_w}, ϕ_J and ϕ_ζ reflect corrections to the terms in the response due to the discrepancies between the section model and the full scale. These correction factors are found from the ratios of the quantities involved for model and full-scale. Through the appropriate selection of turbulence characteristics in the section model test and model length these corrections are relatively small. This last fact should lead to satisfactory reliability.

4. EXPERIMENTAL DETERMINATION OF DESIGN LOAD COMPONENTS

The wind tunnel testing of the section models of the two Sunshine Skyway Bridge alternates provided an opportunity to apply the proposed method. The proposed structure, over Tampa Bay in Tampa Florida is a cable-stayed design with a 366m main span. The concrete alternate used a precast, segmental box girder 29.03m wide and 4.27m deep. Two single strut pylons carry a system of radiating stays located on the longitudinal axis of the bridge (Fig. 4).

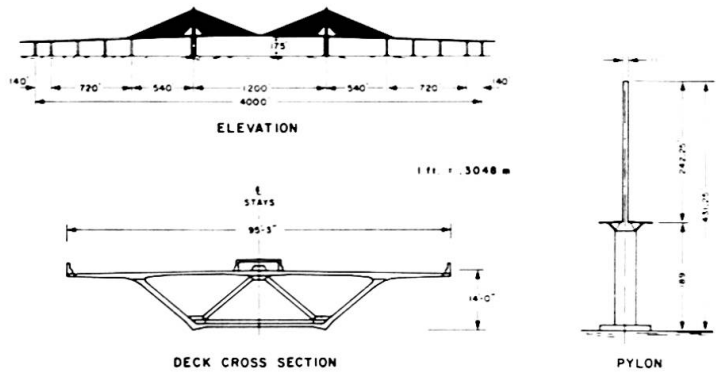

Fig. 4 Sunshine Skyway Bridge

Fig. 5 Section Model in Wind Tunnel

The model of the 1 in 80 scale bridge section shown in Fig. 5 is 7 ft. (≃ 2m) in length corresponding to a 170 m section of the full scale structure. The model was tested with spring mounting giving the correct frequency ratio in lift and torque and 0.5% damping. Measurements of mean and peak dynamic motion are plotted in Fig. 6, and show marked differences between smooth and turbulent flow. With smooth flow there is evidence of some coupling between static lift and torque (i.e. twisting of deck due to torque modifies lift). Although not essential to the method aerodynamic damping and admittance functions were also measured in the experiments.

The large mesh size and bar spacing of the turbulence grid was selected to give a close representation of the natural wind. The measured vertical turbulence intensity behind this grid is found to be 0.05 compared to the expected full scale value of 0.06 over open water. The grid turbulence spectrum and the target full scale spectrum are drawn together in Fig. 10 on a double logarithmic scale. Both have similar form, although the full scale has slightly more energy than does the grid turbulence at lower frequency.

5. DETERMINATION OF DESIGN WIND LOADS

Following equation 8 the wind load from the background turbulence excitation is found through the integration with reduced frequency of the product of the vertical wind spectrum (Fig. 7), Aerodynamic Admittance Function (Fig. 8) (assuming the Sears function), and the Joint Acceptance Function for the particular mode (Fig. 9). The form of these functions is such that the bulk of the energy is in the range of reduced frequency f^* between 0.01 and 0.1 and any uncertainty of the functional values at these low frequencies generally introduce little error. Added to this is the resonant component following equation 8. The resonant modal response, measured in terms of deflection has been converted to an equivalent static load through the modal stiffness:

$$\sigma_{W_{r_z}} = m\,(2\pi f_o)^2\ \sigma_z \quad ; \quad \sigma_{W_{r_\theta}} = I_o\,(2\pi f_o)^2\ \sigma_\theta \qquad (12)$$

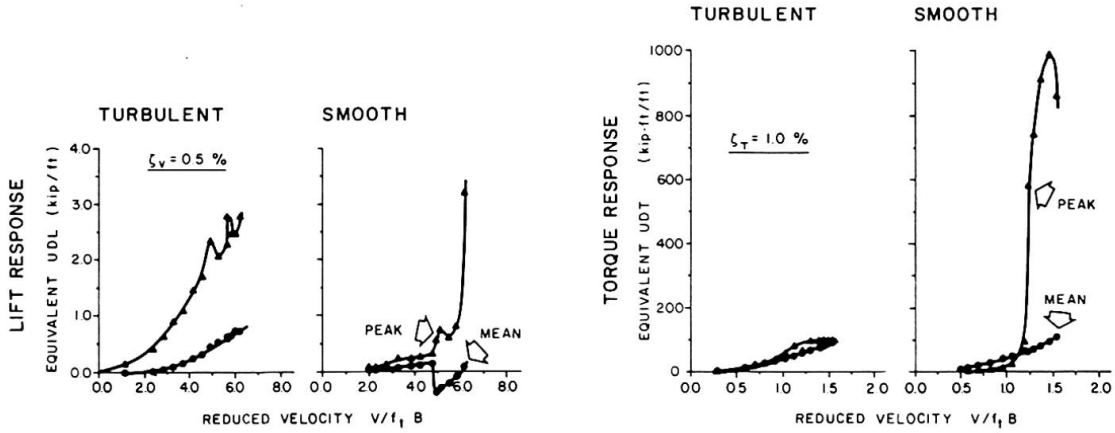

Fig. 6 Section Model Response (Uncorrected)

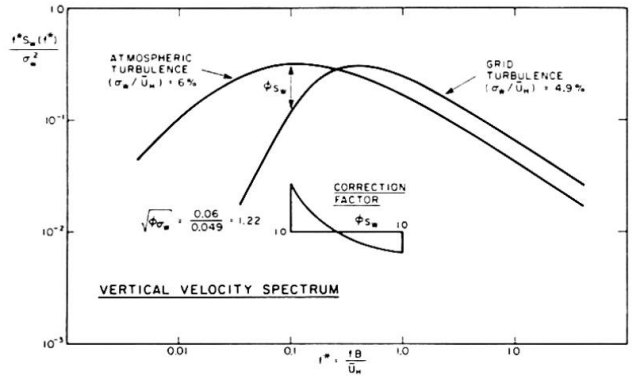

Fig. 7 Vertical Velocity Spectrum

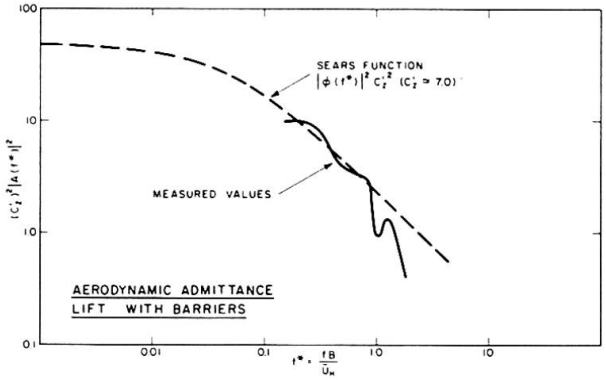

Fig. 8 Aerodynamic Admittance

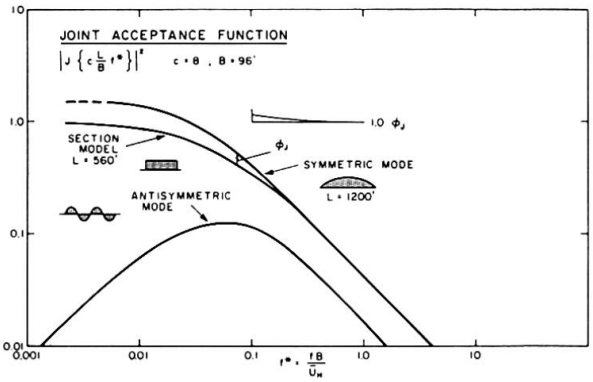

Fig. 9 Joint Acceptance Function

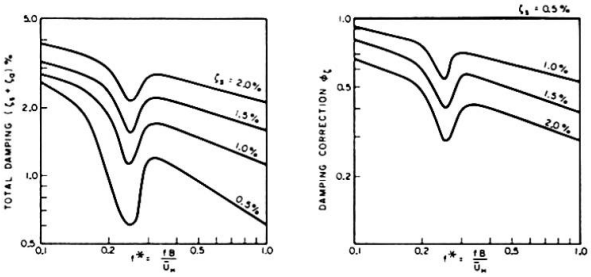

Fig. 10 Damping Functions

The correction terms are determined from the ratios of the quantities involved for full scale and model. That for the turbulence intensity, $\phi_{\sigma w}$ is a constant equal to $(.06/.05)^2 = 1.44$ i.e. the ratio of target full scale to model values. Similarly, the correction factor for the vertical velocity spectrum ϕ_{S_w} is shown in Fig. 7, the joint acceptance function, ϕ_J, in Fig. 9, and the damping, ϕ_ζ, in Fig. 10. The addition of the background and resonant components as in equation (3), result in the loading shown in Figs. 11a and b. The final wind speed scaling will depend upon the final design frequencies of the structure. Thus the example wind loads have been determined for a

nominal wind speed at deck height based on the estimates of vertical and torsional frequencies noted in the figures.

Verification of this procedure, using 1:350 scale aeroelastic models of both the steel and concrete bridges tested in a turbulent boundary layer were excellent (3).

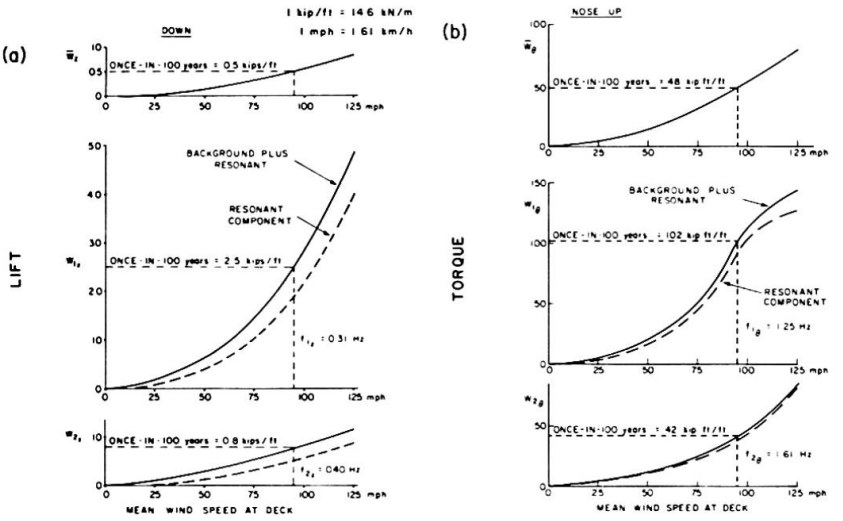

Fig. 11 Wind Load Components on Completed Bridge

6. CONCLUSIONS

A method has been presented whereby wind tunnel section model test results can be incorporated directly into a load format suitable for the definition of the design wind loads of long span structures. The procedure has been verified experimentally with the satisfactory prediction of the response of two full bridge aeroelastic models to boundary layer shear flow.

REFERENCES

1. Davenport, A. G., Isyumov, N., Fader, D. J. and Bowen, C. F. P., "A Study of Wind Action on a Suspension Bridge During Erection and Completion", University of Western Ontario, Faculty of Engineering Science, Research Report BLWT-3-1969, London, Ontario, Canada, May 1969 and March 1970.

2. Davenport, A. G., Isyumov, N., Rothman, H. and Tanaka, H., "Wind Induced Response of Suspension Bridges", Wind Tunnel Model and Full Scale Observations", Proc. 5th Int. Conf. Wind Engineering, Ft. Collins, Colorado, 1979, pp. 807-824.

3. Davenport, A. G. and King, J. P. C., "The Incorporation of Dynamic Wind Loads into the Design Specifications For Long Span Bridges", ASCE Fall Convention, New Orleans, La., 1982.

4. Tanaka, H. and Davenport, A. G., "Wind Induced Response of Golden Gate Bridge", University of Western Ontario, Faculty of Engineering Science Research Report, BLWT-1-1982, Paper accepted for publication by JSD, ASCE, June 1982.

5. Melbourne, W. H., "Model and Full Scale Response to Wind Action of the Cable Stayed Box Girder West Gate Bridge", Practical Experience With Flow Induced Vibrations, Symposium Karlsruhe, Germany, 1979, pp. 625-652.

6. Ukeguchi, N., Sakata, H. and Nishitani, H., "An Investigation of Aeroelastic Instability of Suspension Bridges", Proc. International Symposium on Suspension Bridges, Lisbon, 1966, pp. 273-284.

7. Scanlan, R. H., "An Examination of Aerodynamic Response Theories and Model Testing Relative to Suspension Bridges", Proc. Wind Effects on Buildings and Structures, Tokyo, 1971, pp. 941-951.

Wind Tunnel Model Tests on Wind Sensitive Structures

Essais sur modèle de structures sensibles au vent

Einsatz von Windtunnel für windempfindliche Tragwerke

J.H. WYNHOVEN
Director
John Connell & Assoc.
Melbourne, Australia

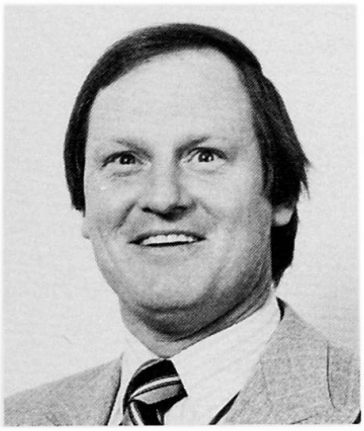

J.J. PEYTON
Managing Director
John Connell & Assoc.
Melbourne, Australia

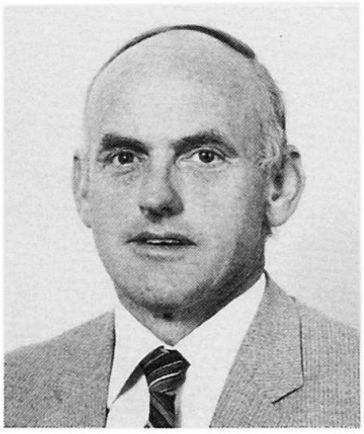

J.A.F. WILLIAMS
Director
John Connell & Assoc.
Perth, Australia

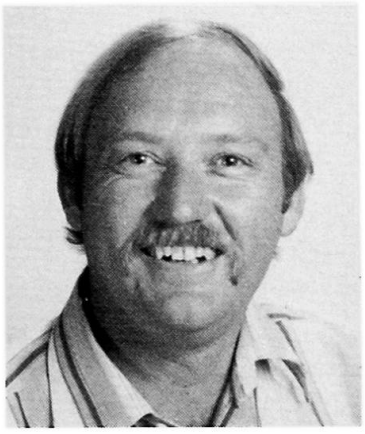

SUMMARY

This paper discusses the use of dynamic modelling applied in wind tunnel testing of a slender large span steel cantilevered grandstand roof, two 50 storey office towers in close configuration, and a 120 metre tall steel lattice cantilever tower. In each case a well documented knowledge of the directional nature of wind was used to permit cost savings to be achieved.

RESUME

Cet article décrit l'utilisation de modèles dynamiques dans une soufflerie pour tester un grand porte-à-faux élancé en acier, une toiture de tribune, deux immeubles-tour de 50 étages et une tour en treillis métallique de 120 m de haut. Dans chaque cas, une étude poussée de la direction et de la nature du vent a été faite pour permettre de substantielles économies.

ZUSAMMENFASSUNG

Dieser Beitrag behandelt den Einsatz dynamischer Modelle im Zusammenhang mit Windkanaluntersuchungen von einem schlanken, weitgespannten, auskragenden, stählernen Tribünendach, von zwei nebeneinander stehenden 50-stöckigen Bürohochhäusern und von einem 120 m hohen stählernen, netzförmigen Turm. In allen Fällen wurde von den genau dokumentierten, örtlich herrschenden Windverhältnissen Gebrauch gemacht und dadurch eine Kosteneinsparung ermöglicht.

1. INTRODUCTION

The Australian Loading Code AS1170, Part 2 - Wind Forces, like other international wind codes, determines wind forces based on wind velocity profiles, terrain category velocity modifiers and drag coefficients which vary with the shape and orientation of members and buildings. Basic design wind speeds for 5, 25, 50 and 100 year return periods are provided for all major centres in Australia. Design wind pressures may then be calculated as follows:

$$P_z = C_p \times 0.6\, V_z^2 \times 10^{-3}\ kN/m^2$$

where P_z = wind pressure at height z

V_z = design wind velocity at height z, m/sec

C_p = pressure coefficient on a surface

It further permits, as an alternative to the above "quasi-static" approach, the carrying out of Wind Tunnel Tests for Dynamic Response, to establish the wind forces. This is permitted providing that:

- the natural wind has been modelled to take account of variation of wind speed with height,
- tests on curved shapes are conducted with due regard to effects of Reynolds numbers,
- the natural wind has been modelled to account for the scale and intensity of the longitudinal component of turbulence,
- the model is scaled with due regard to mass, length, stiffness and damping.

Wind forces are not static loads but a complex dynamic interaction between the wind and the structure that obstructs its path. As the stiffness of a structure decreases the wind excitation increases and the displacement of the structure is magnified beyond that predicted by an "equivalent" static load application.

The real response is very complex to predict as it depends on the stiffness, mass, dimension, shape and orientation of the structure, its location relative to other buildings and topography, as well as the basic wind speed which varies with height, time and direction. The only reliable means to predict the dynamic response of wind sensitive structures is the testing in wind tunnels using dynamic modelling.

This technique has been applied to three different structures for which the application of "quasi-static" loads were considered to be inappropriate. Use was further made of the directional nature of wind which has been documented for Melbourne (Fig. 1) drawing on anemometer data.

All of the dynamic model testing reported in this paper was carried out by Professor W.H. Melbourne at Monash University, Melbourne. [1]

2. WIND TUNNEL TESTING

The 450 KW closed circuit wind tunnel developed and built in the Department of Mechanical Engineering has an overall loop dimension of 10m x 28m and two working sections. One has a cross section of 4m width and 3m height, while the second measures 2m x 2m. This tunnel has been in operation since 1970 and has been used to add enormously to the application of advanced wind engineering techniques to major structures in Australia and the Asian region. Particular use has been environmental wind effects in central city locations, wind forces on cladding elements, dispersion of wind effluents and in particular the dynamic response of wind sensitive structures.

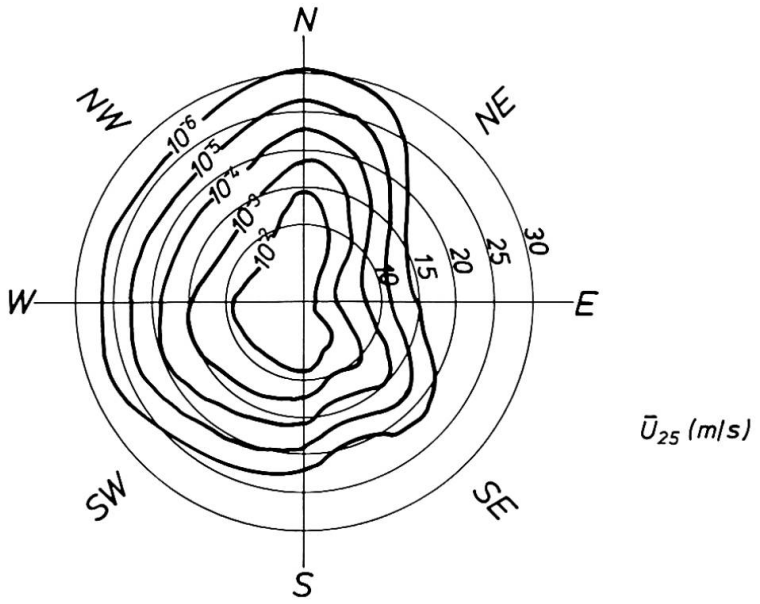

Fig. 1 Directional Wind Speeds, MELBOURNE

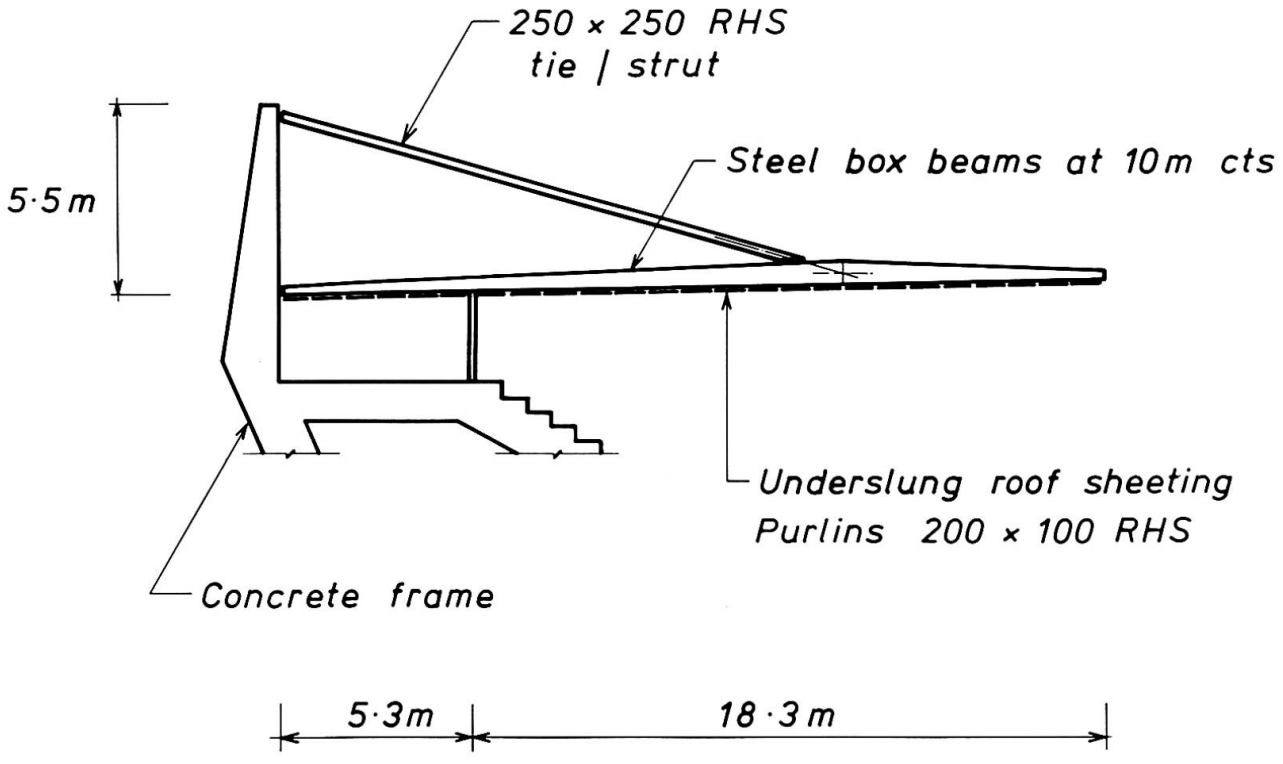

Fig. 2 VFL Park, Waverley, Roof Cross Section

3. VFL PARK, WAVERLEY

This is the home of Australian Rules Football and has been developed to provide seating for over 100,000 spectators. The cantilever roof dimensions are shown on Fig. 2. It forms part of a 150 metre long roof which soars some 25m above the playing field.

A 1:100 scale, aero-elastic model of 8 bays (half of total) was tested for various wind orientations. The members of the roof beams were made from several types of timber, selected to obtain appropriate elastic properties. The roof was made of balsa to which small amounts of additional mass were added to obtain the correctly scaled values. The action of the rear column (reinforced concrete) and main beam (structural steel) was taken to be pure bending while all other members were considered loaded in pure tension or compression for the purposes of scaling. The velocity scale was selected as 0.50.

During wind tunnel testing at low wind speeds, the roof displacement closely followed the deflection pattern of a cantilever. As the wind speed increased a low frequency wave, travelling along the leading edge, started to form (Fig. 3) and was superimposed on the cantilever bending mode. Fig. 4 shows the mean and maximum displacements at the leading edge in the centre of the 8 bay model. The increased contribution from the "cross-wind" action is seen to dominate as the wind speed increases and shows rapid divergence above 25m/sec. This means that at high wind speeds, the real displacement will be up to twice that predicted by the "quasi-static" load obtained by applying the wind loading code.

The significance of the wind tunnel model results must be related to the orientation of the roof and the wind speed acting on the actual structure. Fig. 1 shows the distribution of mean wind speed for Melbourne. Each circle represents the 10 minute mean wind speed measured by anemometer at Essendon Airport, Melbourne, adjusted to a height of 25 metres in open country. The 10^{-6} contour is roughly equivalent to a 100 year return maximum wind speed. The distribution clearly shows considerable variation with orientation. The grandstand faces south and therefore the probability of the design wind load being exceeded is less than 1% per annum which corresponds to designing for a 100 year return wind. If the grandstand faced north, then clearly the stiffness would need to be increased since the mean wind speed from this direction for the same 100 year return period is 36 per cent higher.

The basic design wind speed for Melbourne is 39m/sec for a 50 year return period and to limit excessive dynamic response for wind sensitive cantilevers a stiffness criteria has been adopted which limits the deflection of the cantilever tip to span/200 for the particular wind speed from the direction in which the roof is facing. This criteria has been adopted with success on other wind sensitive roofs including the 28m steel truss cantilever roof at the Victorian Racing Club Grandstand for horse racing in Melbourne. This cantilever roof has suspended at its very tip a 2 storey judges' box and photo-finish camera.

4. COLLINS PLACE PROJECT

This is the largest commercial development project completed in Australia to date. It incorporates two (2) fifty (50) storey towers (ANZ and Collins Towers) linked at its base by a 1 hectare retail/commercial and hotel-lobby area under a vast glassed space frame roof suspended from the towers. The top sixteen (16) storeys of one of the towers is an international hotel containing 375 rooms. The location and orientation of the towers on the site are shown on Fig. 5.

Earlier static model testing in the wind tunnel on a 1/600 scale model indicated that there could be significant aerodynamic interaction between the two towers. This led to a dynamic test being carried out on a 1/384 model and a velocity ratio of 0.20. The towers are of "tube-in-tube" construction with an extremely

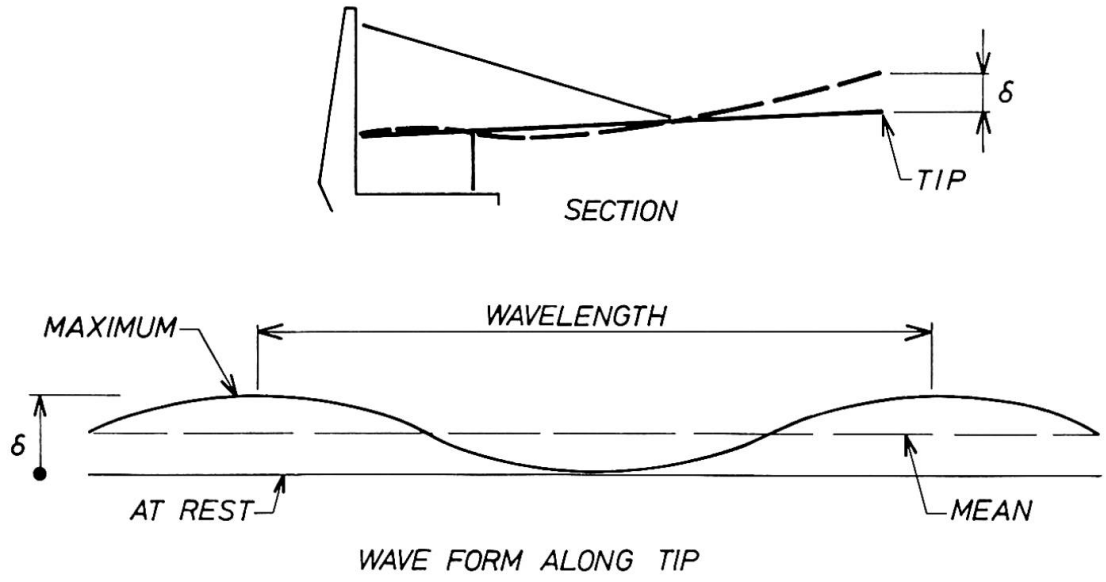

Fig. 3 VFL Park, Waverley, Tip Displacement

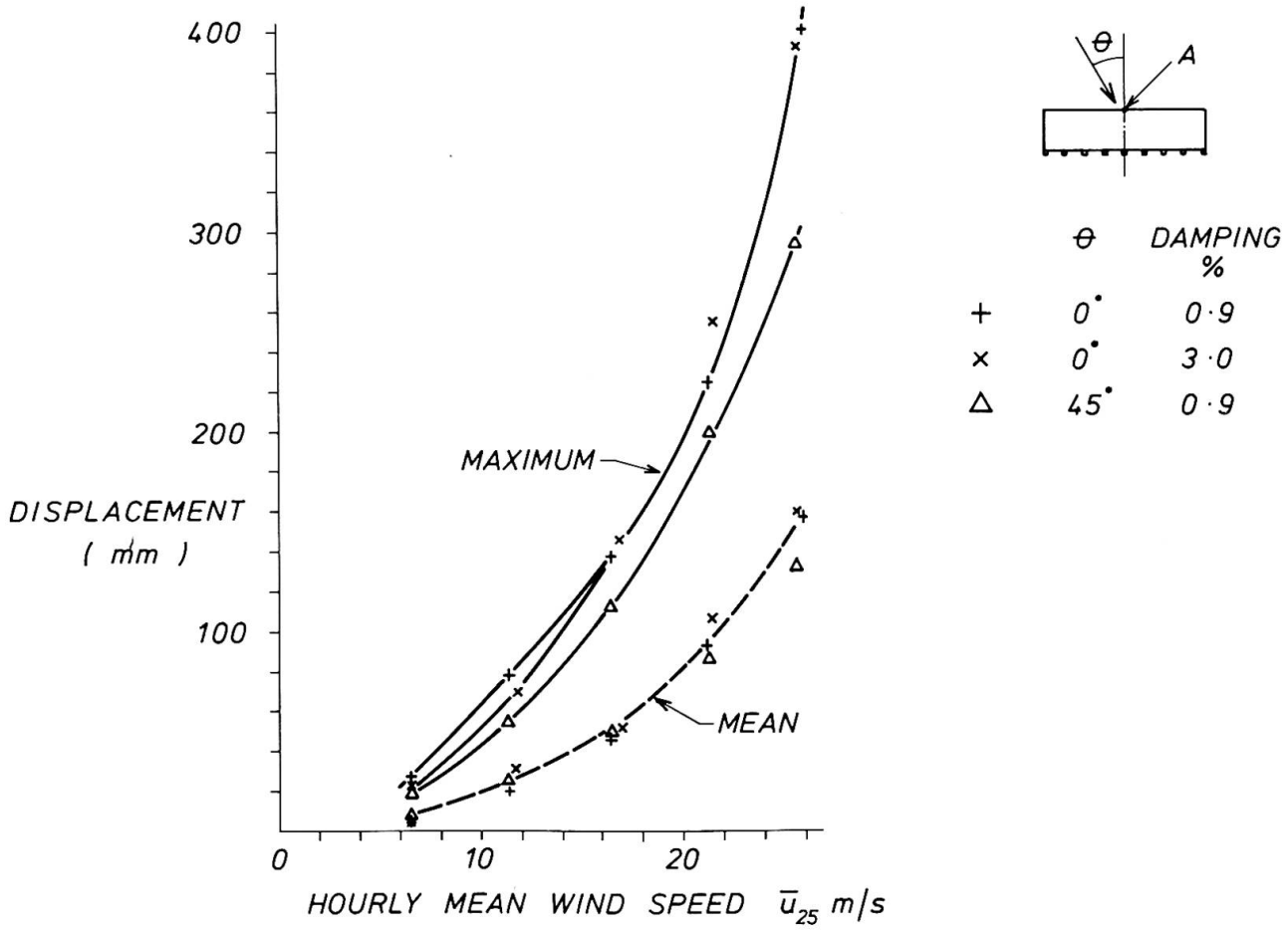

Fig. 4 VFL Park, Waverley, Displacement vs. Wind Speed

stiff facade which permitted the towers to be simulated as rigid blocks placed on spring mounted bases. The tower models were made of Daycel rigid foam with a 1mm plywood skin mounted on steel cantilevers. The positions of the towers on the cantilevers were such as to permit rotation about a pivot point at the footing level of the towers. The cantilevers were strain gauged to allow the overturning bending moments to be measured about two perpendicular horizontal axes at the footing level. Variation in damping was obtained by using oil dashpots at the footing level. The damping used was 1.1% of critical damping and the natural frequency used was $0.3Hz$. A full scale mean hourly maximum wind speed of 30m/sec at a height of 184m above ground level (200m above footing level) was applied.

The design wind loading obtained from the model tests indicated that the interaction between the two towers results in overturning moments about the one axis of approximately 75% of that occurring simultaneously about the other axis. Maximum overturning moments about the base were:

$$M_1 = 1.442 \times 10^6 \text{ kN.m}$$

acting simultaneously with

$$M_2 = 1.055 \times 10^6 \text{ kN.m}$$

The above maximums occur for the ANZ Tower with the wind direction from NW to N from which approximately 50% of the yearly maximum winds occur in Melbourne. These moments are equal to mean plus 3.5 times the standard deviation ($\overline{M} + 3.5\ \sigma_m$) and this corresponds to a 10% probability over a life of 100 years. Higher moments by approximately 3% do occur for the Collins Tower but this is for a wind direction from S to SSE which as discussed earlier, is a considerably lower probability in Melbourne.

The lateral displacement and accelerations at the top of each tower were also calculated and the following values obtained for a 100 year return period.

	displacement	acceleration
ANZ Tower	132mm	3.5% of g
Collins Tower (Hotel)	91mm	1.7% of g

Reliable data on levels of perceptability of motion and acceleration was scarce at that time. However, they were considered less than those predicted on tall buildings then under construction in the USA and were considered acceptable even allowing for the close proximity of the two towers. After several years of occupancy, no complaints have been registered.

5. VICTORIAN ARTS CENTRE UPPER SPIRE

The spire over the Theatres complex rises to a height of 120m above street level and comprises a tapered open latticed spire which rises 84m from its supports (Fig. 6). The Upper Spire has been built using the Mero Spaceframe "ball-joint" connection as shown in Fig. 7. The connection is effectively a "pin-joint" with axial compression being transmitted from the mild steel tube through the cone and sleeve to the node. Axial tension is transmitted from the mild steel tube through the cone and bolt to the node. The bolt, therefore, is never in compression but under wind, experiences a variable tension.

When designing the tower it was considered that the behaviour of the tower could not be predicted by using the "quasi-static" loads from the Wind Code. In fact, interpretation of the resistance to wind offered by the joints and members and the varying degree of shielding offered, was considered to be too great an uncertainty. As the bolts in the connection would be subjected to fluctuating loads under wind, the fatigue life of the bolts needed investigat-

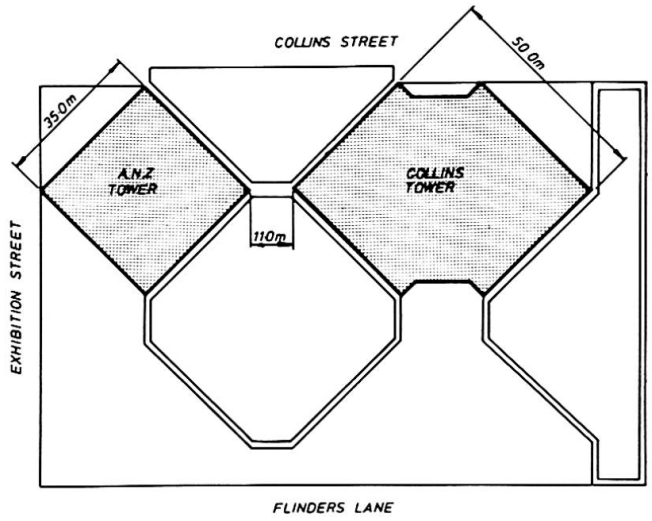

Fig. 5 Collins Place, Melbourne, Site Plan

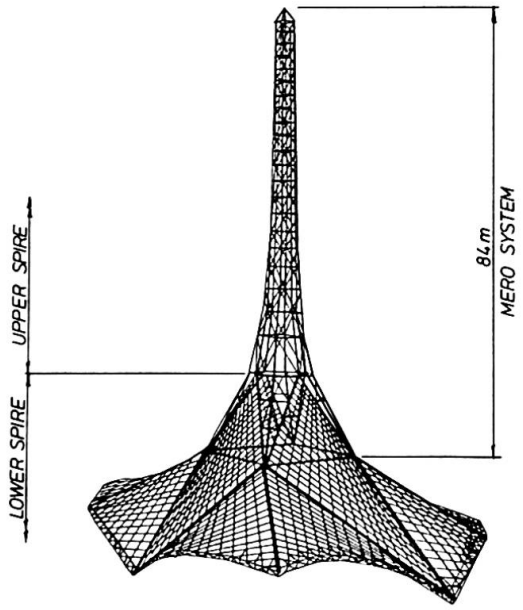

Fig. 6 VAC Upper Spire

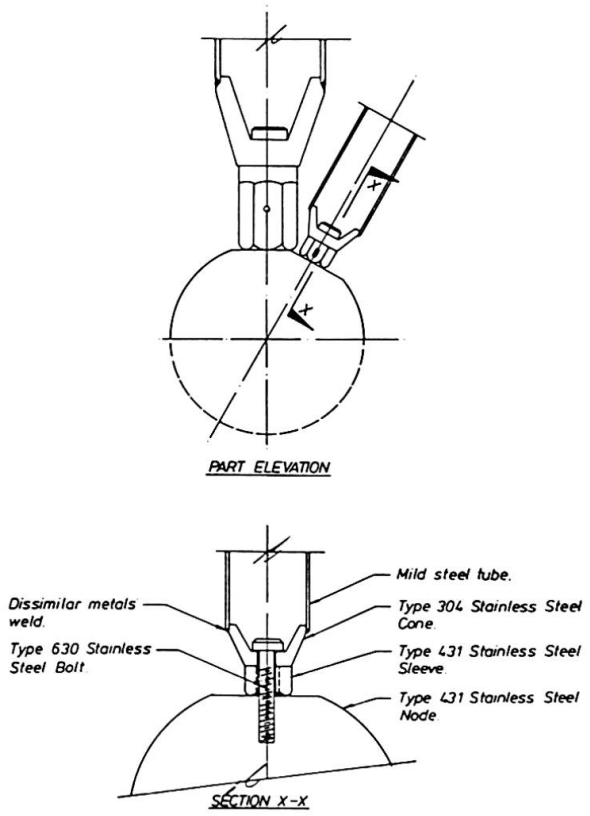

Fig. 7 Mero Connection

ion. An underestimate of bolt forces would considerably affect the life of the structure. A design life of 100 years being the criteria.

A full scale model of the upper six levels of the spire was tested to establish the damping characteristics of the joint system, as this directly affects the dynamic response and therefore the loads. The damping was measured by inducing a natural oscillation and then measuring the degradation using an accelerometer and chart recorder. This was carried out for the condition of torqued bolts and snug-tight bolts. From this, a conservative value for critical damping of 0.004 was adopted for design purposes.

The aeroelastic model for the spire was built to a linear scale of 1:100 using sugar pine with all members loaded purely in tension or compression, the velocity ratio was 0.3.

The results from the model tests provided total overturning moments at the base of the spire approximately 30% less than those obtained by direct application of the Wind Code. This reduction was of great significance in the design and more than offset the cost of wind tunnel testing.

The design loads for fatigue design of the bolts was established by using the natural frequency of vibration, directional wind data (Fig. 1) available for Melbourne, computing the response of the spire in 16 directional areas of wind and for 8 intensities of wind speed. This then permitted the number of cycles of the 8 stress levels that would be experienced over the 100 year design life of the spire to be summated. This data was then used as the stress-cycle history for the fatigue analysis of bolts, members and welds. A limit state design approach being adopted. Without this data a much more conservative approach would need to have been adopted. This being of extra significance as the fatigue life of the bolts decreases with increased diameters.

6. SUMMARY

The use of wind tunnel model testing in predicting the dynamic response of actual structures has permitted a real understanding of the behaviour of structures for those cases where wind loads are a dominant design criteria. Direct application of the "quasi-static" approach of the Wind Code would in the case of wind sensitive structures have resulted in excessive deflection and overstressing. In other cases, a reduced wind loading was able to be applied resulting in considerable cost saving. In all cases, the use of available directional wind data has permitted this to be applied to give direct savings in design loading.

All designs of major structures which are suspected of being sensitive to wind should draw on the advice of experienced wind engineers and use the available wind tunnel facilities for dynamic testing.

REFERENCES

1. Dr. W.H. Melbourne. "Development of Natural Wind Models at Monash University", Fluid Mechanics Conference, Adelaide, Australia. 5th - 9th December, 1977.

Aerodynamic Effects on Suspension Bridges with Inclined Hangers

Effets aérodynamiques des ponts suspendus à câbles inclinés

Aerodynamische Einflüsse auf Hängebrücken mit schrägen Hängern

Toshio MIYATA
Prof. of Civil Eng.
Yokohama Natl. Univ.
Yokohama, Japan

T. Miyata, born 1938, got his Dr. degree in civil engineering at the Univ. of Tokyo, Japan 1969, and has done research work in structural dynamics and wind engineering. He is, now, responsible for a study committee to investigate aerodynamic stability of a very large suspension bridge proposed in Japan.

Hitoshi YAMADA
Res. Assoc.
Yokohama Natl. Univ.
Yokohama, Japan

H. Yamada, born 1955, got his Dr. degree in civil engineering at the Univ. of Tokyo, Japan 1984. He started to work as an university researcher on structural engineering and is now, on official leave to the Univ. of Ottawa, Canada for his research works on wind engineering.

SUMMARY

It has been reported that the inclined hangers of a suspension bridge were so weak after 16 years of service that most would probably have to be replaced. In this paper, it is analytically presented that the fatigue damage of inclined hangers is caused by their essential higher tensile force variations, in contrast with those in traditional vertical hangers. The longitudinal loadings by wind action and traction or braking of heavy vehicles, and the vertical load of inertia forces due to buffeting in gusty winds are assumed, and the latter two factors are concluded to be significant to contribute to the fatigue damage.

RESUME

On a constaté des dommages si importants dans les câbles obliques d'un pont suspendu, qu'après seulement 16 ans de service, on devra probablement en remplacer la plus grande partie. Cet article démontre analytiquement que les dommages de fatigue de câbles obliques sont plus importants que pour les suspentes verticales. Ce fait est dû aux très grandes variations de tension dues au vent et surtout au freinage des véhicules lourds et aux chocs causés par les rafales de vent.

ZUSAMMENFASSUNG

Bei einer Hängebrücke mit schrägen Hängern sollen nach 16 Betriebsjahren die Hänger so schwach sein, dass vermutlich die meisten ersetzt werden müssen. Der Beitrag zeigt auf analytische Weise, dass die Ermüdungserscheinungen an schrägen Hängern auf die – im Vergleich zu traditionellen lotrechten Hängern – wesentlich höheren Spannungsänderungen zurückzuführen sind. Untersucht wird sowohl die Wirkung von in Brückenlängsrichtung wirkenden Lasten infolge Wind und Bremsen von schweren Fahrzeugen als auch von lotrechten Trägheitskräften infolge windinduzierter Schwingungen. Die beiden letzten Faktoren werden als bedeutsam für die festgestellten Ermüdungserscheinungen erkannt.

1. INTRODUCTION

It has been reported [1,2] that the inclined hangers of a suspension bridge were so weak after 16 years of service that most would probably have to be replaced. It is thought that the revolutionary use of inclined hangers may explain their fast deterioration by fatigue, caused by greater restrictions to longitudinal movement in the deck. The use of inclined hangers was originally expected to damp the predicted oscillations of the flexible, streamlined box girder.

In this paper, it is analytically presented that the fatigue damage of inclined hangers is caused by their higher tensile stress variations, in contrast with those in traditional vertical hangers. These tensile stress variations may be attributable not only to the far higher live loads of road traffic, as frequently pointed out, but also to the greater wind-induced buffeting oscillations inevitable to a flexible, winged box girder. In the analyses, assuming the following conditions ; (1) the longitudinal load resulting from traction or braking of heavy vehicles, (2) that by wind action shifted from normal to the bridge axis, and (3) the vertical load corresponding to inertia forces determined according to buffeting in the flexural first mode shape, the estimations of fatigue damage were made.

2. ANALYTICAL PROCEDURE AND ASSUMPTIONS

The displacement and force for the given loadings were calculated by the geometrically nonlinear analysis method, usually applied to the large displacement behaviour of frame work structures, considering the axial force variations in the cables and hangers. The nonlinear variations were confirmed by incrementing the loads step by step up to the assumed maxima. The analyses were made for a model bridge having traditional vertical hangers, with two ropes located at each panel point, as well as for a bridge having inclined hangers, setting the nodal points at all the hanger connections.

The primary dimensions for the analyses were quoted from those of the Severn Bridge [3,4,5] and others were assumed appropriately ; center span length ℓ = 987.6 m, side span length ℓ_1 = 304.8 m, sag-span ratio of cable : 1/12, longitudinal slope : 0.5 % parabolic at center span, one cable (dia. : 50.8 cm, area : 0.116 m^2, $E_c = 2.0 \times 10^7$ t/m^2, weight : 2300 t), one hanger (dia. : 52.8 mm, area : 13.3 cm^2, $E_h = 1.4 \times 10^7$ t/m^2, length : 2.3 m at center and 1.5 m at end to abutment), suspended deck (area : 1.043 m^2, I = 1.21 m^4, $E_s = 2.1 \times 10^7$ t/m^2, steel weight : 11200 t, asphalt thickness : 3.8 cm), tower (flexurality to bridge axis was replaced by an equivalent tensile spring at tower top, having area : 1 m^2, E_t = 165 t/m^2, and length : 1 m). The initial hanger tensions were determined according to the dead load of the girder. The bridge elavations and the hanger connections are as shown in Fig. 1.

3. LONGITUDINAL LOADINGS

3.1 Uniform Wind Loading

Assuming the wind action shifted from normal to the bridge axis, the streamlined box girder of the Severn Bridge would be loaded with the maximum longitudinal drag force (coefficient = about 45 % at most of C_D = 0.6 for normal to the bridge axis) in 50 to 60 degrees orientation from normal [6]. The load intensity is p = 17.7 kN (1.8 tf) /Br. per one panel length (18.3 m), taking account of the design wind speed V_D = 100 mph (44.7 m/s). Fig. 1 shows the hanger tension distribution diagrams for the inclined and the vertical hangers respectively, under the uniform, longitudinal loading on all the spans of the girder. The tension variations in the vertical hangers are very low except those of the extreme end hangers with the shortest length (V1 and V86 in Fig. 1), while those in the inclined hangers are really noticeable within the hanger range different from usual array of isos-

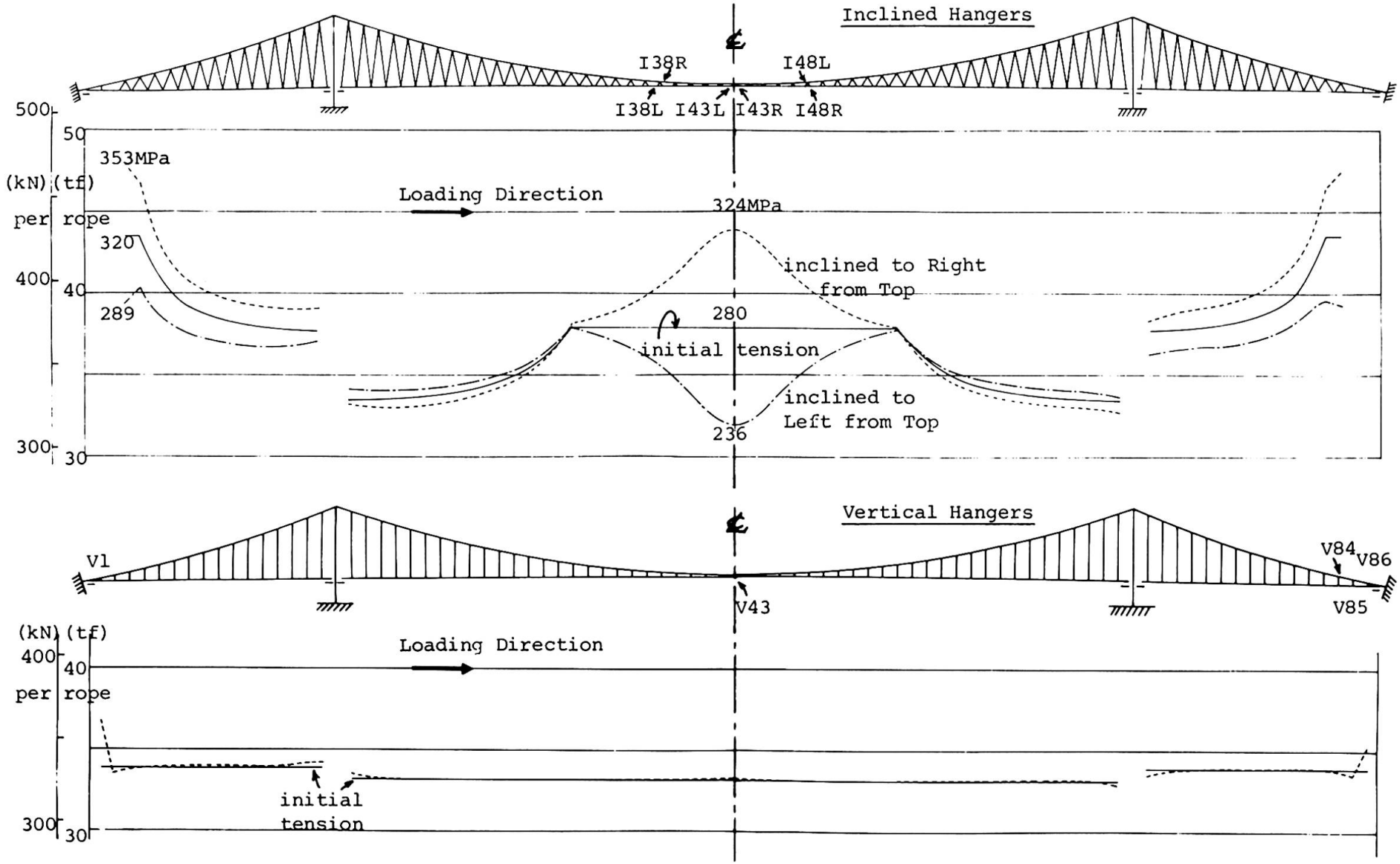

Fig. 1 Hanger Tension Distribution by Uniform Longitudinal Loading for Girder with 17.7 kN(1.8 tf) per one panel length/ Br.

celes triangle in the middle of center span and at the both ends to the abutment of side spans. In this case of loading from left to right, as shown in Fig. 1, the tension variations are different between the hangers inclined to the right from the top and those inclined to the left.

This effect of longitudinal wind loading produces only the tensile stress variation of 44 MPa (4.5 kgf/mm^2) at most at the span center point, which is not so enough to cumulate the fatigue damage, judging from the fatigue strength N.S. curve with 5 % break level in Fig. 4(e), obtained from the tests for hanger ropes [7]. The occurrence of such a strong wind as the design wind speed is quite unusual, and it may be of a return period more than 100 years. This case is concluded not to contribute to the fatigue.

3.2 Uniform Vehicles Traction or Braking Loading

As seen in the preceding analysis, the higher stress variations are essential to the inclined hangers under the longitudinal loading, compared with the vertical hangers. Taking account of the severe longitudinal load resulting from traction or braking of heavy vehicles, the occurrence of much higher stress variations would be expected. Assuming the 25 % intensity (6 kN/m) of the design live load (24 kN/m) for the Severn Bridge as a longitudinal load, p = 110 kN (11.2 tf)/Br. is to be loaded per one panel length. Incidentally, it is referred to the B.S. 5400 Specification for loads of 6.6 [8] that the nominal longitudinal load for type HA shall be 8 kN/m of loaded length. This loading condition means an arrangement of two heavy vehicles with 2 @ 220 kN (22 tf) loaded at each panel point /Br.

The hanger tension distributions are basically similar to those shown in Fig. 1 under such a severe loading on all the spans as well. Aiming at tension variations from the initial one for some specified hangers, Fig. 2 can be obtained, where it is seen that the nonlinearity for the load increment is more remarkable in the vertical hangers, particularly in the extreme end hangers with the shortest length (V1 and V86), and that the almost linear increase of variations in the inclined hangers, for instance, in both hangers at the span cenetr point (I4 3R and L) is so noticeable to produce the higher stress variation of 44 x (11.2/1.8) = 274 MPa (28 kgf/mm^2). As far as the longitudinal displacements of the girder are concerned, in the inclined hangers, the relatively smaller displacements of 13.4 cm in the center span and 5.4 cm in the side spans are calculated, resulting from the greater restriction effects of the inclined hangers to longitudinal movement. On the contrary, in the vertical hangers, the greater displacements are observed with 96.3 cm in the center span, varied almost linearly, and 120 cm in the side spans, varied nonlinearly, although the stress variations in almost all the hangers are very low except the extreme end ones.

Estimate the possibility of fatigue damage for this case of inclined hangers. The repeat numbers of about 1.5 x 10^5, for the stress range of 274 MPa (28 kgf/mm^2) at the span center point, can be taken from the fatigue strength curve with 5 % break level in Fig. 4(e). How often would the occurrence of such a higher stress variation be expected. Judging from the current news that in 1981 the Severn Bridge carried 12 million vehicles [1], the average vehicle numbers loaded at each panel length /Br. is approximately, assuming the heavy vehicle mixed ratio to be 0.25,

$$12 \times 10^6 \times \underbrace{\frac{1}{2}}_{\text{two ways}} \times \underbrace{\frac{1}{365 \times 24}}_{\text{hours/year}} \times \underbrace{\frac{1}{86}}_{\text{panels}} \times 0.25 \fallingdotseq 2 \text{ /hour},$$

which coincides with that of the assumed condition. Furthermore, taking account into 16 years of service mentioned in the beginning, the time length amounts to 16 x 365 x 24 $\fallingdotseq$ 1.4 x 10^5 hours, and corresponds to 2.8 x 10^5 repeat cycles in two ways of the bridge. This analysis would imply a sufficient estimation to induce the fatigue damage for the inclined hangers with higher stress variation. This is the case for the extreme end hangers among the vertical ones as well.

4. VERTICAL LOADING DUE TO BUFFETING

It is a matter of concern to know how high the tension variations for the inclined hangers are under a vertical load. Taking account of the wind-induced buffeting oscillations, which were inevitable to a flexible, winged box girder in gusty winds, the inertia force determined according to a flexural oscillation in the symmetric first mode shape would be a suitable vertical loading to evaluate the fatigue damage. As far as the buffeting oscillations in a winged, plate-like section are concerned, some experimental or theoretical data are available [9,10,11]. Referring to the experimental data (f_T/f_z = 2.8) of vertical RMS responses in a turbulent flow with intensity of 7 % [9], and assuming a possible amplitude of A = 90 cm at the span center point, which probably corresponds to the amplitude at wind speed of about 40 m/s, a set of inertia forces ($mA\omega_z^2\Phi(x)$) of (1) and (2) is determined in the form of 6.32 kN/m (0.645 tf/m) x $\Phi(x)$ /Br. for the girder and 2.62 kN/m (0.267 tf/m) x $\Phi(x)$ /Br. for the cables, as shown in Fig. 3(*a*), where m is the mass, ω_z ($=2\pi f_z$) the circular natural frequency and $\Phi(x)$ the mode shape.

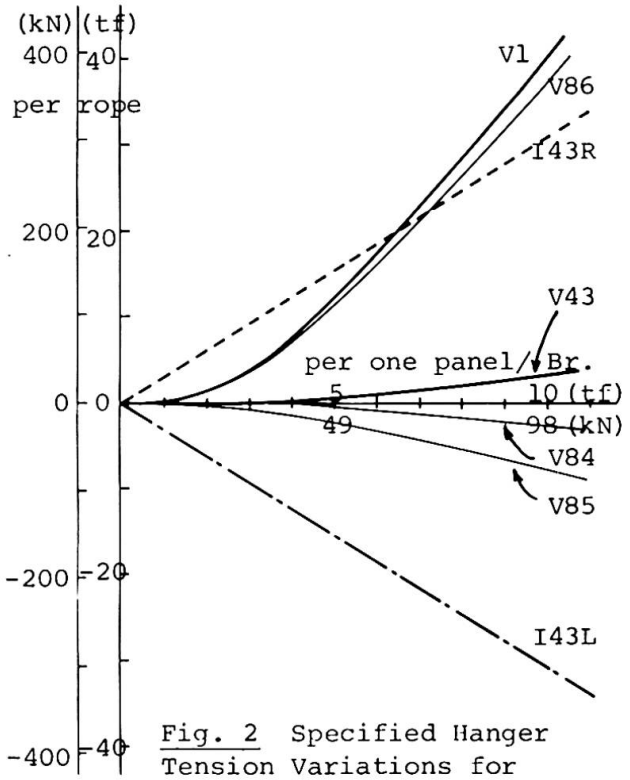

Fig. 2 Specified Hanger Tension Variations for Uniform Longitudinal Loading for Girder

Figs. 3(b) and (c) are the hanger tension distribution diagrams under the vertical loadings of type (1) and (2) for the inclined and the vertical hangers respectively. The nonlinearity in this analysis up to the assumed load intensity is very small for both cases of hangers. On estimating the fatigue damage under buffeting oscillations, the stress variations are to be evaluated in the difference of those for the loadings (1) and (2). The maximum stress range in the inclined hangers in Fig. 3(b) gets to 282 MPa (28 kgf/mm^2) in the vicinity of the hanger I38R, inclined to the right from the top, and also the hanger I48L, inclined to the left. On the contrary, the stress range of vertical hangers is, as shown in Fig. 3(c), 42 MPa (4.3 kgf/mm^2) at most at the span center point, although only the extreme end hangers get 152 MPa (16 kgf/mm^2).

Evaluate the extent of contribution to the fatigue deterioration due to buffeting oscillations, aiming at the inclined hanger with maximum stress variation. For this purpose, the cumulative fatigue damage ratio would be a significant index. Considering the relevant factors ; (*a*) the frequency of occurrence $f(V)$ of wind speed V, (b) the vertical RMS response σ_z of buffeting to wind speed, (c) the peak (amplitude) y distribution of random oscillation z, (d) the relation between stress variation σ_t and peak response y, and (e) the fatigue strength curve (relation between stress range σ_t and repeat numbers N), the cumulative ratio can be calculated by

$$\gamma = \int_V \int_y \{ f(V)p(y,V)/N(y) \}\, dVdy.$$

The respective relations are in detail described in Fig. 4. Using the frequency of occurrence of wind speed given in B.S. 5400 draft [12] and the Rayleigh distribution assumed as the peak distribution p(y,V), the ratio is γ = 0.032 per year, so that over 0.5 for 16 years of bridge service. This may be enough to represent that the wind-induced buffeting oscillations make a significant contribution to the fatigue deterioration.

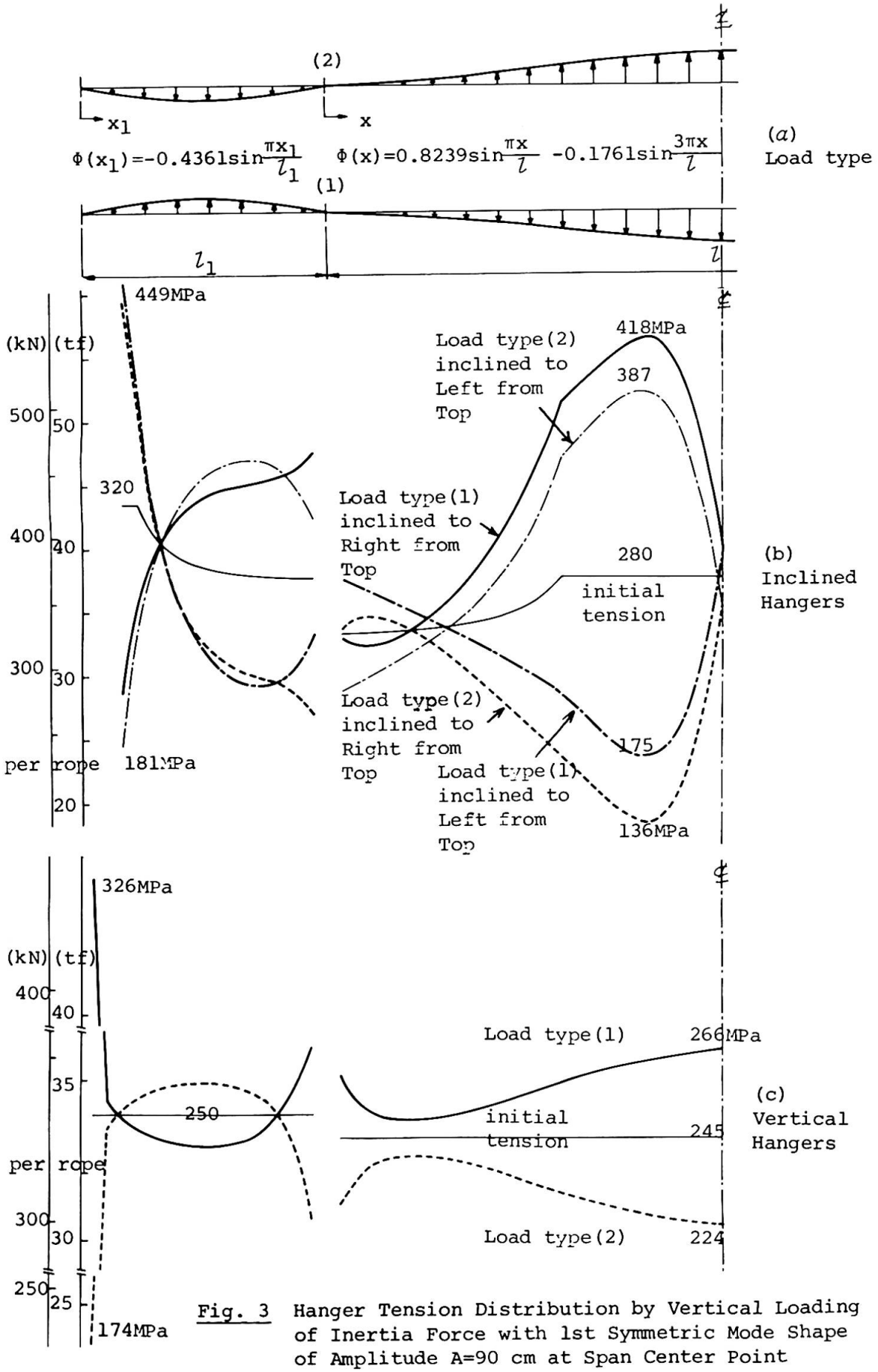

Fig. 3 Hanger Tension Distribution by Vertical Loading of Inertia Force with 1st Symmetric Mode Shape of Amplitude A=90 cm at Span Center Point

(a) Annual Frequency of Occurrence of Wind Speed
$f(V)=3600 f_z p(V)$ (cycle/year)

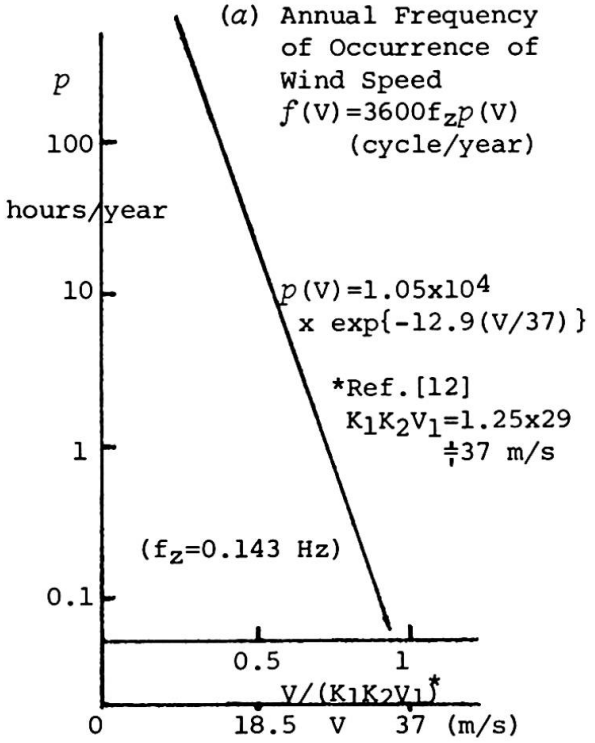

(b) Vertical RMS Response σ_z of Buffeting**

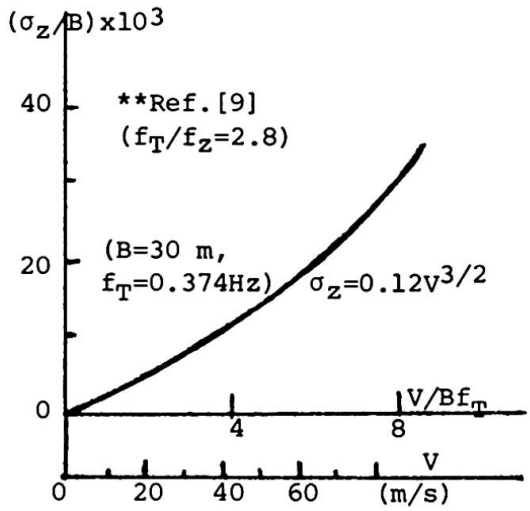

(c) Peak Distribution P(y,V)

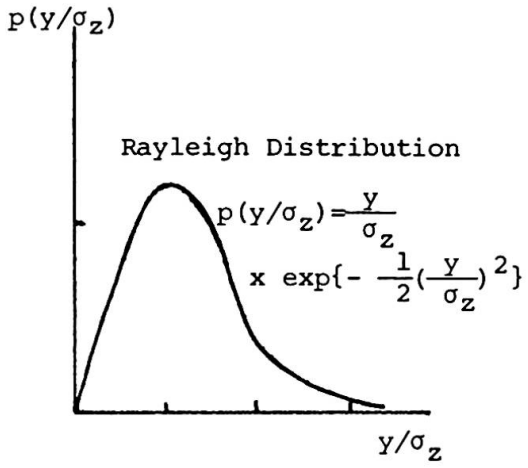

(d) Relation between Stress Variation σ_t and Peak Response y

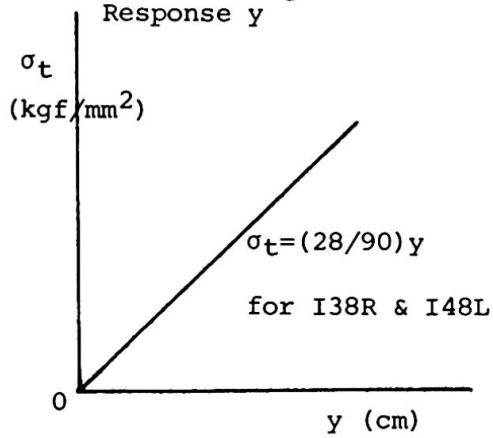

(e) Relation between Stress Range and Repeat Numbers N(y) Ref.[7]

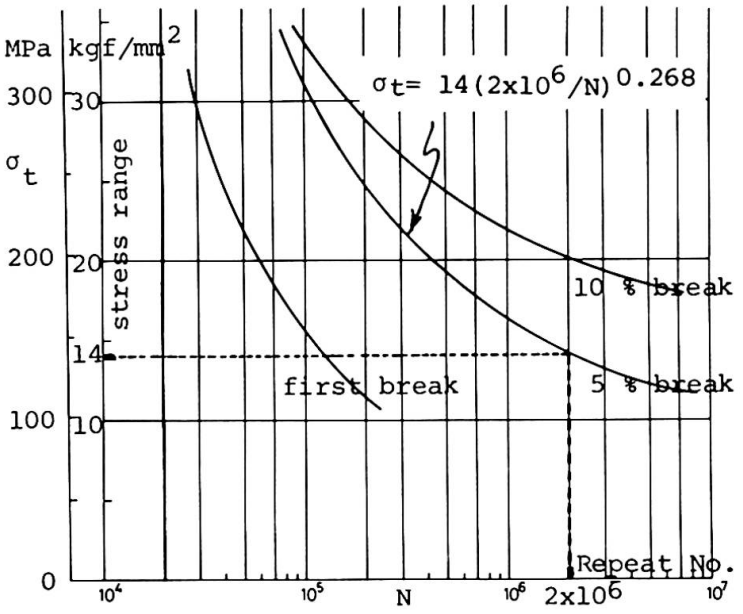

Cumulative Fatigue Ratio

$$\gamma = \int_V \int_y \{f(V)\,p(y,V)/N(y)\}\,dVdy$$

Fig. 4 Cumulative Fatigue Damage Ratio Calculation Flow Description

5. CONCLUDING REMARKS

Under longitudinal or vertical loadings, the tensile force variations in inclined and vertical hangers were analysed, and the estimations of fatigue damage were made taking account of their higher stress variations. Knowledge obtained is as follows ;

(1) The tensile force variations in the inclined hangers are essentially higher in a wider range, particularly in the shorter hangers, compared with those in the traditional vertical hangers, except two extreme end ones.

(2) The longitudinal load resulting from traction or braking of heavy vehicles may be one of important factors to cause the fast deterioration by fatigue. The wind-induced buffeting oscillations may result in a significant contribution to cumulative fatigue damage as well.

(3) As another factor to cumulate the fatigue deterioration, the vertical loading by far heavy vehicles arrangement assumed in 3.2, may be also significant, considering the results of the higher stress range occurred in the analysis in 4. and the studies described in Ref.[13,14].

REFERENCES

1. English bridge cables fail, ENR/ April 8, 1982.
2. Severn Bidge woes mount, ENR/ Dec. 2, 1982.
3. The Severn Suspension Bridge, T.O.Elworthy & Son Ltd., June 1964.
4. Roberts, Sir G., The Severn Bridge, A New Principle of Design, Proc. Symp. Suspension Bridge (Lisbon), Nov. 1966.
5. Severn Suspension Bridge, General Information.
6. Frazer, R.A. and C. Scruton, A Summarized Account of the Severn Bridge Aerodynamic Investigation, NPL Aero Report 222, 1952.
7. Okugawa, A., Tension and Fatigue Tests for Hanger Ropes of Suspension Bridges, Honshi-Giho (Honshu-Shikoku Bridges Technical Report), Vol.2, No.5, July 1978 (in Japanese).
8. British Standards Inst., BS 5400:Part 2:1978, Steel and Concrete and Composite Bridges, Part 2, Specification for Loads.
9. Wardlaw, R.L., H. Tanaka and H. Utsunomiya, Wind Tunnel Experiments on the Effects of Turbulence on the Aerodynamic Behaviour of Bridge Road Decks, Proc. 6th Int. Conf. Wind Engineering (Gold Coast/ Australia), March 1983.
10. Davenport, A.G., N. Isyumov and T. Miyata, The Experimental Determination of the Response of Suspension Bridges to Turbulent Wind, Proc. 3rd Int. Conf. Wind Effects on Structures (Tokyo), Sept. 1971.
11. Miyata, T. and M. Ito, Evaluation of Gusts on Flexible Structures, Pre. Report 9th Congress of IABSE (Amsterdam), May 1972.
12. Bridge Aerodynamics, Thomas Telford Ltd., pp.3-20, 1981.
13. The case against inclined hangers, New Civil Engineer, 15 April,1982.
14. Hanger fatigue in perspective, New Civil Engineer, 29 April, 1982.

Influence of Aerodynamic Stability on the Design of Bridges

Influence de la stabilité aérodynamique sur le projet de ponts

Wirkung der aerodynamischen Stabilität auf den Entwurf von Brücken

J.R. RICHARDSON
Applied Fluid Mech. Div.
NMI Ltd.
Teddington, England

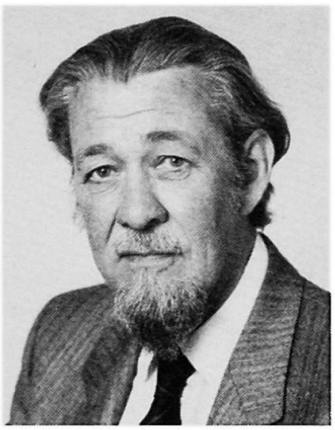

Roy Richardson has worked in the aircraft industry, in private practice, and in government service on the theory and practice of both fluid-dynamics and structures for more than 30 years. At NMI Ltd. his field of research has included offshore structures and wind engineering.

SUMMARY
This article reviews past and present methods of preventing aerodynamic instabilities on long suspension bridges. The current trend in design philosophy is to improve the aerodynamic characteristics and control the inertia, instead of simply increasing the structural stiffness. This has led to some unconventional new forms of road deck, which will enable much greater spans to be built in the future.

RESUME
L'article présente une revue des méthodes anciennes et actuelles pour éviter les instabilités aérodynamiques dans des longs ponts suspendus. La tendance actuelle des projeteurs est d'améliorer les caractéristiques aérodynamiques et de contrôler l'inertie, plutôt que d'augmenter la rigidité structurale. Cette tendance conduit à quelques nouvelles formes de tablier, qui conduiront à l'avenir à des travées plus larges.

ZUSAMMENFASSUNG
Dies ist ein Beitrag über frühere und gegenwärtige Methoden der Verhinderung aerodynamischer Instabilität bei grossen Hängebrücken. Die heutige Planungstendenz geht dahin, die charakteristischen aerodynamischen Eigenschaften zu verbessern und die Trägheitskräfte zu kontrollieren, anstatt einfach die Steifigkeit zu erhöhen. Das hat zu einigen unkonventionellen neuen Formen von Fahrbahnträgern geführt, die in Zukunft das Bauen viel grösserer Spannweiten ermöglichen werden.

1. INTRODUCTION

The design philosphy for very long-span bridges has become increasingly influenced by the problem of aerodynamic stability. Past efforts to combat this problem by providing high torsional stiffness in the deck have become uneconomic. Long bridges are invariably cable supported, so that the resulting heavier deck increases the dead-load on the cables. Alternative solutions can, however, be achieved by a proper understanding of the problem.

There is an historic parallel between bridge and aircraft design during the past 40 years. Bridges were getting longer and aircraft were going faster. Stiffness was overtaking strength as the design criterion for both types of structure. In the aeronautical field a great deal of flutter research had already been done [1], but the Tacoma disaster in 1940 left bridge designers starting almost from scratch. Although research was quickly commissioned [2], this relied heavily upon aircraft experience.

Solutions to the aircraft flutter problem were invariably sought through changes of stiffness and inertia distribution, because the aerodynamic configuration was determined by its efficiency as a vehicle. Bridge design followed this route, although deck symmetry gave little scope for inertia changes, so that stiffness was the goal in practice. In recent years, however, more attention has been devoted to modifying the aerodynamic properties of the road deck in an effort to reduce the economic penalty of high stiffness.

2. AERODYNAMIC STABILITY

2.1 The Aeroelastic Triangle

Many years ago, Collar [1] gave an illuminating description of the nature of aeroelastic stability. His triangle (Fig.1) shows the three fundamental kinds of force - structural stiffness, aerodynamic and inertia - which can combine to give various phenomena. Those which involve only two kinds of force are the most easily understood. Stiffness and inertia combine to give structural vibrations. Stiffness and aerodynamics can lead to divergence - a kind of aerodynamic buckling. Finally inertia and aerodynamics determine the stability of a rigid aircraft - a problem irrelevant to bridges.

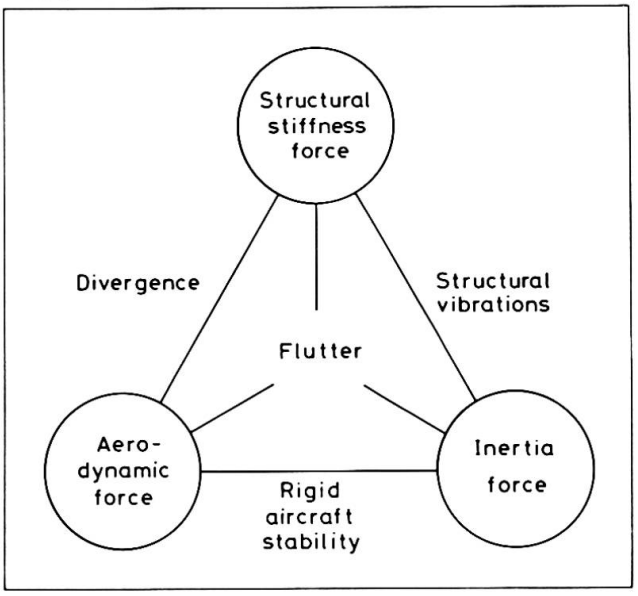

Fig.1 Aeroelastic triangle.

Flutter is more esoteric, being caused by a combination of all three forces. It is a growing oscillation which occurs above some critical wind speed, and it can easily destroy the structure. Below this speed the air forces damp each of the vibration modes.

2.2 Types of Instability

In this paper we are concerned only with true instabilities, not with resonant vibrations due to forcing from shed vortices or turbulence. Two unstable

phenomena can occur on bluff deck sections, such as those with plate stiffening girders. One is a motion in pure bending - called "galloping" - caused by negative aerodynamic damping at certain wind inclinations. The other, in pure torsion, is also due to negative aerodynamic damping. As will be shown, even a slender deck has little aerodynamic damping in torsion. However, since we intend to avoid such unstable deck sections, we will concentrate upon divergence and coupled flutter.

When the deck is twisted, the wind gives it both a lift force and a pitching moment. The latter tends to increase the angle of twist since the lift centre acts at the quarter point of the deck on the windward side. It is thus a negative torsional stiffness which increases with wind speed. At some critical wind speed it overcomes the torsional stiffness of the structure and buckles the deck statically. This is "divergence".

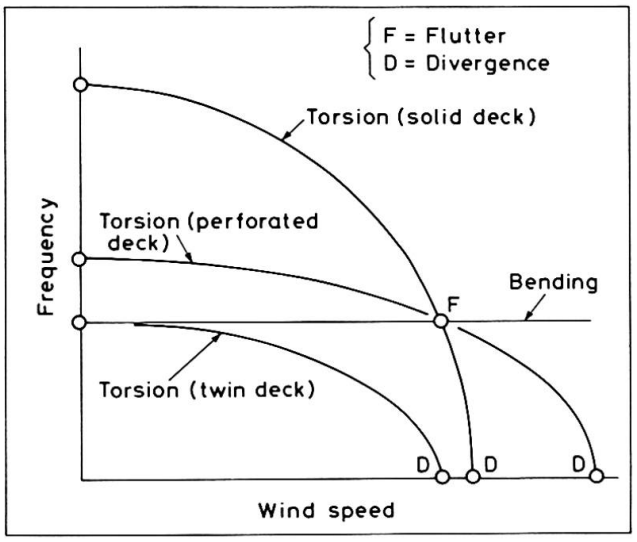

Fig.2 Flutter and divergence.

The same destabilising moment is responsible for "flutter". At wind speeds below divergence the torsion frequency is finite, but lower than that in still air (Fig.2). The bending frequency, on the other hand, remains sensibly constant because the aerodynamic forces give damping instead of stiffness forces in this mode. The two frequencies therefore coincide at a wind speed below that of divergence. Secondary forces then couple the bending and torsion modes to produce an unstable oscillation.

This simplified explanation ignores the effect of aerodynamic damping which, although a secondary force, can be significant in some circumstances.

2.3 Effect on Design

When the physical nature of the aerodynamic-structural-inertia interaction is understood, the designer has the opportunity to vary all three forces in an optimum manner to ensure bridge stability at minimum cost. First, however, practical ways of changing each kind of force must be considered.

3. STRUCTURAL STIFFNESS

3.1 Bending

Very long spans are invariably suspension bridges, whose bending stiffness and frequencies are determined naturally by gravity and the elastic properties of the cables. Secondary stiffness, provided by stay-cables or girder stiffness have a significant effect only for relatively short spans. Little opportunity thus exists to alter the bending characteristics.

3.2 Torsion

In conventional bridge design, flutter is avoided by increasing the torsional stiffness. This can be achieved in a variety of ways.

Girders attached to the deck extremities, in the manner of earlier bridges (Fig.3a), give resistance to twisting. This is obtained from warping of the deck - or differential bending of the girders - which is efficient only for very short spans. Furthermore the bending stiffness is increased in proportion, so that the frequency ratio remains essentially unchanged.

When a second lateral shear bracing, as pioneered by Steinmann, is added below the road deck, it forms a torsion truss with the side girders and the deck itself (Fig.3b). This dramatically increases the torsional stiffness, because shear rather than bending forces are involved. Since the bending stiffness is unaltered the frequency ratio is greatly improved.

Another type of lattice truss, the "monocable", has been proposed by Leonhardt (Fig.3c). In this design a triangular box is formed by a single suspension cable at the apex and the road deck at the base. The nearly vertical shear panels are provided by inclining the hangers in the manner of a Warren girder, so that they double as both strength and stiffness members. Although the "box" area increases towards the towers, the shear efficiency of the hangers is reduced in this region because they become nearly vertical to maintain a constant spanwise pitch. The torsion stiffness may therefore be lower at the towers than at mid-span.

A streamlined steel torsion box was first used by Freeman Fox and Partners on the Severn crossing (Fig.3d). It uses steel more efficiently than a truss, and owes much to aircraft practice. Nevertheless it has the same limitations as other box structures, because its depth must increase when greater spans are contemplated. Its limit-span may have been reached with the Humber bridge.

When, for other reasons, the need for torsional stiffness can be reduced, widely spaced cables present an alternative to torsion boxes (Fig.3e), as has been proposed by W C Brown of Freeman Fox & Partners. Although two towers are needed at each pier, and transverse beams to support the central road, this solution has much to commend it.

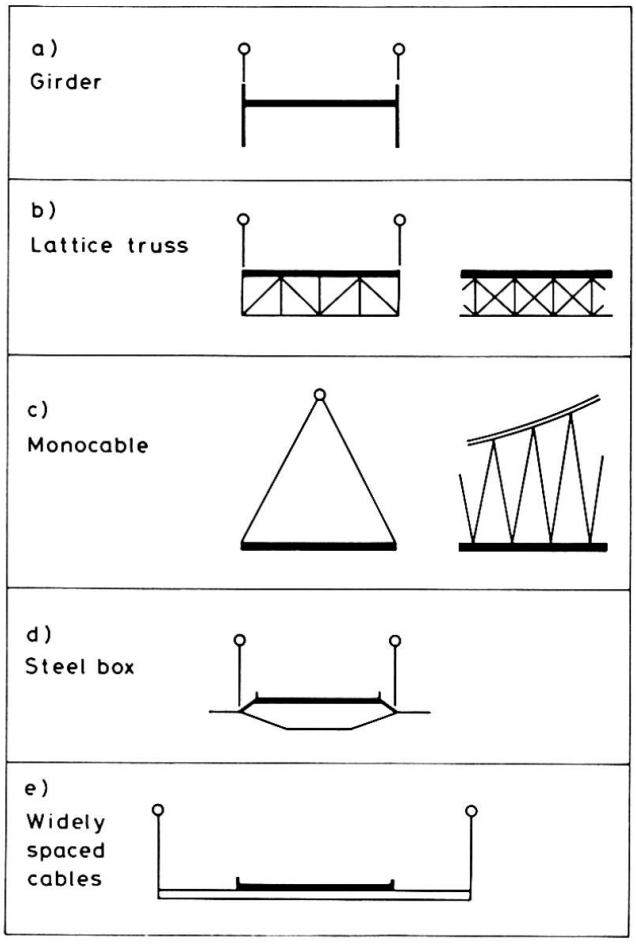

Fig.3 Types of torsional stiffening.

4. AERODYNAMIC FORCES

Since our purpose is to review the design implications of various deck configurations, we will consider only the steady or quasi-steady forces acting on the opaque segments of thin road decks. Unsteady aerodynamic effects, which reduce the lift and cause phase lags, and bluffness which causes separation of the flow will be largely ignored. Two types of force are involved. Aerodynamic

stiffness is proportional to displacement and damping is proportional to velocity. The bending mode has no aerodynamic stiffness since the angle to the wind is unchanged. However, it has considerable damping, because its vertical velocity combines with the wind speed to give an effective angle of attack. The torsion mode has aerodynamic stiffness which is identical in form to that caused by bending velocity, since the deck is at an angle to the airstream. Its damping is more complex, however, because the vertical velocities increase linearly from the centre of the deck. These aerodynamic forces on various deck configurations will be described in turn.

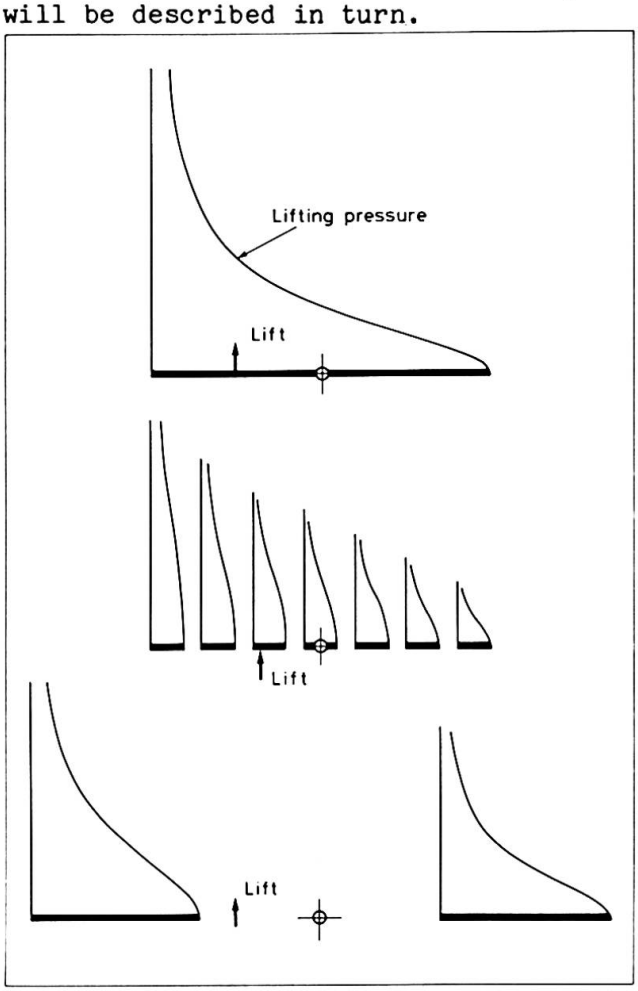

Fig.4 Lift due to pitch angle.

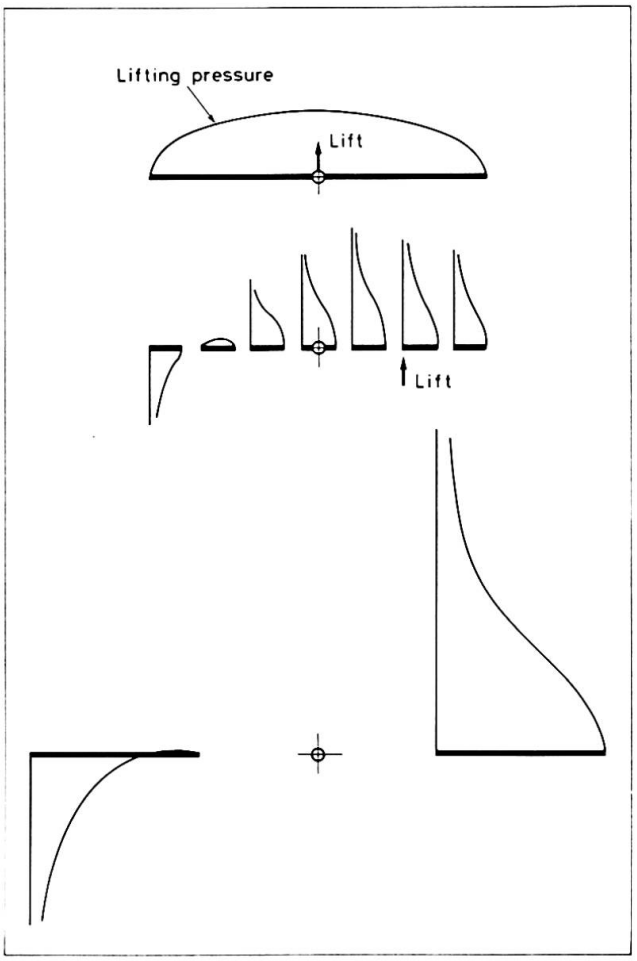

Fig.5 Lift due to pitch velocity.

4.1 Conventional Decks

A thin opaque road deck behaves like a wing. At an angle of twist, or when subjected to a vertical velocity, the wind causes lifting pressures which give both lift and pitching moment (Fig.4). The lift centre is at the quarter point of the deck and thus provides the destabilising moment discussed previously. Torsion velocity gives an elliptical lift distribution (Fig.5). This has a lift but no moment, so that the torsion damping is theoretically zero. Unsteady aerodynamic effects make this damping positive, but bluffness may have the opposite effect. The flutter speed of a conventional road deck can thus be sensitive to its aerodynamic shape.

4.2 Double Decks

On truss-stiffened bridges the lower shear bracing is often replaced by a second road deck. The aerodynamic forces on the two decks then resemble those on

biplane wings. The total lift force, due to angle of twist, is reduced as the gap between the decks become less. The centre of lift, however, moves ahead of the quarter-chord so that the effect on the destabilising moment is less pronounced. Unfortunately the quasi-steady torsion damping is still theoretically zero because the lift distribution due to torsional velocity is still symmetric. This can be alleviated to some extent by separating the vertical position of the torsion and drag centres, so that horizontal velocities of the deck contribute to its torsional damping [3].

4.3 Perforated Decks

Although small aerodynamic slots have been used on many bridges, the idea of a true perforated deck is due to W C Brown. Experimental and theoretical work at NMI [4,5] has uncovered some important facts about this concept. When multiple slots are introduced in a thin road deck the lifting force due to wind inclination is reduced directly in proportion to the deck "solidity". Furthermore, the centre of lift is moved closer to the midchord so that the moment is proportional to the square of the solidity. Thus, with a typical solidity of 70%, the destabilising moment is reduced to 49% of that of a solid deck (Fig.4). This means that the torsional frequency can be reduced to maintain the same flutter speed (Fig.2).

An additional advantage of deck perforations is that positive damping occurs in the torsion mode. The lift distribution due to pitch velocity (Fig.5) is no longer symmetrical, having a downward force on the windward side.

4.4 Twin Decks

A logical extension of the perforated deck is the twin deck. When the two traffic carriageways are separated laterally, leaving a huge "slot" between them, some remarkable aerodynamic effects take place [6]. In an inclined wind the lift distribution gives exactly the same total lift and moment as the unseparated decks. The lift centre is unaffected by the separation (Fig.4).

Pitch velocity, however, results in a very different lift distribution to that of a solid deck (Fig.5). The windward deck has a large downward force on it, so that the aerodynamic damping in the torsion mode is highly positive.

The implications of these facts will be described in later sections of this paper.

5. INERTIA FORCES

Bridge decks are symmetrical and must be stable in winds blowing from either direction. The opportunity to shift the mass centre to the windward side, and thus prevent flutter by "mass balancing" as on aircraft, is therefore severely limited. During the construction phase of the Humber bridge, the author's suggestion of temporary water bags on each side of the deck, one of which could be drained when the direction of a high wind was known, proved successful. Such a measure for a completed bridge would, however, add to the dead load.

The radius of gyration of the mass in the torsion mode is therefore the only inertia parameter which can be varied by the designer. On a conventional bridge this is invariably less than half the distance between the cables, so that the still air torsion frequency is always higher than that of bending, even without

a torsion box. If the radius of gyration could be increased to lower the torsion frequency to that of bending, flutter (but not divergence) could be eliminated. Unfortunately, this leads to nearly zero damping of the torsion mode on a conventional deck. However, a perforated or twin deck does not suffer from this problem when the still air frequencies coincide, because each has an inherent damping in torsion.

6. FUTURE DESIGN

A variety of means of controlling the aerodynamic, inertia and structural stiffness forces independently have been presented. When individual possibilities are combined together, a number of new forms for stable large-span bridges emerge. Three of these will be described.

6.1 The Proposed Tsing-Ma Bridge

The design of this bridge was recently completed by Mott, Hay and Anderson, as part of the system to join Lantau Island to the mainland in Hong Hong. Its deck structure is a conventional lattice-truss designed to carry motor traffic and commuter trains on two levels. Streamlined fairings cover the ends of the truss to reduce the drag and vortex excitation, and large aerodynamic slots are provided under the railway lines and between the carriageways on the upper deck (Fig.6). Its aerodynamic characteristics are thus a combination of the double and slotted decks. Tests at NMI Ltd [7] proved it to be stable in typhoon winds.

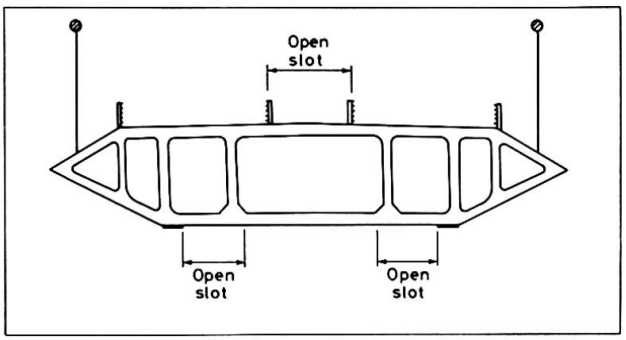

Fig.6 The Tsing-Ma design.

6.2 The Proposed Messina Bridge

Freeman, Fox and Partners have combined the principles of the perforated deck and widely spaced cables in a design for a bridge across the Messina Straits with a mainspan of 3300m (Fig.7). The central roadway contains multiple slots which are covered by grills, and is supported on transverse beams connected to the hangers. Twin railway tracks under the road are braced to the crossbeam extremities by stay cables. Since the deck has no significant torsional stiffness, twisting is resisted by the widely spaced suspension cables. Despite the the fact that its bending and torsion frequencies are much closer together than is usual, the bridge has been shown to be stable in high winds because the deck slots reduce the destabilising aerodynamic moment (Fig.2).

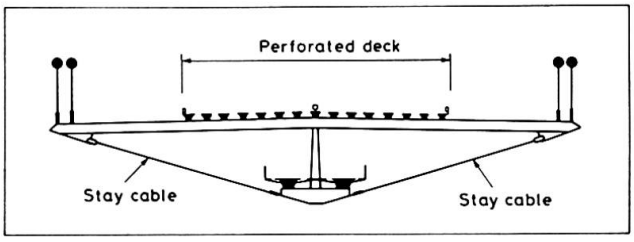

Fig.7 The Messina Straits design.

6.3 Twin Bridges

The twin-bridge (Fig.8), as yet only a design concept [6], uses the physical properties of all three types of force to give aerodynamic stability. Torsional

stiffness is provided by widely spaced cables. The radius of gyration of the deck is raised by suspending each half under one of the (pairs of) cables, leaving a large gap between them which is traversed by crossbeams at intervals along the span. This equalises the bending and torsion frequencies. The separation of the deck halves does not increase the destabilising aerodynamic moment, so that the divergence speed is not affected. However, it provides considerable aerodynamic damping in torsion. Flutter is therefore completely eliminated by the frequency coincidence (Fig.2), without incurring the serious consequences of poor torsional damping.

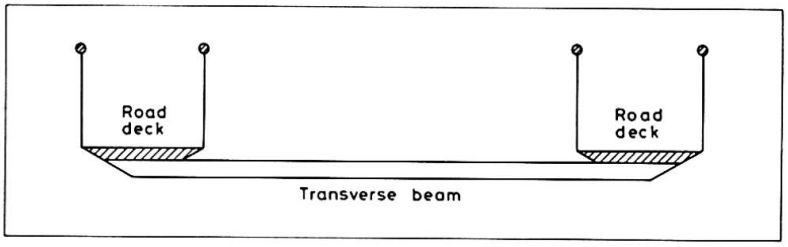

Fig.8 The twin-bridge concept.

The advantage of such a design is that the road decks can be shallow and light in weight, thus reducing the amount of steel required in the cables.

7. CONCLUDING REMARKS

A recent trend in bridge design is to seek better aerodynamic forms for the road deck, to avoid providing heavy torsion boxes which become increasingly uneconomic as longer spans are contemplated. Modifications to the inertia properties can also be used to advantage. Future bridges of much greater length are now possible, but they will look very different from current designs.

REFERENCES

1. COLLAR A.R., The Expanding Domain of Aeroelasticity. J.Royal Aero. Soc. Vol L, August 1946.

2. BLEICH F., McCULLOUGH C.B., ROSENCRANS R. and VINCENT G.S., The Mathematical Theory of Vibration in Suspension Bridges. U.S. Department of Commerce, Washington, 1950.

3. IRWIN H.P.A.H., Centre of Rotation for Torsional Vibration of Bridges. Journal of Industrial Aerodynamics. 4, 1979.

4. WALSHE D.E., TWIDLE G.G. and BROWN W.C., Static and Dynamic Measurements on a Model of a Slender Bridge with a Perforated Deck. International Conference on the Behaviour of Slender Structures. The City University, London, 1977.

5. RICHARDSON J.R., Aerodynamic Forces on Perforated Bridge Decks. NMI Report 118, 1981.

6. RICHARDSON J.R., The Development of the Concept of the Twin Suspension Bridge. NMI Report 125, 1981.

7. CURTIS D.J., HART J.J., SCRUTON C. and WALSHE D.E., An Aerodynamic Investigation for the Suspended Structure of the Proposed Tsing-Ma Bridge. Engineering Structures, Butterworths, (to be published).

CN Tower, Toronto: Model and Full Scale Response to Wind

Essais sur modèle et comportement réel au vent de la Tour CN, Toronto

CN Tower, Toronto: Berechnungsmodell und gemessenes Verhalten unter Windbelastung

Nick ISYUMOV
Univ. of Western Ontario
London, ON, Canada

Alan G. DAVENPORT
Univ. of Western Ontario
London, ON, Canada

Jaak MONBALIU
Univ. of Western Ontario
London, ON, Canada

Nick Isyumov obtained his undergraduate degree in Engineering Science in 1960 and his Ph.D. in 1971, both from the University of Western Ontario. He is the Manager and Associate Research Director of the Boundary Layer Wind Tunnel Laboratory.

Alan Davenport obtained his B.A. and M.A. from Cambridge University England in 1954 and 1958. In 1957 he received his M.A. Sc. from the University of Toronto and a Ph.D. from the University of Bristol in 1961. He is a Professor in Civil Engineering and the Director of the Boundary Layer Wind Tunnel Laboratory.

Jaak Monbaliu received a Civil Engineering degree in 1982 from the Catholic University of Leuven, Belgium. He is currently studying towards his Masters at the University of Western Ontario.

SUMMARY
The design of the 555 m high free standing CN Tower in Toronto for the action of wind was based on the findings of a comprehensive wind tunnel model study. This paper presents an overview of that study and provides comparisons with actual observations. The program of full-scale measurements, started in 1976, has provided information on properties of the wind and the response of the tower. The comparisons, although limited, are favourable and lend confidence to wind tunnel modelling techniques.

RESUME
Le projet de la tour CN à Toronto, de 555 m de hauteur, a été réalisé sur la base d'une étude approfondie et d'essais aérodynamiques sur modèle. Les résultats de l'étude sont présentés et comparés avec les mesures effectuées sur la tour. Le programme de mesures en vraie grandeur, commencé en 1976, donne des informations sur les caractéristiques du vent et le comportement de la tour. Les comparaisons, bien que limitées, sont positives et favorables aux techniques utilisées pour les essais en soufflerie.

ZUSAMMENFASSUNG
Die Berechnung des 555 m hohen, frei stehenden CN Tower in Toronto für Windbelastungen basiert auf den Erkenntnissen aus umfassenden Modellversuchen im Windtunnel. Dieser Beitrag gibt eine Übersicht über die Resultate dieser Versuche und enthält Vergleiche mit Messungen am Bauwerk. Das umfassende Messprogramm, gestartet 1976, lieferte Informationen über die Windeigenschaften und über das Verhalten des Turmes. Die Vergleiche, wenn auch begrenzt im Umfang, sind vielversprechend und stärken das Vertrauen in Modellversuche im Windtunnel.

1. INTRODUCTION

The approximately 555-m high CN Communications Tower in Toronto has now been operational for nearly a decade. The action of wind on this unique tower, which remains the world's tallest free standing structure, was extensively studied in a wind tunnel model study, carried out at the Boundary Layer Wind Tunnel Laboratory during the design of the tower. This study provided information on the overall wind loads and responses of the structure, the action of wind on various components, and its effects on the tower performance including transmission quality. A program of monitoring and recording the wind induced response of the tower and some meteorological data was started in 1977. Participants in this co-operative study included the Department of Civil Engineering at the University of Toronto, the Atmospheric Environment Service of Environment Canada, the Division of Building Research of the National Research Council and the Boundary Layer Wind Tunnel Laboratory (BLWTL).

This paper describes the wind tunnel model studies carried out for this tower with emphasis on the aeroelastic simulation. An overview is provided of the program of monitoring and recording of the wind induced response of the full scale tower and some properties of the wind. Finally, this paper presents some results of the full scale program along with comparisons obtained from the wind tunnel model study. The analysis of the full scale data is continuing and the presented information is of an initial rather than a comprehensive nature.

2. WIND TUNNEL MODEL STUDIES

A comprehensive program of wind tunnel model studies was carried out to provide information on various wind related questions affecting the design of the structure. This program continued over a period of some 6 years and included the following main parts:

i) Aeroelastic and section model wind tunnel tests were carried out to evaluate an earlier version of the tower. It was subsequently replaced by the present tower configuration which was found to be aerodynamically and economically more effective.

ii) An aeroelastic model simulation of the tower was carried out at a geometric scale of 1:450 in turbulent boundary layer flow conditions representative of wind at the project site from various compass directions. This part of the study defined the wind loads on the concrete shaft and the steel antenna and provided information on the wind induced response of the tower. This included data on the displacements and rotations of the antenna mast and the accelerations of the tower at the restaurant and other levels.

iii) A static pressure model was tested at a geometric scale of 1:450 to provide information on the local peak pressures and suctions on the elevator shaft glazing, at the restaurant and upper observation levels and at the lower accommodation levels, including the pool lobby and other lower buildings at the tower base. It is noteworthy that some of the highest local exterior suctions found in the entire study occurred on the pool lobby.

iv) A limited study of pedestrian level winds at the base of the tower was made using the pressure model of the tower and lower accommodation levels. These measurements indicated relatively high wind speeds, particularly near the three tapered legs of the shaft.

v) A partial model of the upper accommodation levels and adjacent parts of the shaft was studied at a geometric scale of 1:60 to examine the action of wind on the air-supported radome enclosing the microwave transmission equipment just

below restaurant level. The radome was modelled aeroelastically and information was provided on the internal pressurizaton required to limit deformations and assure its performance at high wind speeds.

vi) Analytical estimates were made to evaluate the effectiveness of two tuned mass dampers attached to the antenna mast. These two auxiliary mass absorbers were designed to ensure a minimum level of damping in the second, fourth and fifth modes of vibration of the tower. While the aeroelastic model study did not indicate excessive movements of the antenna mast, these dynamic absorbers were added to increase the reliability of performance.

vii) Some initial observations of the full-scale response were made during the construction of the tower. These measurements provided important validations of assumed tower properties. The most significant of these were made after the completion of the concrete shaft. These confirmed the structural damping used in the aeroelastic model study and the anticipated mass and stiffness properties.

viii) Meteorological data for the Toronto area were analysed to arrive at a statistical model of the probability distribution of gradient wind speed and wind direction for the area. This model provided an estimate of the probability of exceeding particular levels of wind speed from different azimuth directions and was used in the synthesis of the wind tunnel model findings to provide predictions of various wind induced full scale effects.

Only the aeroelastic model simulation is discussed in further detail at this time. A photograph of the 1:450 scale aeroelastic model mounted in the wind tunnel is shown in Fig. 1. The aeroelastic model was designed to simulate the exterior geometry of the tower and its stiffness, mass and damping properties. Details of aeroelastic similarity requirements are described elsewhere (1,2,3). Aeroelastic similarity was achieved by maintaining the equality of the following non-dimensional ratios in model and in full scale:

$$\textit{mass scaling:} \qquad \frac{\rho_s}{\rho} = \frac{\textit{inertia forces of tower}}{\textit{inertia forces of flow}} \qquad (1)$$

$$\textit{stiffness properties:} \qquad \frac{EI}{\rho V^2 L^4} = \frac{\textit{elastic forces of tower}}{\textit{inertia forces of flow}} \qquad (2)$$

$$\textit{damping:} \qquad \zeta_s = \frac{\textit{dissipated forces in tower}}{\textit{inertia forces of tower}} \qquad (3)$$

where ρ_s, ρ, E, I, V, L and ζ_s are representatively the bulk density of the tower, the air density, the elastic modulus or equivalent, the second moment of area the wind speed, a characteristic length and the structural damping expressed as a proportion of critical damping. Gravity forces were not modelled as the stiffness of the tower is dominated by elastic forces. The velocity scale, determined by the maximum speed of the wind tunnel and practical considerations of satisfying equation (2), was 1:5. This established the time scale at 1:90. The aerodynamics of the tower are largely determined by its sharp edged geometry and Reynolds number scaling was not a major consideration.

The model was constructed using a metalized epoxy commercially available under the trade name Devcon A. This material has a low modulus of elasticity and values of a density and damping comparable to those of concrete. The model tower was con-

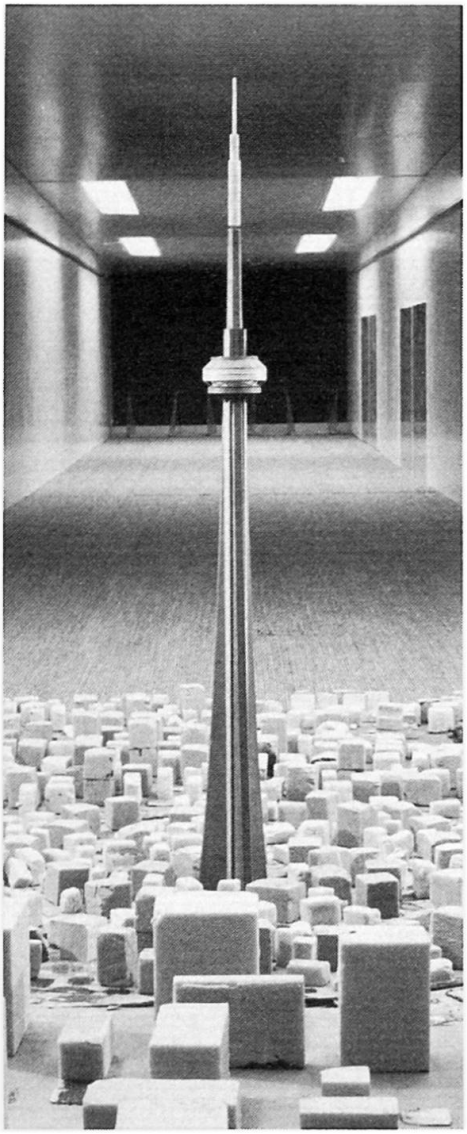

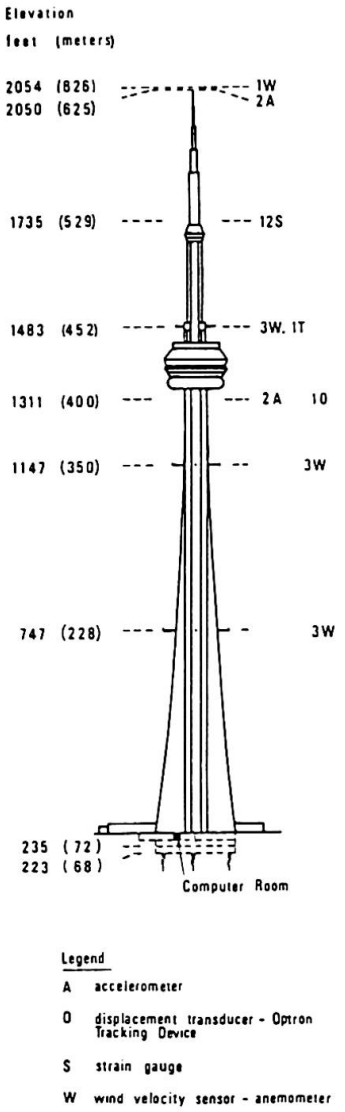

Fig. 1 View of Aeroelastic Model of Tower in Wind Tunnel and Summary of Full Scale Wind and Response Sensing Instrumentation of Full Scale Tower

structed using sheets of Devcon A precast to the correct thickness. These sheets, with a thickness as low as 0.25 mm in some cases, were cut and glued to form the shape of the tower shaft. The structural properties of the antenna mast were simulated by a specially fabricated spline using aluminum and hypodermic tubing. This spline was enclosed by non-structural radomes made of styrofoam to the correct exterior dimensions.

The instrumentation of the aeroelastic model included a strain-gauged balance capable of measuring the static and dynamic overturning and torsional moments at the base of the tower; accelerometers at the restaurant level; and strain-gauges on the antenna spline which measured the overturning moments at the base of the antenna mast in two orthogonal directions. The model was tested in turbulent boundary layer flow conditions representative of natural wind at the project site for a full range of wind directions and a range of wind speeds. In most of the tests model wind speeds simulated full scale values up to about 55 m/s (125 mph). Higher wind speeds were examined in selected cases.

3. OVERVIEW OF FULL SCALE MONITORING PROGRAM

The instrumentation used to measure the properties of the wind and the tower response is summarized in Fig. 1. Bendix-Friez anemometers and directional vanes are located at elevations of 228, 350, 452 and 626 metres. The top level has a single anemometer. The other levels have three anemometers each located on a boom extending 9.1 m (30 ft) beyond the end wall of each of the three tapered legs. Other instrumentation shown in Figure 1 include accelerometers at elevations of 400 and 625 m, an Optron tracking device at an elevation of 400 m and strain-gauges on the antenna mast at an elevation of 529 m. Details of other instrumentation, including other strain-gauges, gas analyzers and temperature probes, can be found elsewhere (4,5,6). The data acquisition and recording system was capable of sampling 80 channels of data continuously at a rate of 5 Hz. In the normal operating mode, the sampled data are analyzed in real time and only 10 minute average data are logged on magnetic tape. During strong winds all data are recorded on magnetic tape. These two data bases are respectively referred to as "average" and "high speed" data. Details of procedures used and assessments of data reliability and quality can be found elsewhere (4,5,6,7). Not all of the instrumentation functioned reliably and the assessment of data quality has become an important aspect of data analysis.

3.1 Wind Structure

The anemometers at elevations 228, 350 and 452 m despite the 9.1 m booms, are within the aerodynamic influence of the tower and the measured wind speeds and directions must be corrected. Correction factors, which relate the recorded wind speeds and directions to ambient values were obtained from wind tunnel model tests at the BLWTL (8). While the top anemometer at elevation 626 m, has functioned throughout most of the program, the operation of the other anemometers has been intermittent. There are few "high speed" records for which all anemometer levels were operational. While "averaged data" have been used to examine the structure of the mean and turbulent wind (7), more high speed data are necessary before any conclusions can be drawn. Generally, the wind speed at the top anemometer is significantly higher than that at the 452 m and other levels. The intensity of turbulence at the top anemometer is significant. Typical values for winds over land and off-the-lake are about 10 and 5 percent respectively. A typical time history of the wind speed at the top anemometer is given in Fig. 2. A spectrum of the longitudinal component of turbulence, measured at the top anemometer, is presented in Fig. 3. The overall shape is seen to approximately follow the Davenport spectrum (9). The peak wave length in this case has been adjusted to give best fit to the measured data.

Trends to date suggest that the boundary layer at the tower location is significantly deeper than conventionally assumed. Unfortunately more detailed assessments must await further data. For example, there are suggestions that the top anemometer, assumed to require no corrections, may in fact for some wind directions be within the aerodynamic influence of the antenna top.

3.2 Overall Tower Response

Time histories of some of the tower responses during June 20th, 1980 are shown in Fig. 2. These records, taken over approximately 1 hour, are typical of the "high speed" tower data. The wind speed at the top anemometer and the east-west displacement of the tower, measured by the Optron system at the 400 m level, are shown for the full duration of the record. Five minute portions of the wind speed and displacement records are shown at an expanded time scale. Also shown, are the east-west and north-south accelerations at the 400 m level.

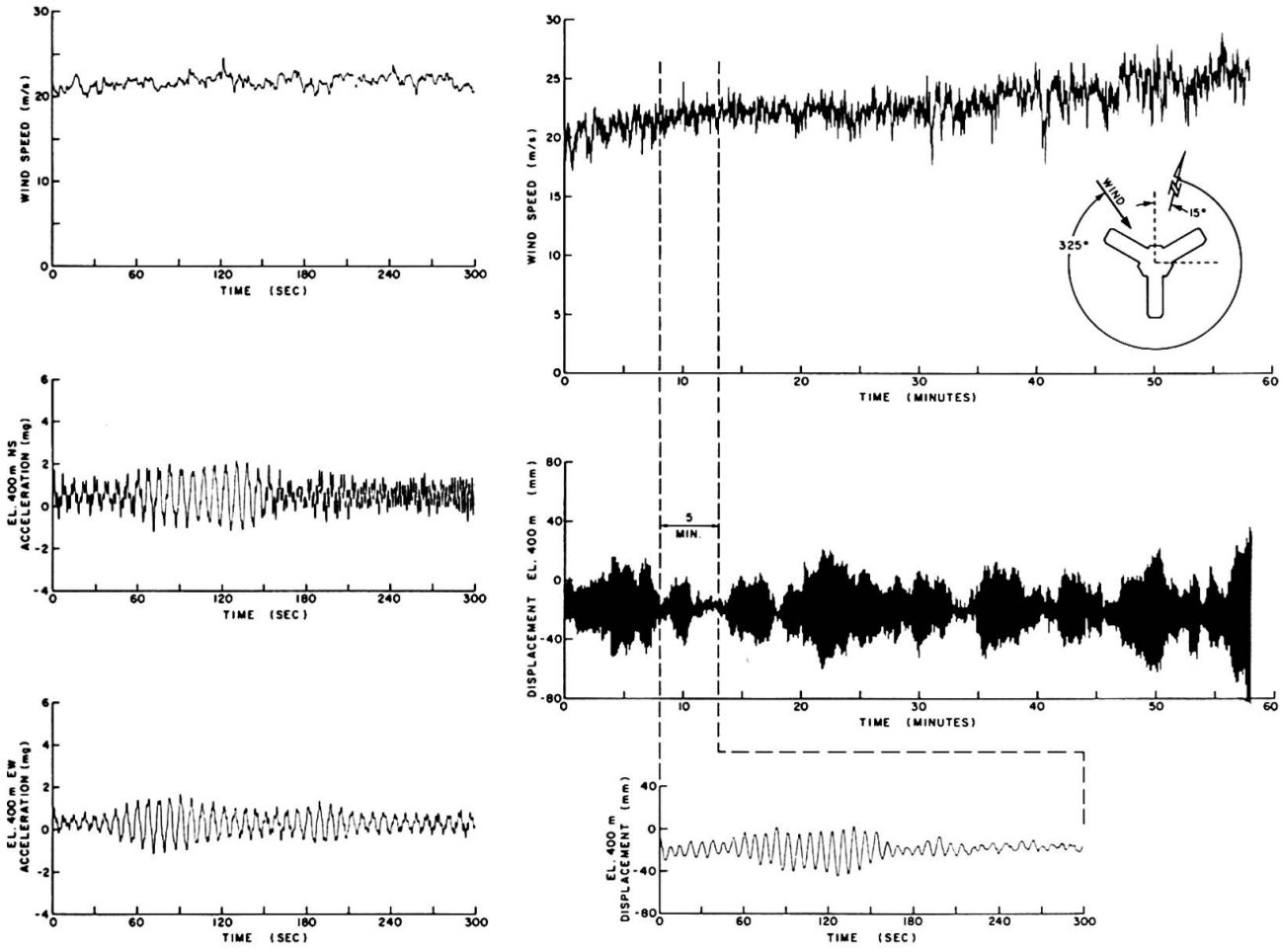

Fig. 2 Time Histories of the Wind Speed at Top Anemometer and Some Tower Responses During June 20, 1980

The wind speed is seen to increase somewhat over the length of the record. Loss of stationarity becomes a concern for longer records. This poses difficulties for spectral analysis as longer records are required to achieve a proper resolution and to reduce statistical variability. Of the various measures of the tower response, the accelerometers at the 400 m and the 626 m levels are found to provide the most reliable measures of the wind induced response. The Optron record, shown in Fig. 2, had to be adjusted in order to correct for instrument drift. The measured displacement is also sensitive to temperature variations. For example, on sunny days there is a pronounced diurnal movement of the tower which follows the sun.

Examining the expanded time history of the tower displacement, the dynamic response is seen to be predominantly in the fundamental mode of vibration. This is consistent with the findings of the aeroelastic wind tunnel study which showed that the wind induced dynamic response of the concrete shaft primarily comprised oscillations in the fundamental mode of vibration. Higher modes of vibration, however become significant for the movements of the antenna mast. Spectra of a number of wind tunnel model and full scale responses are shown in Fig. 4. As seen from the spectra of the base bending moments, both the along wind and across wind dynamic responses of the tower shaft are principally in the fundamental mode of vibration. Spectra of the antenna base moment measured in the aeroelastic study, however indicate significant contributions from higher modes of vibration. The overall behaviour of the tower, predicted by the aeroelastic model, is generally confirmed by the full scale tower data. Spectra of the acceleration at the 400 m level and strain gauges near the antenna are in

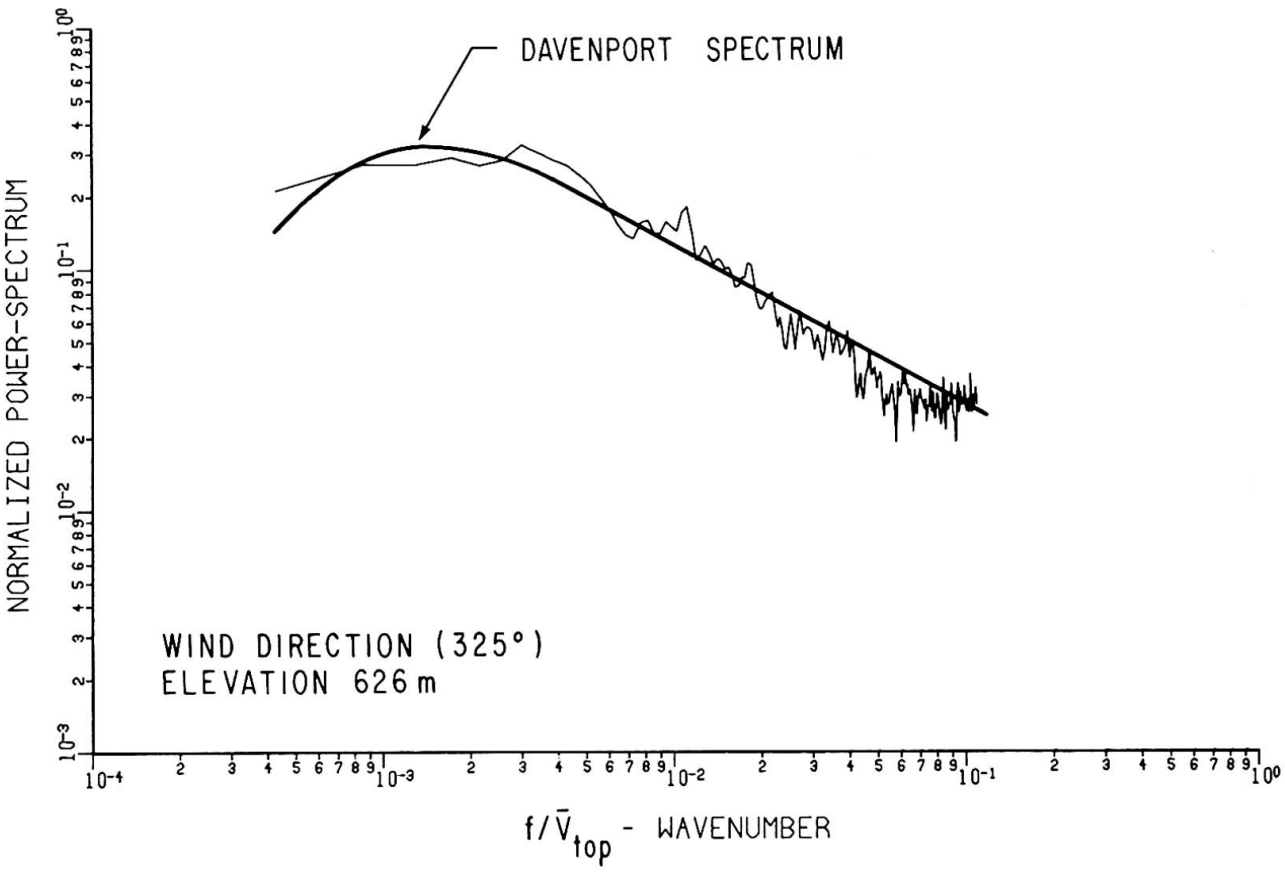

Fig. 3 Power Spectrum of Wind Speed at Top Anemometer During June 20, 1980

general agreement with the model study. As seen from the spectra of the accelerations at elevation 626 m, the higher modes of vibration become important near the top of the antenna. The dynamic response of the tower in the along-wind direction is found to be greater than that in the across-wind direction. This confirms aeroelastic model tests which indicated that the drag response dominated for wind speeds of practical interest.

Table 1 summarizes the frequencies of the tower in its first seven modes of vibration. This includes analytical estimates carried out in 1974 with the final projected tower stiffness and mass data measurements of the frequencies of vibration of the tower near its completion in November of 1976. These measurements, made near the base of the antenna, did not indicate any contributions from the 3rd, 6th and 7th mode of vibration. Current estimates are also shown in Fig. 1. Generally, the observed frequencies agree well with analytical estimates which used projected tower properties. Extensive material testing and full scale observations at the completion of the concrete shaft (10) provided improved estimates of the tower properties. Measurements of the tower frequencies to-date have not indicated significant changes with time or with wind speed.

The damping of the structure in its fundamental mode of vibration was initially estimated to be in the range of .5 to .75 per cent of critical (10). Limited estimates of the damping so-far (7) indicate that the structural damping in the fundamental mode of vibration is somewhat below 1% of critical and the total damping including contributions of aerodynamic damping is in excess of 1%.

3.3 Comparisons of Wind Induced Accelerations

Comparisons of wind tunnel and full scale horizontal accelerations for selected

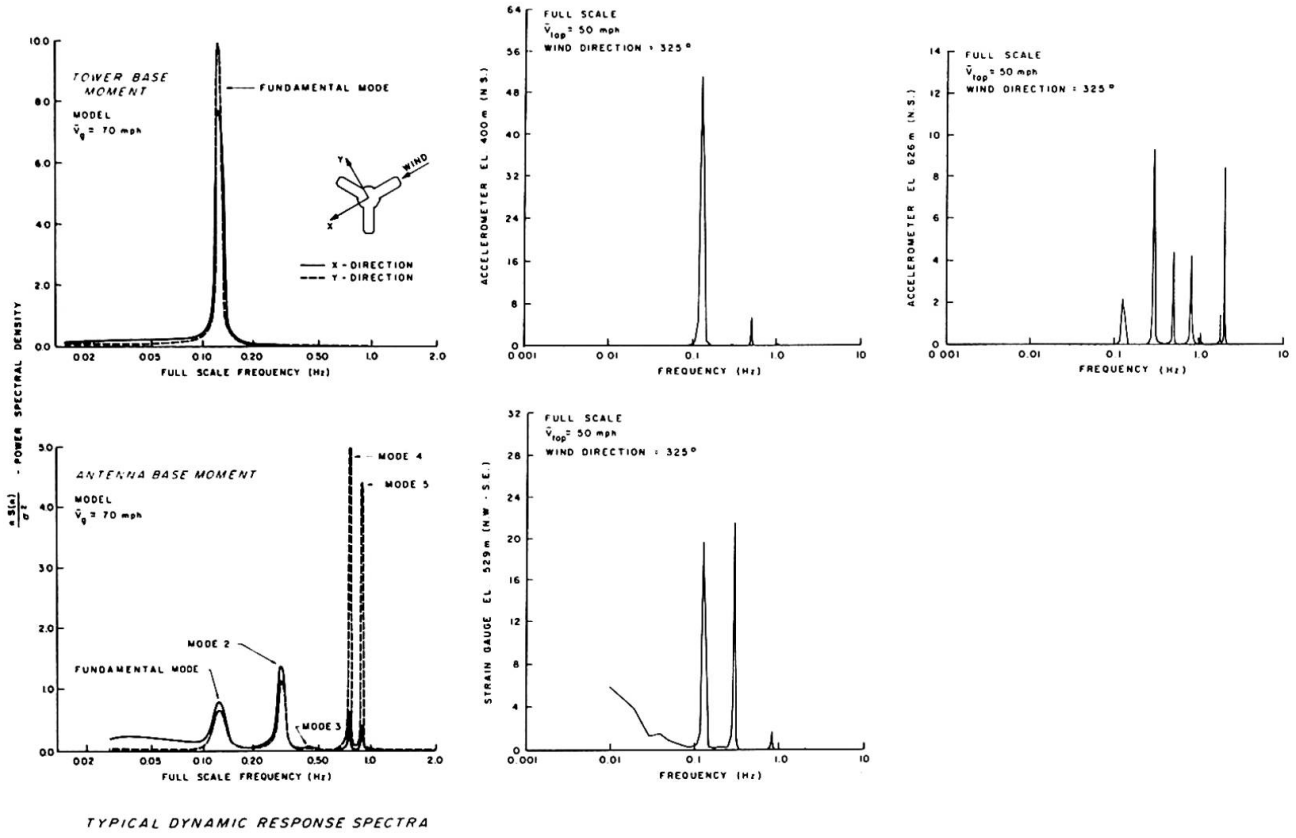

TYPICAL DYNAMIC RESPONSE SPECTRA

Fig. 4 Some Response Spectra From Wind Model Study and Full Scale Observations

TABLE 1

FREQUENCIES OF MODES OF VIBRATION OF TOWER

Mode of Vibration	Analytical Estimate (1)	Measurements Near Completion(2)	From Current Tower Data
1	.124	.129	.127
2	.266	.305	.298
3	.486	-	.483
4	.815	.838	.815
5	1.03	1.07	1.02
6	1.83	-	1.78
7	2.02	-	2.03

(1) Based on final projected tower properties in 1974.
(2) Taken on November 25, 1976 near base of antennna.

wind directions during the period of June 16 to June 22, 1980 are shown in Fig. 5. The comparison is based on the resultant RMS acceleration in both full scale and model. While there is considerable scatter in the full scale observations, the accelerations of the tower at both 400 and 626 m levels tend to approach the wind tunnel data at higher wind speeds. The lowest wind speed examined in the wind tunnel study corresponded to about 25 m/s at gradient height.

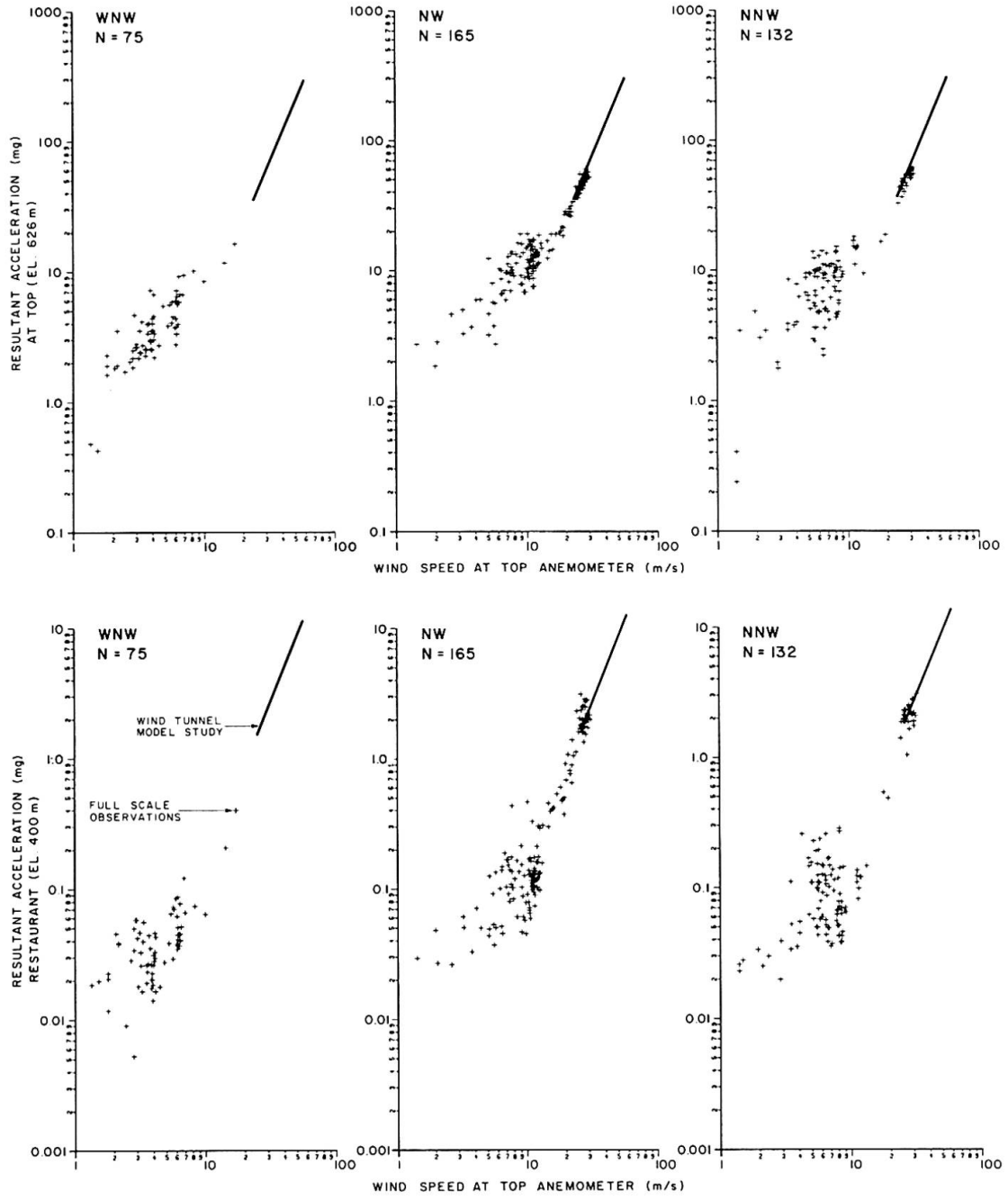

Fig. 5 **Comparisons of Observed Resultant RMS Accelerations With Wind Tunnel Data**

Examining the individual components of the resultant acceleration, the drag accelerations are found to be dominant in both full scale and in the aeroelastic study. While the agreement with the aeroelastic study is good for the data shown in Fig. 5, other directions in particular from the south, showed less favourable agreement. This relates to the overall question of full scale data quality and must wait the analysis of further data before more complete comparisons with the aeroelastic study can be made.

4. CONCLUDING REMARKS

Although the full scale monitoring program has been operational for a number of years, data comparable to the findings of the wind tunnel model study are just now becoming available. Generally there appear to be no surprises in the observed response of the tower. Its dynamic properties tend to be consistent with its design values and indications so far suggest that the wind tunnel model study provided representative estimates of the wind induced response of the tower. Somewhat more unexpected are the properties of the wind. The boundary layer appears to be deeper and the turbulence intensity higher than conventionally anticipated.

Evaluations of the full scale tower response are complicated by difficulties with data quality. Work is currently in progress to improve corrections to the anemometer data to allow for aerodynamic influence of the tower and to generally assure the quality of the data.

ACKNOWLEDGEMENT

The authors would like to acknowledge contributions by Messrs C. Ruigrok and M. Mikitiuk to the development of programs for data handling and analysis.

REFERENCES

1. Whitbread, R. E., "Model Simulation of Wind Effects on Structures", Conf. on Wind Effects on Bldgs. and Structs., Nat. Phys. Lab., June 1963.

2. Vickery, B. J., "Aeroelastic Modelling of Chimneys and Towers", Intl. Workshop on Wind Tunnel Modelling Criteria and Techniques, Nat. Bur. Stds., Gaithersburg, Maryland, April 1982, pp. 21.

3. Isyumov, N., "Aeroelastic Simulation of Building and Structures", ASCE Fall Con., October 1982, New Orleans, Louisiana.

4. Harrison, R. G., "A Study of the Structural Response of the CN Tower During Windstorms", M.A. Sc. Thesis, Dept. of Civ. Engin., Univ. of Toronto, Toronto, Ontario, 1978.

5. Bunjamin, H. H., "Instrumentation of the CN-Tower", M.A. Sc. Thesis, Dept. of Civ. Engin. Univ. of Toronto, Toronto, Ontario, 1981.

6. Collins, M. P., Birkemoe, P. C. and Bunjamin, H., "Structural Behaviour of the CN Tower During a Windstorm", ASCE Nat. Conf., October 1980.

7. Ruigrok, C., "A Preliminary Study of Full-Scale Data From the CN-Tower, Toronto, Canada", M. Eng. Thesis, Fac. of Eng. Sc., Univ. of Western Ontario, London, Ontario, 1984.

8. Davenport, A. G. and Isyumov, N., "The Influence of the Boom Length on Wind Speed Measurements for the CN-Tower, Toronto", The Univ. of Western Ontario, Fac. of Eng. Sc. Res. Rept., BLWT-SS1-1974, January 1974.

9. Davenport, A. G., "The Spectrum of Horizontal Gustiness Near the Ground in High Winds", Ph.D. Thesis, Univ. of Bristol, England, 1961.

10. Isyumov, N. and Brignall, J., "Some Full-Scale Measurements of Wind-Induced Response of the CN Tower, Toronto", J. of Indust. Aero., 1 (1975) pp. 213-219.

System Damping Effects on Cable-Stayed Bridges

Vibration et amortissement des ponts haubannés

Systemdämpfungseffekte von Schrägseilbrücken

Ken-ichi MAEDA
Dr. Eng.
Kawada Industries
Tokyo, Japan

Ken-ichi Maeda, born in 1949, got his Dr. Eng. in 1984 at Osaka University. His major field of activity is long-span bridge engineering. He is at present manager of the Research Laboratory, Kawada Industries, Inc.

Masahiro YONEDA
Res. Eng.
Kawada Industries
Tokyo, Japan

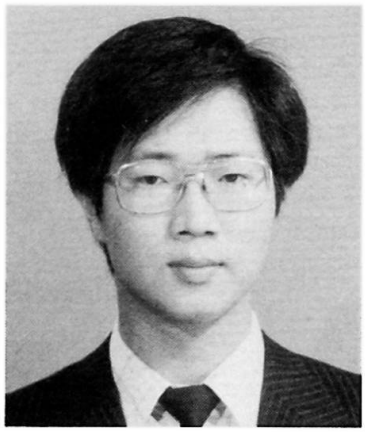

Masahiro Yoneda, born in 1954, got his M. Eng. in 1980 at Kanazawa University. His major field of activity is wind effects on structures. He is employed at the Research Laboratory, Kawada Industries, Inc.

Yukio MAEDA
Prof. Dr.
Osaka University
Osaka, Japan

Yukio Maeda, born in 1922, got his B.E. at Hokkaido University and Dr. Eng. at University of Tokyo. Since 1969 he is Professor of Structural Engineering, Osaka University. At present he is Vice Chairman of Technical Committee, IABSE.

SUMMARY

For the purpose of obtaining basic data on wind resistant design, wind-induced characteristic responses with system damping effects on cable-stayed bridges are studied. The causes of the system damping are defined, and an analytical technique involving time series response using results of a sectional model wind tunnel test is proposed. Then, from an actual bridge test and an analysis of an actual design example, general features are discussed.

RESUME

Dans le but d'obtenir les charges statiques et dynamiques du vent, nécessaires au dimensionnement des ponts suspendus, on étudie les réponses dynamiques du système. Ces réponses dynamiques et leur amortissement ont été étudiées de manière analytique, sur modèles en soufflerie et in situ.

ZUSAMMENFASSUNG

Um grundlegende Daten für die Bemessung auf Wind zu erhalten, werden die charakteristischen Reaktionen unter Windbelastung anhand der Systemdämpfungseffekte von Schrägseilbrücken untersucht. Die wichtigsten Ursachen der Systemdämpfung werden definiert und ein analytisches Verfahren, bei dem die Ergebnisse aus einem Modellversuch im Windkanal verwendet werden, wird vorgeschlagen und anhand eines Versuchs an einer Brücke erörtert.

1. INTRODUCTION

The system damping effect which would prevent bending oscillations of cable-stayed bridges and secure hereby their dynamic safety, was first pointed out by F. Leonhardt[1]. However, judging from the results of full-scale measurements of several bridges built in Japan, the system damping effect cannot be considered as characteristics common to all of the cable-stayed bridges. Namely, it seems that the governing cause and real response are not completely clarified yet, and the development of analytical study is indispensable as well as further actual bridge tests. Because the effects on wind-induced responses, principally observed at a few actual bridge tests and during the construction, are difficult to be directly examined by full-model wind-tunnel tests. Consequently, there are many problems remaining unsolved, and the application to a design has not been generally carried out yet.

In these circumstances, the purpose of the present study is to obtain basic data on the application of the effects of system damping to a wind resistant design. In this paper, first, by investigating the behaviour of so-called internal resonance, the authors define governing causes of the system damping of cable-stayed bridges. Then, the authors treat bending aeolian oscillations among various kinds of wind-induced responses, and propose an analytical technique of time series response using unsteady aerodynamic forces given by a sectional model wind-tunnel test, taking into consideration the internal resonance. Next, the validity of the definition and the analytical technique is confirmed by an actual bridge test. Moreover, the time series response analysis of an actual design example is performed using the results of a spring-mounted model test. Finally, the authors attempt to conclude general features of the present study.

2. DEFINITION OF GOVERNING CAUSES

In this chapter, the authors define that the function of staying cables as a damped absorber[2] in Fig.1 (tuned mass damper in a wide sense) and the beating phenomena (from another angle, a main girder and particular cables exchange their oscillation energy) are governing causes of the system damping of cable-stayed bridges, when so-called internal resonance in terms of bending oscillations of a main girder and of transverse local oscillations of cables remarkably occurs. The defined causes are examined by using a solution of a complex eigenvalue problem concerning a simple simulation model of cable-stayed bridges.

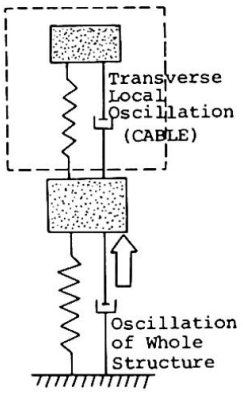

Fig.1 Damped absorber

Fig.2 shows the simulation model with 2-degree of freedom for a study on the defined causes. The equation of free damping oscillation may be given as follows :

$$\begin{bmatrix} m_g+m_c/2 & 0 \\ 0 & m_c \end{bmatrix}\begin{bmatrix} \ddot{x}_g \\ \ddot{x}_c \end{bmatrix}+\begin{bmatrix} c_g & 0 \\ 0 & c_c \end{bmatrix}\begin{bmatrix} \dot{x}_g \\ \dot{x}_c \end{bmatrix}+\begin{bmatrix} k_{gg} & k_{gc} \\ k_{gc} & k_{cc} \end{bmatrix}\begin{bmatrix} x_g \\ x_c \end{bmatrix}=\begin{bmatrix} 0 \\ 0 \end{bmatrix} \quad (1)$$

where $\ddot{x}$, $\dot{x}$, x, m, c and k express the acceleration, the velocity, the displacement, the mass, the structural damping coefficients and the stiffness, respectively. And suffix g or c indicates the values of a girder or a cable, respectively.

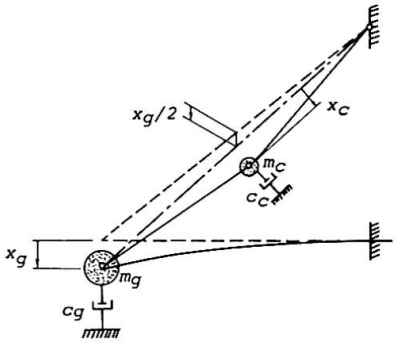

Fig.2 Simulation model

If a model as shown in Fig.3, in which the transverse oscillation of the cable is neglected, and another model with only the transverse oscillation of the cable in Fig.4 are presumed here, the equations of motion is respectively given from Eq.(1) as follows :

$$(m_g+m_c/2)\ddot{x}_g+c_g\dot{x}_g+k_{gg}x_g=0 \quad \cdots\cdots\cdots\cdots (2)$$

$$m_c\ddot{x}_c+c_c\dot{x}_c+k_{cc}x_c=0 \quad \cdots\cdots\cdots\cdots (3)$$

Then, when ω_g and ω_c, h_g and h_c are respectively the natural circular frequencies and the structural damping constants of the models with 1-degree of freedom, the following equations are obtained :

$$\left.\begin{aligned} c_g &= 2(m_g+m_c/2)h_g\omega_g \\ k_{gg} &= (m_g+m_c/2)\omega_g^2 \end{aligned}\right\} \cdots\cdots (4) \qquad \left.\begin{aligned} c_c &= 2m_c h_c \omega_c \\ k_{cc} &= m_c\omega_c^2 \end{aligned}\right\} \cdots\cdots (5)$$

As an extreme case where the internal resonance occurs, the assumption $\omega_g=\omega_c=\bar{\omega}$ is made here. Thus, by substituting Eq.(4), Eq.(5) and the equations $x_g=X_g e^{i\Omega t}$, $x_c=X_c e^{i\Omega t}$, as a conventional approach, into Eq.(1), the following equation is obtained :

$$e^{i\Omega t}\begin{bmatrix} -\Omega^2+2ih_g\bar{\omega}\Omega+\bar{\omega}^2 & k_{gc}/(m_g+m_c/2) \\ k_{gc}/m_c & -\Omega^2+2ih_c\bar{\omega}\Omega+\bar{\omega}^2 \end{bmatrix}\begin{bmatrix} x_g \\ x_c \end{bmatrix}=\begin{bmatrix} 0 \\ 0 \end{bmatrix} \cdots\cdots (6)$$

From the condition of existence of significant solution of the above equation, two sets of the conjugate complex roots, Ω_1 and Ω_2, can be approximately derived as follows :

$$\left.\begin{aligned} \Omega_1 &\fallingdotseq i\{(h_g+h_c)/2\}\bar{\omega}\pm\sqrt{\bar{\omega}^2[1-\{(h_g+h_c)/2\}^2]-\alpha} \\ \Omega_2 &\fallingdotseq i\{(h_g+h_c)/2\}\bar{\omega}\pm\sqrt{\bar{\omega}^2[1-\{(h_g+h_c)/2\}^2]+\alpha} \end{aligned}\right\} \cdots\cdots (7)$$

where $\alpha=\{k_{gc}/(m_g+m_c/2)\}(k_{gc}/m_c)$. Moreover, the normalized natural modes, $\{\Phi_1\}$ and $\{\Phi_2\}$, can be obtained from Eq.(6) as follows :

$$\{\Phi_1\}=[\sqrt{1/\{2(m_g+m_c/2)\}},\ -\sqrt{1/(2m_c)}]^T,\quad \{\Phi_2\}=[\sqrt{1/\{2(m_g+m_c/2)\}},\ +\sqrt{1/(2m_c)}]^T \cdots\cdots (8)$$

Hence, by paying attention to bending aeolian oscillations due to wind forces acting on the girder, the following equation may be expressed for each time step:

$$\{\Phi_1\}^T[F_I]\{\Phi_1\}=\{\Phi_2\}^T[F_I]\{\Phi_2\}=\frac{1}{2}(\{\Phi_g\}^T[F_I]\{\Phi_g\}) \cdots\cdots (9)$$

where $[F_I]$ is the unsteady aerodynamic damping matrix which will be described in the next chapter, and $\{\Phi_g\}=[\sqrt{1/(m_g+m_c/2)},\ 0\ ]$ is the normalized mode when the transverse oscillations of the cable are neglected.

Therefore, it will be known that the bending oscillations due to wind forces acting on the girder are produced by two kinds of similarly coupled natural modes, $\{\Phi_1\}$ and $\{\Phi_2\}$, which are excited almost at the same time by means of the natural circular frequencies, $\omega_1=\sqrt{\bar{\omega}^2-\alpha}$ and $\omega_2=\sqrt{\bar{\omega}^2+\alpha}$, close to each other. Furthermore, it will be known that the following conditions can be easily satisfied, and that the total damping constant to each mode is increased as compared with the case where the internal resonance hardly occurs :

$$2\{(h_g+h_c)/2\}\omega_1-h_g^*/2 > 2h_g\omega_g-h_g^*,\quad 2\{(h_g+h_c)/2\}\omega_2-h_g^*/2 > 2h_g\omega_g-h_g^* \cdots\cdots (10)$$

where $h_g^*=\{\Phi_g\}^T[F_I]\{\Phi_g\}$. Also, it will be apparently known that beating phenomena remarkably occur, and amplitudes of the girder are periodically decreased, but without expending the energy. Consequently, it can be judged that the defined causes will be governing factors of the system damping of cable-stayed bridges.

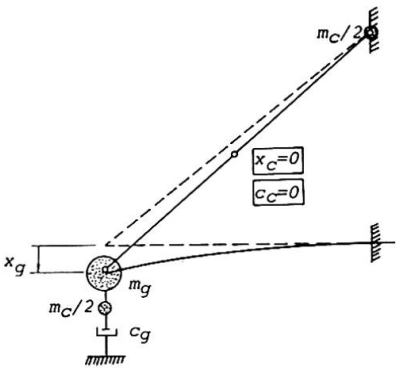

Fig.3 Model($x_c=0$)

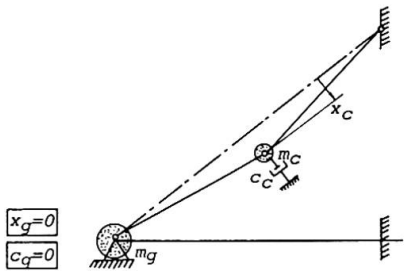

Fig.4 Model($x_g=0$)

3. ANALYTICAL TECHNIQUE USING RESULTS OF WIND-TUNNEL TEST

In this chapter, the authors deal with bending aeolian oscillations among various kinds of wind-induced responses, and propose an analytical technique of time series response using unsteady aerodynamic forces given by a sectional model wind-tunnel test, taking into consideration the internal resonance. Because, the system damping effect on cable-stayed bridges is difficult to be directly examined by full-model wind-tunnel tests.

To an analytical model of cable-stayed bridges with cables replaced by links for

considering their transverse local oscillations, the linearized equations of motion[3] may be given on the basis of the several assumptions as follows :

$$[M]\{\ddot{y}\}+[C]\{\dot{y}\}+[K]\{y\}=[F_I]\{\dot{y}\} \quad \cdots\cdots(11)$$

where $[M]$ is the mass matrix, and $[K]$ is the tangential stiffness matrix in a static equilibrium state. Also, $[C]$ is the structural damping matrix, and $[F_I]$ is the unsteady aerodynamic damping matrix. By performing the natural vibration analysis for the equation $[M]\{\ddot{y}\}+[K]\{y\}=\{0\}$, two kinds of similarly coupled natural modes of i-th and j-th orders, $\{\Phi_i\}$ and $\{\Phi_j\}$, and the natural circular frequencies close to each other, ω_i and ω_j, can be obtained when the internal resonance remarkably occurs. Moreover, if the normalization $\{\Phi_K\}^T[M]\{\Phi_K\}=1 \ (k=i,j)$ has been performed, Eq.(11) can be transformed into the following 2nd order differential equation relative to the generalized coordinates, q_i and q_j :

$$\ddot{q}_k+(2h_k\omega_k-\{\Phi_k\}^T[F_I]\{\Phi_k\})\dot{q}_k+\omega_k^2 q_k=0 \quad (k=i,j) \quad \cdots\cdots(12)$$

where h_i and h_j are the structural damping constants. But, being different from the conventional cases where only one kind of natural modes is considered, values assumed in a wind-tunnel test cannot be used as these constants. Also, these constants must be evaluated by taking account of degree of the internal resonance.

When h_g and h_c, ω_g and ω_c, $[C_g]$ and $[C_c]$, and $\{\Phi_g\}$ and $\{\Phi_c\}$ respectively express the structural damping constants, the natural circular frequencies, the damping matrices, and the normalized natural modes of the model neglecting transverse local oscillations of cables and also of the model for only transverse oscillations of cables, the following equations can be constituted :

$$2h_k\omega_k=\{\Phi_k\}^T[C]\{\Phi_k\}=\left[\{\Phi_{k,g}\}^T,\ \{\Phi_{k,c}\}^T\right]\begin{bmatrix}[C_g], & [0]\\ [0], & [C_c]\end{bmatrix}\begin{Bmatrix}\{\Phi_{k,g}\}\\ \{\Phi_{k,c}\}\end{Bmatrix} \quad (k=i,j) \quad \cdots\cdots(13)$$

$$2h_g\omega_g=\{\Phi_g\}^T[C_g]\{\Phi_g\}, \qquad 2h_c\omega_c=\{\Phi_c\}^T[C_c]\{\Phi_c\}$$

where $\{\Phi_{k,c}\}$ expresses only the transverse local oscillation component of the cables in $\{\Phi_k\}$, and $\{\Phi_{k,g}\}$ expresses $\{\Phi_k\}$ from which this component has been deducted. Thus, from the above equations and the fact that $\{\Phi_i\}$ and $\{\Phi_j\}$ are similar to each other, it seems that these values, h_i and h_j, may be evaluated by the following approximate expression :

$$2h_k\omega_k\fallingdotseq 2h_g\omega_g(\{\Phi_{k,g}\}^T\{\Phi_{k,g}\})/(\{\Phi_g\}^T\{\Phi_g\})+2h_c\omega_c(\{\Phi_{k,c}\}^T\{\Phi_{k,c}\})/(\{\Phi_c\}^T\{\Phi_c\}) \quad (k=i,j) \quad (14)$$

The validity of evaluating the structural damping constants by Eq.(14) will be confirmed in the next chapter.

Hence, by giving the matrix $[F_I]$, Eq.(12) can be expressed definitely. This matrix can be calculated by using the unsteady aerodynamic lift coefficient C_{LZI} obtained from the sectional model wind-tunnel test with the dimensionless amplitude Z_r and the reduced wind velocity U_r at each angle of attack. However, differently from the conventional cases, it is required to give U_r and Z_r corresponding to two kinds of natural circular frequencies close to each other and similarly coupled natural modes. These values may be computed as follows. Namely, the value of U_r may be given corresponding to the average value $(\omega_i+\omega_j)/2$ of the frequencies. On the other hand, the value of Z_r may be given corresponding to the equivalent amplitude vector $\{Z_p\}$ which can be expressed by the following equation in each time step :

$$\{Z_p\}=\sqrt{(q_i\{\Phi_i\}+q_j\{\Phi_j\})^2+\left(\frac{\dot{q}_i\{\Phi_i\}+\dot{q}_j\{\Phi_j\}}{(\omega_i+\omega_j)/2}\right)^2} \quad \cdots\cdots(15)$$

Therefore, by integrating Eq.(12) in succession with a small interval and applying the mode superposition method, the time series response analysis of bending aeolian oscillations can be performed taking into consideration the internal resonance. Furthermore, the proposed analytical technique can be easily extended to other kinds of wind-induced oscillations.

4. EXAMPLE OF FULL-SCALE MEASUREMENT

In this chapter, in order to confirm the validity of the defined causes and of evaluating the structural damping constants by using Eq.(14), the results of an actual cable-stayed PC bridge test are introduced and examined.

The bridge tested is as illustrated in Fig.5, in which it was anticipated at the time of design that the internal resonance would occur under completed conditions after grouting of HiAm-anchor cables. The tests conducted were a dropping load test and a moving load test. The weight, dropping position and moving speed of a loading car were about 2.0 t , the midpoint of the span and 30km/h, respectively. For the sake of comparison, the dropping test was made not only after grouting, but also before the grouting.

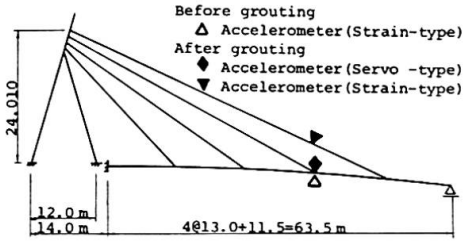

Fig.5 Cable-stayed PC bridge

Fig.6 shows the computed results of natural circular frequencies and modes together with the measured values. Fig.7 and Fig.8 show the recorded waveforms of the respective items of measurement at the dropping and moving load tests, respectively. Moreover, Table 1 shows the calculated values of damping constants by substituting the reasonable values, h_g=0.00477 and h_c=0.00637, into Eq.(14), corresponding to the measured values of logarithmic decrement, δ_g=0.03 and δ_c=0.04.

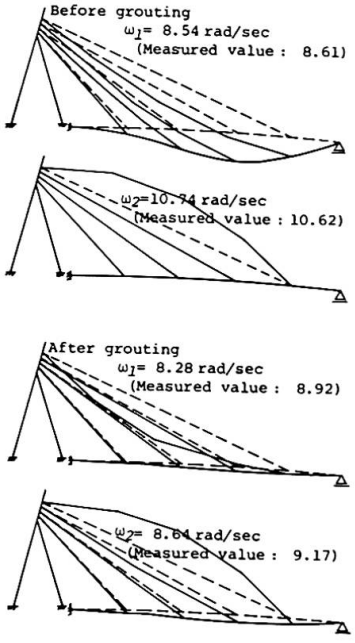

Fig.6 Natural circular frequencies and modes

Hence, it will be seen from Fig.6 that after the grouting, unlike before the grouting, two kinds of similarly coupled modes having close frequencies to each other exist apparently due to the internal resonance. Also, it will be seen from Fig.7 and Fig.8 that in the case of residual free oscillations after the grouting, amplitudes of the main girder are rapidly decreased, and that changes in the amplitude apparently due to the beating phenomenon are observed.

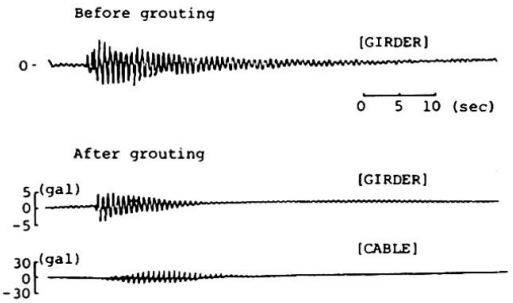

Fig.7 Dropping load test

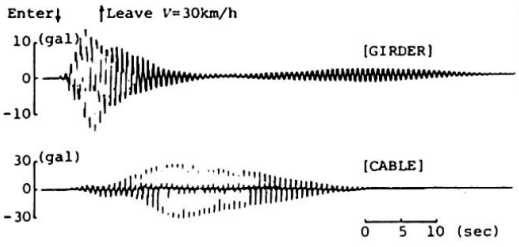

Fig.8 Moving load test

	ORDER	MODE	CALCULATED V. (δ_g=0.03, δ_c=0.04)	
Before grout.	1st	OSCILLATION OF GIRDER	δ_1	0.030
			h_1	0.00477
	2nd	OSCILLATION OF CABLE	δ_2	0.040
			h_2	0.00637
After grout.	1st	COUPLED OSCILLATION OF GIRDER AND CABLE	δ_1	0.037
			h_1	0.00589
	2nd		δ_2	0.033
			h_2	0.00525

Table 1 Damping constants

While, from Table 1, it will be known that the values of h_1 and h_2 corresponding to the coupled natural modes after the grouting are larger than the value of h_g. Also, it will be known that the sum of h_1 and h_2 after the grouting is equal to the sum of h_g and h_c, and that before the grouting, the value of h_1 corresponding to the non-coupled mode of the main girder is equal to the value of h_g.

Therefore, from the above considerations, it may be maintained that in actual bridges, the system damping due to the defined causes can occurs actually. The actual bridge for the test has satisfied the required conditions for the internal resonance incidentally in the design, and in case of multi-cable-stayed bridges,

possibilities of satisfying the conditions would have been higher. Thus, the defined causes may be considered to be a governing factor of the system damping experienced in the past. Furthermore, it may be considered that evaluation of the damping constant by Eq.(14) is appropriate, as one of the features of the proposed analytical technique.

5. TIME SERIES RESPONSE ANALYSIS FROM SPRING-MOUNTED MODEL TEST

In this chapter, a time series response analysis of bending aeolian oscillations with respect to an actual design example are performed using unsteady aerodynamic coefficients obtained from a spring-mounted model test. Then, it will be tried to obtain basic data for a wind resistant design related to the system damping effects of cable-stayed bridges.

5.1 Calculation Model Corresponding to Actual Design Problem

An actual design example to be considered is a multi-cable-stayed bridge[4] as shown in Fig.9 and Table 2. In the original design, this bridge has not satisfied the required conditions of the internal resonance. Thus, an additional mass is considered here corresponding to an actual problem for a comparison with the static design.

Consequently, in the case of this bridge with HiAm-anchor cables, by increasing the thickness of grouting, four kinds of calculation models are used here, in which characteristics of cables at the 10th and 11th levels are given as shown in Table 3.

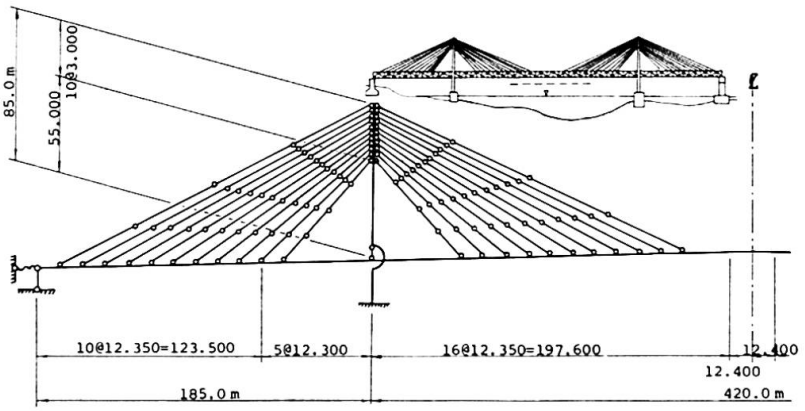

Fig.9 Skeleton

	AREA (m^2)	INERTIA (m^4)	Y.MODULUS (t/m^2)
GIRDER	1.0635 ~ 1.5747	40.538 ~ 65.585	21000000.0
TOWER	1.4780 ~ 2.2520	4.568 ~ 9.054	21000000.0
CABLE	0.0225 ~ 0.0419	0.0	20500000.0
SPRING (length : 3.0 m)	1.0	0.0	36000.0

Table 2 Sectional values

CABLE		MODEL	SECTIONAL VALUES AREA (m^2)	LENGTH (m)	DENSITY (t/m^3)	TOTAL WEIGHT (t)	NO. OF φ7mm - WIRE	PE - PIPE OUTSIDE DIAMETER	PE - PIPE WEIGHT (kg/m)	REQUIRED VALUE OF GROUT AREA (cm^2)	REQUIRED VALUE OF GROUT WEIGHT (kg/m)	REQUIRED VALUE OF GROUT DENSITY (t/m^3)	CIRCULAR FREQUENCY (rad/sec)
CENTER SPAN	10th	*MODEL-1,-1L*	0.03586	179.554	11.0	70.827	(117×4) ×2	φ125mm	15.04	474.54	76.913	1.62	3.324
		MODEL-2L											
		MODEL-3L			18.282	117.714		φ200mm	37.36	1781.83	315.723	1.77	2.578
	11th	*MODEL-1,-1L*	0.03586	191.907	11.0	75.700	(117×4) ×2	φ125mm	15.04	474.54	76.913	1.62	3.128
		MODEL-2L			16.192	111.430		φ180mm	30.72	1372.09	247.417	1.80	2.578
		MODEL-3L											
SIDE SPAN	10th	*MODEL-1,-1L*	0.04186	180.791	11.0	83.247	(136×4) ×2	φ140mm	18.56	632.85	109.458	1.73	3.097
		MODEL-2L											
		MODEL-3L			15.873	120.125		φ200mm	37.36	1725.15	294.690	1.71	2.578
	11th	*MODEL-1,-1L*	0.04186	193.208	11.0	88.965	(136×4) ×2	φ140mm	18.56	632.85	109.458	1.73	2.910
		MODEL-2L			14.025	113.429		φ180mm	30.72	1315.42	223.918	1.70	2.578
		MODEL-3L											

Table 3 Characteristics of HiAm-anchor cables

Namely, *MODEL-1* and *MODEL-1L* correspond to the cases where transverse local oscillations of the cables are neglected and considered without adjusting distributed

mass, respectively. *MODEL-2L* corresponds to the case where the requirements for the internal resonance are satisfied by adding a mass to the four uppermost cables at the 11th level. *MODEL-3L* corresponds to the case where the same adjustment is made to four cables at 10th level in addition to the 11th level.

5.2 Natural Oscillation Characteristics

The natural circular frequencies and modes concerning the 1st order symmetric oscillation of the main girder are shown in Fig.10. Namely, the mode superposition method is applied by paying attention to the modes shown in this figure. However, in *MODEL-1L*, the mode of the 10th order is apparently not excited by the unsteady aerodynamic forces acting on the main girder, but is indicated there as reference.

5.3 Structural Damping Constants

By considering four cases of h_C, the values of structural damping constants h_i and h_j corresponding to each mode evaluated by Eq.(14) are used, namely, for *CASE-1*, *CASE-2*, *CASE-3* and *CASE-4*, in which a value of 0.03 is used as the logarithmic decrement $\delta_g=2\pi h_g$, the values of $\delta_C=2\pi h_C$ are varied from 0.0 to 0.0075, to 0.0150 and to 0.0300, respectively.

5.4 Unsteady Aerodynamic Force

As the unsteady aerodynamic lift coefficient C_{LZI}, a value is applied corresponding to the reduced wind verocity U_r=1.992 shown in Fig.11, which is formulated by the least square method by using V-A-δ curve (wind velocity-amplitude-logarithmic decrement curve)[5] obtained from the results of a wind-tunnel test of the spring-mounted model in the case of an angle of attack of 5-degrees. For reference, ratio of C_{LZI} to dimensionless amplitude $z_r=z_0/B$ is also shown in Fig.11.

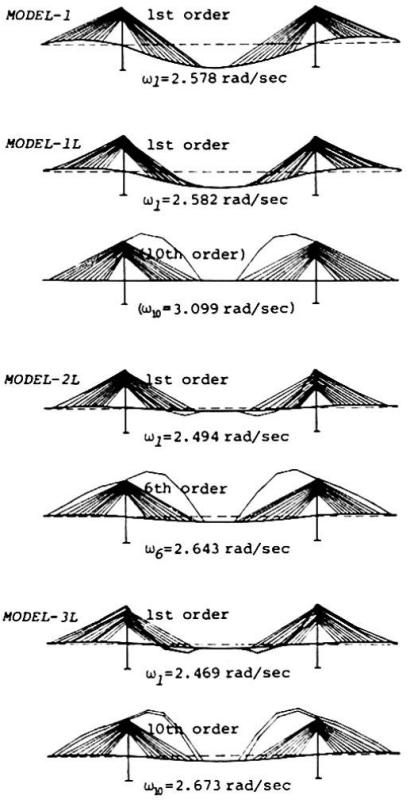

Fig.10 Natural circular frequencies and modes

5.5 Results and Consideration

A part of calculated results of the time series response analysis is shown in Fig.12, when the initial value of vertical displacement amplitude at 1/2 point of the main girder is 0.150 m.

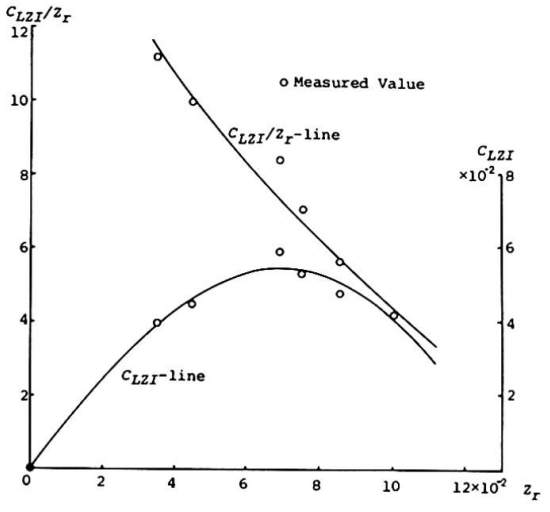

Fig.11 Unsteady aerodynamic force

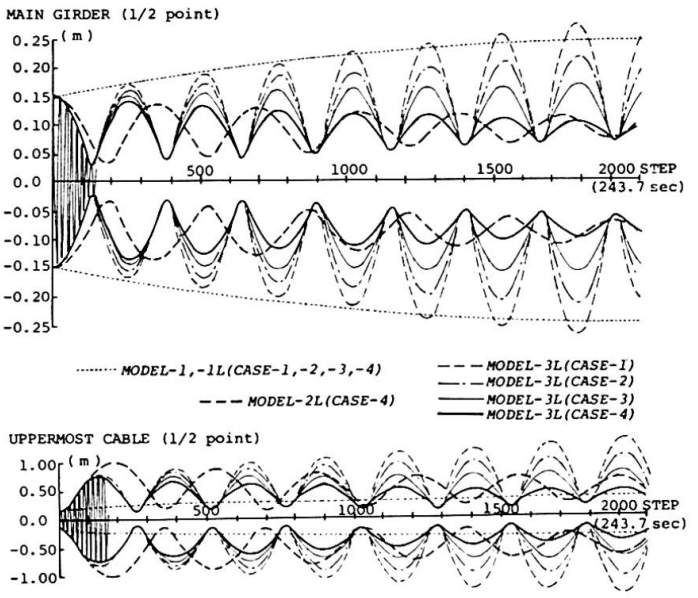

Fig.12 Amplitudes to steady state

This figure shows an envelope of the response amplitudes from the initial development stage to the steady state of vertical displacements at 1/2 points of the main girder and the uppermost cable of the center span. From this figure, it will be known that there is almost no difference between *MODEL-1* and *MODEL-1L*, and that, in the case of *MODEL-2L* and *MODEL-3L*, the amplitude is gradually decreased periodically. Moreover, in the case of *MODEL-3L*, it will be known that the steady state amplitude slightly increases in *CASE-1* where the function of the cable as a damped absorber is neglected, but becomes considerably small in *CASE-2* and *CASE-3* compared to *MODEL-1L*. Also, it will be known that, in *CASE-4*, the development of oscillations is even restricted in the case of *MODEL-2L* and *MODEL-3L*.

6. CONCLUSIONS

From the afore-mentioned discussions, the following conclusions may be drawn :

(1) It can be judged that the defined causes are governing factors of the system damping of cable-stayed bridges, which are the function of staying cables as a damped absorber (tuned mass damper in a wide sense) and the beating phenomena when the internal resonance in terms of bending oscillations of a main girder and of transverse local oscillations of cables remarkably occurs.

(2) By enhancing the action of cables as a damped absorber by using materials with higher damping capacity, it is not difficult to even restrict the occurrence of wind-induced oscillation of main girders of cable-stayed bridges by means of the system damping effect.

(3) It is positively predictable that the examination of the system damping effect due to the defined causes will become not negligible in the wind resistant design of cable-stayed bridges. Especially, by satisfying the requirements for the internal resonance by adjusting a distributed mass of particular cable of multi-cable-stayed bridges, the system damping effect enables to considerably reduce steady state amplitudes and are effective for improving the aerodynamic stability without an impediment to the static design.

(4) For the examination of the system damping, the proposed analytical technique of time series response taking into consideration the internal resonance is appropriate, which is easily extended to other kinds of wind-induced oscillations by using results of sectional model wind-tunnel tests.

Finally, the authors would like to express the deepest appreciation to Prof. M. Ito (University of Tokyo), to Prof. Y. Ohchi (Hosei University) and to Dr. H. Yamaguchi (Saitama University) for their valuable advices during the present study, and also to Mr. M. Yasuda and Dr. S. Narui (Honshu-Shikoku Bridge Authority) for their valuable data given to the authors.

REFERENCES

1) Leonhardt, F. et al. : Cable-Stayed Bridges, IABSE SURVEYS, S-13/80, 1980.

2) Den Hartog, J.P. : Mechanical Vibrations, 4th Edition, McGraw-Hill Book Inc., 1956.

3) Y. Kubo, M. Ito and T. Miyata : Nonlinear Analysis of Aerodynamic Response of Suspension Bridges in Wind, Proc. of JSCE, No.252, 1976 (in Japanese).

4) Japan Society of Civil Engineers : Report of Technical Research and Study on 'Hitsuishijima-Bashi' and 'Iwagurojima-Bashi' Cable-Stayed Bridges, Part III, 1980 (in Japanese).

5) Honshu-Shikoku-Bridge Authority : Report of Wind-Tunnel Tests for Main Truss Girder of 'Iwagurojima-Bashi' Cable-Stayed Bridge, Part II, 1980 (in Japanese).

Conclusions to Seminar VI
Windeinwirkungen auf Tragwerke

Ernst GEHRI
Dipl. Bauing.
Eidg. Techn. Hochschule
Zürich, Schweiz

Die heute zur Verfügung stehenden Berechnungsmethoden weisen in der Regel einen wesentlich höheren Genauigkeitsgrad auf, als die auf das betrachtete Tragwerk einwirkenden Kräfte. Dies gilt insbesondere für die Erfassung der Windeinwirkungen.

Im Einführungsbericht setzte MELBOURNE zum Ziel des Seminars das Tragwerksverhalten unter den effektiven Windeinwirkungen besser zu erfassen und zugleich einfache Entwurfs- und Bemessungsverfahren aufzustellen. Inwieweit wurde dieses Ziel erreicht?

Die auf die Bauwerke einwirkenden Windkräfte sind stark von den geographischen und topographischen Eigenschaften des betrachteten Gebietes abhängig. Die heute in den nationalen Vorschriften eingeführten Werte sehen grossräumige Festlegungen vor, die deshalb eher als Richtwerte anzusehen sind. Oertliche Unstetigkeiten infolge der Topographie (Täler, Berge, usw.) können dadurch nicht erfasst werden. Zudem beeinflusst die Rauhigkeit des Geländes (Bebauung, Bepflanzung) die Struktur des Windes in dem oftmals wichtigen bodennahen Bereich. MELBOURNE weist insbesondere darauf, dass die maximalen Windwerte nur in einem meist genau definierbaren Richtungsbereich auftreten. Angaben über die Windgeschwindigkeiten bezüglich Richtung (Windrose) sind demnach entscheidend für die Erfassung realistischerer Windeinwirkungen. Einen guten Einblick über die Struktur des natürlichen Windes ergeben die Messungen von ISYUMOV et al. am CN Tower in Toronto.

Bei schlanken, windempfindlichen Tragwerken sollten bei der Festlegung der Windkräfte die aeroelastischen Eigenschaften des Tragwerkes beachtet werden. MELBOURNE zeigt eindrücklich wie dadurch die Verteilung der Windkräfte und somit auch die daraus resultierende Beanspruchung stark variieren kann.

Die meisten Seminarbeiträge befassten sich mit aerodynamischen Stabilitätsuntersuchungen von Brücken, was in Anbetracht des Teilnehmerkreises nicht erstaunlich ist. IRWIN zeigt eindrücklich wie durch an sich geringfügigen Aenderungen an der Querschnittsform oder durch die Anordnung von z.T. unterbrochenen Verkleidungen die aerodynamische Stabilität wesentlich verbessert werden kann. Analoge Verbesserungen können ebenfalls durch den Einbau von Dämpfern erreicht werden. Durch relativ einfache Entwurfsmassnahmen kann somit das Problem aeroelastischer Instabilität wesentlich entschärft werden. ITO/YAMAGUCHI untersuchten den Einfluss von windinduzierten Verformungen des Tragwerkes auf die kritische Windgeschwindigkeit bei Hängebrücken. DAVENPORT/KING versuchen die bisherige getrennte Behandlung statischer und aerodynamischer Windeinwirkungen zu vermeiden. Das Vorgehen ist zukunftsweisend, erlaubt es doch ausgehend von Windkanalversuchen an einem Modellquerschnitt die Entwurfswindlasten genauer festzulegen.

Der Beitrag von MIYATA/YAMADA befasst sich mit dem unterschiedlichen Verhalten von Hängebrücken mit lotrechten und schrägen Hängern. Wie die Autoren dabei feststellen, sind aber nicht die Windkräfte primäre Ursache der höheren dynamischen Beanspruchung schräger Hänger, sondern die aus den Verkehrslasten resultierenden Beanspruchungen.

RICHARDSON diskutiert verschiedene Möglichkeiten zur Verbesserung der aerodynamischen Stabilität weitgespanntester Hängebrücken. Er schlägt dabei vor die Steifigkeit des Tragwerkes wesentlich zu erhöhen und die aerodynamischen Kräfte durch Längsschlitze zu vermindern. Für weitgespannte Brücken folgt daraus als geeigneteste Lösung das Zwei-Brücken-Konzept (Zwei miteinander gekoppelte Hängebrücken).

MAEDA et al. befassen sich mit einem Teilaspekt, nämlich mit dem Systemdämpfungseffekt von Schrägseilbrücken. Insbesondere wird hier der Einfluss der Schrägkabeln als Dämpfer untersucht und dabei aufgezeigt, wie durch den Einsatz von Hüll- und Füllmaterialien mit höherem Dämpfungsvermögen eine wesentliche Verbesserung erzielt werden kann.

Von besonderem Interesse sind die Darlegungen von WYNHOFEN et al. da sie einerseits Hochbauprobleme behandeln und andernseits die Bedeutung von Windkanaluntersuchungen an dynamischen Modellen aufzeigen.

Das durchgeführte Seminar - die intensiv geführte Diskussion hat dies auch bestätigt - führte zu einem besseren Verständnis über die Windeinwirkungen, wobei im Vordergrund die Probleme bei weitgespannten Brücken standen. Das weniger spektakuläre, aber dennoch volkswirtschaftlich bedeutungsvolle Problem der Windeinwirkungen auf Verkleidungen (Dacheindeckungen, Fassaden, usw.) blieb deshalb unbehandelt.